UNIVERSIDADE FEDERAL DO RIO GRANDE DO SUL
Instituto de Ciências Básicas da Saúde
Departamento de Bioquímica Prof. Tuiskon Dick
Programa de Pós-Graduação em Ciências Biológicas: Bioquímica

Metabolismo Energético Cerebral é Modulado em Ambos os Hemisférios em Um Modelo Experimental de Isquemia Focal Permanente

Yasmine Nonose

Dissertação apresentada ao Curso de Pós-Graduação em Ciências Biológicas: Bioquímica, da Universidade Federal do Rio Grande do Sul, como requisito para obtenção do título de Mestre em Ciências Biológicas: Bioquímica.

Porto Alegre, 29 de fevereiro de 2016

UNIVERSIDADE FEDERAL DO RIO GRANDE DO SUL
Instituto de Ciências Básicas da Saúde
Departamento de Bioquímica Prof. Tuiskon Dick
Programa de Pós-Graduação em Ciências Biológicas: Bioquímica

Metabolismo Energético Cerebral é Modulado em Ambos os Hemisférios em Um Modelo Experimental de Isquemia Focal Permanente

Yasmine Nonose

Orientador: Dr. Adriano Martimbianco de Assis

Dissertação apresentada ao Curso de Pós-Graduação em Ciências Biológicas: Bioquímica, da Universidade Federal do Rio Grande do Sul, como requisito para obtenção do título de Mestre em Ciências Biológicas: Bioquímica.

Banca examinadora:

1. Profª Drª Christianne Gazzana Salbego – Membro do Programa de Pós-Graduação em Ciências Biológicas: Bioquímica, ICBS/UFRGS (relatora)
2. Prof. Dr. Carlos Alexandre Netto – Membro do Programa de Pós-Graduação em Ciências Biológicas: Bioquímica, ICBS/UFRGS
3. Profª Drª Rosalia Mendez-Otero – Instituto de Biofísica Carlos Chagas Filho, Centro de Ciências da Saúde, Universidade Federal do Rio de Janeiro (UFRJ)

Porto Alegre, 29 de fevereiro de 2016

A presente dissertação foi desenvolvida no Instituto de Ciências Básicas da Saúde, Universidade Federal do Rio Grande do Sul, sendo financiado pela Coordenação de Aperfeiçoamento de Pessoal de Nível Superior (CAPES), pelo Conselho Nacional de Desenvolvimento Científico e Tecnológico (CNPq), pelo Instituto Nacional de Ciência e Tecnologia em Excitotoxicidade e Neuroproteção (INCT-EN) e pela Pró-Reitoria de Pesquisa desta Universidade (PROPESQ/UFRGS).

"*Nothing in life is to be feared, it is only to be understood.*

Now is the time to understand more, so that we may fear less".

"Nada na vida deve ser temido, e sim compreendido.

Agora é a hora de compreendermos mais, para que possamos temer menos"

Madame Marie Curie,

Prêmio Nobel de Física (1903) e Química (1911).

AGRADECIMENTOS

Ao meu orientador, Dr. Adriano de Assis, por me receber no laboratório 28, por estar sempre presente quando precisei, pela amizade e por todas as oportunidades que nossa convivência me proporcionou. Obrigada por todo apoio, incentivo e reconhecimento.

Ao Prof. Dr. Diogo Souza, que também me acolheu no laboratório 28 e sempre foi muito atencioso com todos. Obrigada pelas conversas sobre ciência, sobre a vida e por ser uma pessoa tão generosa.

À minha família, que sempre incentivou meus estudos. Em especial, um grande obrigada ao meu pai, que me acompanhou incansavelmente em todas as etapas do mestrado e também em muitas comemorações ao longo desses dois anos.

Aos colegas que participaram dos experimentos desenvolvidos nesse projeto: Bruna, Leo, Roberto, Zimmer, Samuel e Gianina; e aos Professores Dr. André Quincozes e Dr. Luc Pellerin. É um prazer trabalhar com vocês.

Aos integrantes do Grupo de Neuroenergética & Neuroproteção Jussemara, Leonardo, Pedro, Rodrigo e Vitória por todo apoio e amizade.

A todos os queridos colegas e ICs do laboratório 28 por tornarem todos os dias prazerosos e divertidos, por serem pessoas maravilhosas e comprometidas com o trabalho que fazemos e por todo o aprendizado que me proporcionaram. Obrigada também aos colegas do laboratório 26 por todas as conversas, orientações, cafés compartilhados e amizade.

Aos meus grandes amigos e amigas, em especial à Fernanda, Letícia, Manuela, Aline, Deborah, Márcio, Stefano, Gustavo e Ramiro, que sempre torceram por mim incondicionalmente e comemoraram comigo cada pequena conquista ao longo do mestrado.

A todos os funcionários do ratário e do Departamento de Bioquímica.

Às mulheres que me inspiraram a seguir na pesquisa científica, em especial à Profª Drª Magdolna Maria Vozári-Hampe, à Profª Drª Iraci Lucena da Silva Torres e à minha “doutoranda” Joanna Ripoll Rozisky. Obrigada por todos os ensinamentos.

Agradeço especialmente o apoio financeiro das instituições: CNPq, CAPES, FAPERGS e INCTEN.

Por fim, agradeço a todos que, de alguma maneira, contribuíram para a realização desse trabalho.

ÍNDICE **PÁG.**

PARTE I

RESUMO

A isquemia cerebral (IC) ainda é uma das principais causas de mortalidade e deficiência adquirida em humanos. A maioria dos sobreviventes necessita de assistência médica contínua, o que significa que é preciso investigar as vias que levam à reparação e à recuperação da função cerebral atingida. O conhecimento de mecanismos que atuam na fase de recuperação oferece uma maior janela temporal para atuação farmacológica. Assim, o objetivo deste trabalho foi investigar o envolvimento das alterações do metabolismo energético, do sistema glutamatérgico e de parâmetros astrocitários após indução de isquemia focal permanente (FPI) *in vivo*. Ratos Wistar machos adultos (90 dias) foram divididos em dois grupos: Sham e Isquemia. A isquemia foi induzida por termocoagulação, enquanto os animais Sham foram submetidos apenas à craniotomia. Análises *ex vivo* foram realizadas em ambos os hemisférios cerebrais, separadamente. Após 2 dias, a isquemia aumentou a captação e a oxidação de glicose, glutamato e lactato no hemisfério ipsilateral à lesão. Tanto a captação de glutamato quanto a oxidação de lactato se mostraram aumentadas também no hemisfério contralateral no mesmo período, indicando que o lactato derivado do glutamato possa ser responsável por manter o metabolismo cerebral logo após FPI. A Análise da captação de [^{18}F]FDG em microPET mostrou que, *in vivo*, a captação de glicose ipsilateral está prejudicada, sugerindo que a insuficiência de fluxo sanguíneo na região está por trás dessa alteração. A análise por *Real Time* PCRq mostrou que a expressão de mRNA dos transportadores GLAST e GLT-1 estava diminuída no hemisfério isquêmico. A expressão de GLT-1 também estava diminuída no hemisfério contralateral nos dois tempos analisados, indicando uma regulação diferente para esse transportador. O imunoconteúdo de GLAST mostrou diminuição contralateral, contribuindo para a hipótese de que a GFAP pode ser importante para reter esse transportador na membrana plasmática. Após 2 dias, foi observado um aumento de MCT4 contralateral, enquanto que o MCT2 encontrava-se diminuído. Os níveis proteicos de MCT4 continuaram elevados após 9 dias no hemisfério contralateral, com aumento também no ipsilateral, sugerindo que esse transportador tem um papel mais ativo a curto e a médio prazos após IC. A análise de parâmetros astrocitários por imunohistoquímica demonstrou reatividade na área de peri-infarto e um maior conteúdo de GFAP. O aumento do número de processos centrais primários é o maior responsável pela forma mais radial da astroglia reativa. Em conjunto, nossos resultados sugerem que o metabolismo energético possa estar regulado de forma a conter a expansão do insulto isquêmico e, assim, auxiliar a recuperação metabólica após indução de lesão isquêmica. Além disso, destacamos o envolvimento do lactato como um substrato energético essencial para recuperação do dano isquêmico e, também, para iniciar os mecanismos de compensação no hemisfério contralateral.

ABSTRACT

Cerebral ischemia (IC) is still a leading cause of death and acquired deficiency in humans. Most survivors need further medical care, which makes essential the investigation of mechanisms that lead to brain repair and recovery. Considering that knowledge of the mechanisms behind brain repair and recovery offers a greater time window for pharmacological manipulation of potential therapeutic targets, the aim of this work was to investigate the involvement of changes in the energy metabolism, glutamatergic system and astrocytic parameters in an animal model of focal permanent ischemia (FPI). Adult male Wistar rats (90 days) were divided in 2 groups: Sham and Ischemia. FPI was induced surgically by themocoagulation, while sham animals were only submitted to craniotomy. *Ex vivo* analyses were performed in both brain hemispheres separately. At 2 days post-FPI, brain ischemia significantly increased ipsilateral uptake and oxidation of glucose, glutamate and lactate. Interestingly, glutamate uptake and lactate oxidation were also contralateraly augmented, indicating that glutamate-derived lactate may be responsible for maintaining brain metabolism after focal ischemia. MicroPET evaluation showed that *in vivo* [^{18}F]FDG uptake is impaired, indicating that blockage of cerebral blood flow may be the reason for diminished uptake when compared to the *ex vivo* analyses. RT-PCRq analysis showed that mRNA expression of glutamate transporters GLAST and GLT-1 was reduced in the ischemic hemisphere. The expression of GLT-1 was also reduced in the contralateral hemisphere in both time points analyzed, indicating a different regulation for this transporter. GLAST immunocontent by western blot showed a contralateral decrease 9 days after FPI, contributing to the possibility that GFAP can be important to retain this transporter in the plasma membrane. We also observed an increase in MCT4 protein levels in the contralateral hemisphere, while MCT2 was decreased, 2 days following FPI. MCT4 levels were still elevated at 9 days, also showing ipsilateral increase, suggesting that this transporter has a more active role in both short and medium term after IC. The analysis on astrocytic parameters presented greater reactivity in the peri-infarct area and a higher content of GFAP in the areas analyzed. Morphological changes, especially due to increased number of primary central processes, are responsible for most radially reactive astroglia. Together, our results suggest that energy metabolism may be regulated to contain the expansion of the ischemic insult and thus help the metabolic recovery after ischemic injury. In addition, we point out the involvement of lactate as an essential energy substrate for the recovery of ischemic damage, and also to start the compensation mechanisms in the contralateral hemisphere.

LISTA DE ABREVIATURAS

ATP: Adenosina Trifosfato

AVE: Acidente Vascular Encefálico

EAAC1: *Excitatory Amino Acid Carrier*, carreador de aminoácido excitatório 1

EAAT: *Excitatory Amino Acid Transporter*, transportadores de aminoácidos excitatórios

FPI: *Focal Permanent Ischemia*, isquemia focal permanente

GFAP: *Glial Fibrillary Acidic Protein*, proteína glial fibrilar ácida

GLAST: *Glutamate-Aspartate Transporter*, transportador glutamato-aspartato

GLT-1: Glutamate Transporter 1, transportador de glutamato 1

IC: Isquemia Cerebral

Km: Constante de Michaelis Menten

MCAO: Middle Cerebral Artery Occlusion, oclusão da artéria cerebral média

MCT: *Monocarboxilic acid Transporter*, transportador de ácidos monocarboxílicos

OMS: Organização Mundial da Saúde

RA: Reatividade Astrocitária

rt-PA: *Recombinant Tissue Plasminogen Activator*, ativador de plasminogênio tecidual

RT-PCRq: *Real Time - quantitative Polymerase Chain Reaction*, Reação em Cadeia da Polimerase quantitative em tempo real.

SNC: sistema nervoso central

LISTA DE FIGURAS

1. INTRODUÇÃO

1.1. Isquemia Cerebral

A isquemia cerebral (IC) é uma das maiores causas de mortalidade e morbidade em humanos atualmente (Castillo *et al.*, 2003), sendo conhecida clinicamente como acidente vascular encefálico (AVE) e popularmente como derrame. Dados da Organização Mundial de Saúde (OMS) revelam que o AVE permaneceu sendo a segunda maior causa de morte ao redor do mundo durante a última década (OMS, 2010). Aproximadamente 15 milhões de pessoas sofrem AVE no mundo todo a cada ano; dessas, 5 milhões morrem e outros 5 milhões ficam permanentemente incapacitadas (OMS, 2002). No Brasil, segundo o Ministério da Saúde, são registradas cerca de 68 mil mortes por AVE anualmente. A doença representa a primeira causa de morte e incapacidade no país, gerando um grande impacto econômico e social (Ministério Da Saúde, 2012).

A IC é caracterizada por uma redução severa ou por um bloqueio do fluxo sanguíneo ao cérebro (Dirnagl *et al.*, 1999), podendo ser transitória ou permanente. Além disso, pode ser originada por: (a) rompimento de uma artéria ou vaso sanguíneo, causando sangramento (AVE hemorrágico); ou (b) por obstrução de uma ou mais artérias (AVE isquêmico). Em ambos os casos, o suprimento insuficiente de oxigênio e glicose à demanda metabólica cerebral resulta em morte celular poucos minutos após o início do bloqueio da circulação (Broughton *et al.*, 2009).

Mais de 80% dos casos de AVE são de origem isquêmica (American Stroke Association, 2012), podendo ser desencadeados por:

I) **Hipoperfusão:** quando o fluxo sanguíneo cerebral é interrompido ou reduzido por parada cardíaca, afetando o cérebro por inteiro (IC global);

II) **Trombose ou Embolismo:** quando o fluxo sanguíneo é interrompido ou reduzido em uma região cerebral específica (IC focal). Ocorre devido à obstrução de um vaso sanguíneo por um coágulo, sendo esta a causa mais prevalente de AVE isquêmico.

Há outras causas de infarto cerebral e sua distinção é essencial para o tratamento dos pacientes. Entretanto, essas causas apresentam uma menor incidência e não fazem parte do objetivo deste trabalho.

Em 1995, foi demonstrado que a administração de rt-PA (*recombinant tissue plasminogen activator,* ativador de plasminogênio tecidual) melhorava o prognóstico em grupos de pacientes cuidadosamente selecionados que sofreram AVE isquêmico agudo (*National Institute of Neurological Disorders And Stroke*, 1995). Entretanto, ainda hoje o rt-PA é a única substância aprovada para o tratamento do AVE isquêmico (*Guidelines for management of ischaemic stroke and transient ischaemic attack,* 2008). É importante ressaltar que, apesar de seu uso ter se provado seguro e eficaz, sua utilização se restringe a 5% dos pacientes (Fonarow *et al.*, 2011), provavelmente devido à janela temporal reduzida e pelos riscos de complicações hemorrágicas. Dessa forma, há uma demanda urgente por tratamentos aplicáveis mais abrangentes.

O conhecimento dos eventos moleculares associados à morte celular causada pela IC, bem como daqueles envolvidos nas estratégias celulares de sobrevivência, é fundamental para o desenvolvimento de terapias clinicamente efetivas e, consequentemente, para a diminuição da morte neuronal. A busca pelo entendimento de tais eventos é de extrema relevância, uma vez que não há protocolo terapêutico clinicamente eficaz que possa reduzir a incidência e/ou as sequelas neurológicas resultantes da isquemia (Parnham and Sies, 2000).

1.1.1. Propagação da lesão isquêmica

Diversos processos neuroquímicos são iniciados pela IC focal. O conjunto desses acontecimentos é conhecido como cascata isquêmica (Brouns and De Deyn, 2009), um fenômeno heterogêneo que pode ser descrito como uma insuficiência energética celular devido à hipoperfusão local seguida de excitotoxicidade, estresse oxidativo, inflamação pós-isquemia, disfunção da barreira hematoencefálica, entre outros, culminando na morte neuronal, glial e endotelial (Figura 1). Uma vez iniciada, a cascata isquêmica pode durar horas ou dias, mesmo após a restauração da circulação sanguínea (Zivin, 1998). Apesar da reperfusão ser essencial para a restauração das funções celulares, ela paradoxalmente causa um dano secundário, comumente referido como dano de reperfusão (Eltzschig and Eckle, 2011; Duehrkop and Rieben, 2014).

Inicialmente, o dano isquêmico conduz à insuficiência bioenergética devido à diminuição de oxigênio e glicose, o que reduz ou impede a síntese de

ATP através da glicólise e da fosforilação oxidativa. A diminuição de ATP intracelular rapidamente conduz à disfunção do transporte iônico dependente de energia, como a Na^+/K^+ ATPase. Consequentemente, ocorre a despolarização dos neurônios e da glia (Katsura *et al.*, 1994; Martin *et al.*, 1994), a ativação de canais de cálcio voltagem-dependente e a liberação de aminoácidos excitatórios no espaço extracelular, como o glutamato (Phillis *et al.*, 1996). Simultaneamente, o transporte desse neurotransmissor, que é dependente do gradiente eletrogênico, está desabilitado, causando seu acúmulo na fenda sináptica. A contínua estimulação dos receptores ácido-amino-3-hidróxi-5-metil-isoxazol-4-propiônico (AMPA), cainato e N-metil-D-Aspartato (NMDA) pelo glutamato resulta na perda da homeostase do cálcio e na ativação de eventos intracelulares que culminam na morte celular. Esse fenômeno é conhecido como excitotoxicidade glutamatérgica.

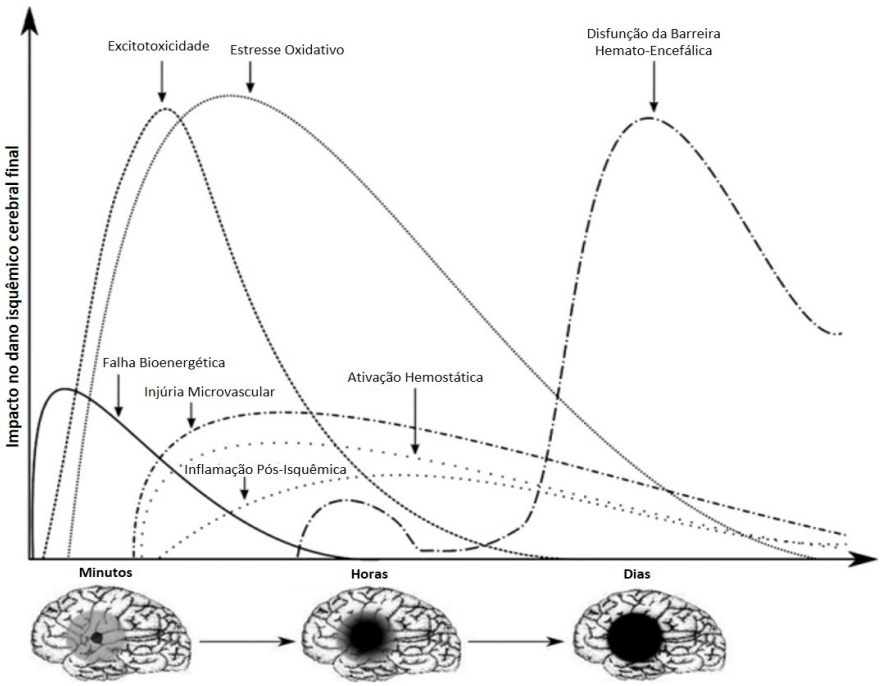

Figura 1. Representação do perfil do dano isquêmico focal agudo ao longo do tempo e dos mecanismos patofisiológicos principais. A contribuição de cada fenômeno no dano isquêmico cerebral final é representada pelo eixo Y. Já a progressão da lesão isquêmica mediante ausência de reperfusão é ilustrada no eixo X. Adaptado de Brouns e De Deyn (2009).

Dessa forma, pode-se inferir que a limitação de reservas energéticas cerebrais e a elevada dependência do metabolismo aeróbico da glicose, apesar de contribuírem enormemente para a vulnerabilidade do tecido cerebral, não são os únicos processos responsáveis pelo dano isquêmico. A conectividade

intercelular intrínseca e os mecanismos de sinalização, normalmente responsáveis pelo processamento de informações, tornam-se danosos em condições isquêmicas, auxiliando na evolução do infarto (Calabresi *et al.*, 2000).

1.1.2. *Core* isquêmico e Zona de Penumbra

Na IC focal, pode-se distinguir duas regiões pertinentes: o *core* isquêmico e a zona de perfusão intermediária. O *core* isquêmico consiste nas regiões cerebrais mais prejudicadas pela hipoperfusão, as quais tornam-se rápida e permanentemente danificadas, sofrendo morte celular por meio de processos como lipólise, proteólise, desagregação de microtúbulos, insuficiência bioenergética e quebra da homeostase iônica (Brouns and De Deyn, 2009). Já a zona de perfusão intermediária, localizada ao redor do centro da lesão, é classificada como tecido funcionalmente comprometido, mas ainda viável estruturalmente, uma vez que apresenta alguma perfusão oriunda da circulação colateral (Bandera *et al.*, 2006). Essa área é denominada zona de penumbra, em referência à área ao redor de uma sombra projetada por um objeto opaco, como o da sombra da Terra ou da Lua sobre uma região durante um eclipse parcial. Dessa forma, o termo “penumbra” é particularmente apropriado, uma vez que define as características do tecido ao redor da lesão bem como sua localização física em torno do *core* isquêmico (Astrup *et al.*, 1981; Donnan *et al.*, 2007).

Alterações fisiológicas, bioquímicas e bioenergéticas ocorrem em um ritmo mais lento na zona de penumbra. O insulto isquêmico se propaga na penumbra por meio de despolarizações esporádicas, as quais resultam da liberação de glutamato do *core* isquêmico (Lipton, 1999). Apesar da utilização de glicose aumentar na região, os níveis de ATP não resistem e decaem a 50% dos valores basais após 3,5 horas o início da IC focal (Yao *et al.*, 1995).

A zona de penumbra é o tema central de diversas pesquisas relacionadas ao AVE devido ao seu potencial de recuperação. Se for administrado um tratamento efetivo (tanto para reestabelecer o fluxo sanguíneo como para inibir algum componente da cascata isquêmica), a zona de penumbra pode ser salva, diminuindo a área cerebral atingida pela lesão

isquêmica e resultando em um melhor prognóstico para o paciente. Entretanto, a progressão do dano isquêmico no espaço-tempo eventualmente impedirá a sua recuperação, o que restringe o salvamento da penumbra a algumas horas após o início da IC (Brouns and De Deyn, 2009).

1.1.3. Modelos animais de IC

Existe uma grande variedade de modelos animais de AVE desenvolvidos, todos com o objetivo de identificar os mecanismos por trás da IC e de desenvolver novos tratamentos. Os modelos animais são indispensáveis, uma vez que proporcionam: (a) um método reprodutível, controlado e padronizado para analisar a patofisiologia do AVE, bem como o efeito de possíveis fármacos; (b) aceso direto ao tecido cerebral para realização de análises; (c) detecção e avaliação de eventos que contribuam com a patofisiologia da doença logo após seu início; e (d) interação entre os tecidos vascular e cerebral, melhor mimetizando a patologia em humanos (Fluri *et al.*, 2015).

A maioria dos experimentos é realizada em pequenos animais, sendo o emprego de ratos como animal de experimentação a decisão mais comum, uma vez que apresenta inúmeras vantagens, como baixo custo de obtenção e de manutenção e grande aceitabilidade pela perspectiva ética. Além disso, o rato é amplamente utilizado em estudos de IC por apresentar uma vasculatura cerebral e uma fisiologia semelhantes aos humanos, pelo fácil monitoramento de parâmetros fisiológicos e pela homogeneidade relativa entre linhagens (Strom *et al.*, 2013).

Um dos métodos mais utilizados para indução de IC focal envolve a oclusão da artéria cerebral média (MCAO), uma vez que essa artéria e suas ramificações são os vasos cerebrais que mais frequentemente são afetados pelo AVE isquêmico em humanos, representando aproximadamente 70% dos infartos cerebrais (Garcia, 1984; Bogousslavsky *et al.*, 1988; Hossmann, 1991; Takizawa and Hakim, 1991). A oclusão intra-arterial por sutura é o método mais utilizado em roedores, sendo empregado em mais de 40% dos experimentos em neuroproteção após IC (Howells *et al.*, 2010). Esse modelo permite a oclusão tanto permanente quanto transitória da artéria cerebral média, além de

ter uma elevada taxa de sucesso na indução do infarto. Entretanto, o grau e a área atingida dependem da duração da oclusão, seu local de indução e do fluxo sanguíneo colateral. Além disso, essa técnica pode levar à hemorragia sub-araconóide ou à inadequada oclusão, dependendo do tipo de sutura empregada (Fluri *et al.*, 2015). Devido a esses fatores, há certa preocupação com as diferenças patofisiológicas entre os modelos de MCAO permanentes e transitórios. Resultados discrepantes podem contribuir grandemente para o fracasso dos agentes neuroprotetores empregados em ensaios clínicos.

Outros modelos bastante empregados incluem a realização de craniotomia, permitindo acesso às artérias cerebrais e, principalmente, às ramificações distais da artéria cerebral média. Nessa dissertação, o modelo escolhido foi o de IC focal permanente induzida por termocoagulação (Szele *et al.*, 1995), visto que a técnica é de fácil desenvolvimento, apresenta uma menor variabilidade e um menor tamanho de lesão, possibilitando um melhor acompanhamento das regiões afetadas pelo AVE focal posteriormente à indução da isquemia, ao longo do tempo, em um tamanho de área significativo para as análises visadas. Além disso, a indução de IC focal por essa técnica nos permite utilizar um número menor de animais e realizar análises mais precisas no metabolismo energético cerebral e eventuais drogas neuroprotetoras (Hansel, 2014).

1.2. Metabolismo energético cerebral

Apesar de representar apenas 2% do peso corporal total, o cérebro humano é responsável pelo consumo de 25% de toda a glicose circulante e por 20% do oxigênio disponível no organismo em condições de repouso (Magistretti, 1999). A manutenção e a restauração do gradiente iônico dissipado pelos potenciais de ação, bem como a captação e reutilização de neurotransmissores, são os principais processos que contribuem para a elevada demanda bioenergética do tecido cerebral (Alle *et al.*, 2009). Além disso, a limitação de reservas energéticas cerebrais o torna altamente dependente do fluxo sanguíneo e do metabolismo aeróbico da glicose para a síntese de ATP. Como consequência, o cérebro é extremamente vulnerável ao dano isquêmico em comparação com outros tecidos (Dugan and Choi, 1999).

Após a hipoperfusão local induzir a falha bioenergética e comprometer a síntese de ATP através da fosforilação oxidativa, os processos celulares dependentes de energia são prejudicados. A insuficiência de glicose leva à utilização do glicogênio cerebral, o qual se encontra majoritariamente nos astrócitos, bem como toda a maquinaria necessária para sua síntese e catabolismo. Em condições anóxicas, o glicogênio está mais disponível para degradação do que a glicose, uma vez que não necessita consumir uma molécula de ATP para iniciar o processo (Ibrahim, 1975; Hamprecht *et al.*, 2005). Entretanto, suas reservas são esgotadas pelas despolarizações contínuas na região da penumbra. Adicionalmente, a falta de oxigênio conduz à glicólise anaeróbica, que produz uma grande quantidade de lactato (Nicoli *et al.*, 2003; Brouns *et al.*, 2008). Níveis elevados de lactato são considerados não somente um marcador do metabolismo anaeróbico durante IC, mas também uma possível causa de dano secundário, o que levaria à expansão da lesão isquêmica (Brouns *et al.*, 2008).

O cérebro adulto, em condições fisiológicas, utiliza praticamente só glicose como substrato energético. Entretanto, a utilização de outros substratos também é possível em determinadas circunstâncias. Os corpos cetônicos são consumidos preferencialmente durante o desenvolvimento do sistema nervoso central (SNC) ou durante jejum prolongado, bem como o lactato é utilizado durante períodos de atividade física intensa e ativação neuronal (Belanger *et al.*, 2011).

Por muito tempo, o lactato foi considerado somente um produto final da glicólise anaeróbia com nenhuma função no metabolismo. Porém, na década de 50, um estudo conduzido por McIlwain revelou que o tecido cerebral pode utilizar monocarboxilatos como substrato energético no lugar de glicose (McIlwain, 1956). O grupo desses compostos inclui o lactato, o piruvato e os corpos cetônicos. Por serem substâncias hidrofílicas, os ácidos monocarboxílicos não difundem através da membrana plasmática. Existem transportadores específicos para carrear esses compostos através da barreira hemato-encefátlica e através das membranas de cada tipo celular. A família dos transportadores de monocarboxilatos (MCT, *monocarboxylate transporter*) é composta de 14 membros, dentre os quais somente os 4 primeiros, MCT 1 –

4, mostraram atuar por meio de um sistema de co-transporte de monocarboxilatos e prótons por um mecanismo de simporte. Esses transportadores são distintos um do outro não somente por sua cinética, mas também pela sua distribuição tecidual e localização celular (Pierre and Pellerin, 2005).

O MCT1 está presente em quase todos os tecidos, incluindo músculo, rim, fígado e coração. No SNC de roedores adultos, o MCT1 está localizado mais abundantemente nas células endoteliais formadoras de vasos (Baud *et al.*, 2003), podendo ser encontrado em astrócitos e, raramente, em neurônios. Já o MCT2 apresenta expressão mais marcada em córtex, hipocampo e cerebelo, sendo encontrado mais especificamente em células neuronais de roedores jovens e adultos. Importantemente, o MCT2 é o principal transportador neuronal no cérebro de roedores, sendo associado com o transporte de ácidos monocarboxílicos em projeções axonais e também no terminal pós-sináptico. O MCT3 é exclusivamente expresso no epitélio pigmentado retinal (Philp *et al.*, 1998; Philp *et al.*, 2001), enquanto o MCT4 foi encontrado primeiramente no músculo esquelético, onde tem uma expressão elevada (Dimmer *et al.*, 2000). Em cérebro de roedores, estudos indicam que o MCT4 é expresso exclusivamente em astrócitos de diversas regiões cerebrais.

Ao longo dos anos, diversos estudos confirmaram que o lactato é eficientemente oxidado no cérebro e, particularmente, pelas células neuronais. Esses resultados conduziram à hipótese da existência de uma lançadeira de lactato astrócito-neurônio *in vivo*, pela qual os astrócitos forneceriam aos neurônios um substrato energético complementar durante um período de grande atividade. Além disso, já foi demonstrado que o lactato tem a capacidade de preservar atividade neuronal e função cerebral durante episódio hipoglicêmico e até mesmo é um substrato obrigatório na recuperação pós-hipóxia (Phillis *et al.*, 2001; Pellerin, 2003). O lactato revelou ser importante para o metabolismo energético cerebral, o que inclui seu potencial neuroprotetor no SNC, além de abrir novas possibilidades para o entendimento da interação neurônio-glia.

1.3. Sistema glutamatérgico

O aminoácido glutamato é o principal e o mais abundante neurotransmissor excitatório do SNC de mamíferos, tendo importante participação no processo de comunicação intercelular, crescimento e diferenciação (Nedergaard *et al.*, 2002). Entretanto, níveis excessivos desse neurotransmissor na fenda sináptica levam à excitotoxicidade, um fenômeno que ocorre em diversas desordens e que está envolvida na patofisiologia de dano cerebral isquêmico (Brouns and De Deyn, 2009).

Sabe-se que o glutamato não é metabolizado no ambiente extracelular. Portanto, as sinapses glutamatérgicas são reguladas pelos transportadores de aminoácidos excitatórios (EAAT, *excitatory amino acid transporter*) que estão presentes tanto em células gliais como nos neurônios (Danbolt, 2001). Já foram identificadas 5 isoformas desses transportadores: EAAT1 ou GLAST (*glutamate-aspartate transporter*, transportador de glutamato e aspartato) e EAAT2 ou GLT-1 (*glutamate transporter* 1, transportador de glutamato 1), encontrados principalmente em astrócitos; EAAT3 ou EAAC1 (*excitatory amino acid carrier*, carreador de aminoácido excitatório 1); EAAT4, encontrado principalmente em neurônios; e EAAT5 (Danbolt, 2001; Had-Aissouni, 2012).

Em condições fisiológicas, a excitotoxicidade glutamatérgica é evitada pelo astrócito, uma célula glial especializada em diversas funções tanto regulatórias quando de suporte (Allen and Barres, 2009). Os astrócitos são responsáveis pela remoção do excesso de neurotransmissores da fenda sináptica por meio de transportadores; no caso do glutamato, os principais transportadores envolvidos são o GLT-1 e o GLAST (Rothstein *et al.*, 1994). Ambos medeiam o transporte de glutamato do meio extracelular para o intracelular por meio do co-transporte de três íons Na^+ e um íon H^+, somado à extrusão de um íon K^+. Dessa forma, o transporte de glutamato é dependente do gradiente de sódio oriundo da Na^+ / K^+-ATPase (Danbolt, 2001), tornando a captação de glutamato um processo custoso energeticamente.

Durante as condições patofisiológicas da isquemia, o gradiente eletroquímico das membranas celulares não é mantido, prejudicando o transporte de glutamato, aumentando ainda mais sua concentração no terminal sináptico e contribuindo para a progressão do insulto isquêmico (Anderson and Swanson, 2000; Phillis *et al.*, 2000; Bonde *et al.*, 2003). Além disso, a falha

bioenergética decorrente pode acarretar no transporte reverso de glutamato (do meio intra para o extracelular) e, consequentemente, em um aumento ainda mais acentuado dos níveis desse neurotransmissor na fenda sináptica (Malarkey and Parpura, 2008). A hiperestimulação dos receptores que medeiam os efeitos do glutamato resulta em um aumento da permeabilidade ao Ca^{2+}, que, no citosol, é um importante segundo mensageiro e influencia diversas funções celulares, incluindo a regulação da proliferação e da sobrevivência celular, bem como pode levar à morte celular por necrose ou apoptose (Orrenius *et al.*, 1996). Diferentemente do *core* isquêmico, a região da penumbra apresenta um metabolismo energético parcialmente preservado. O fluxo sanguíneo restrito, somado às alterações impostas pela propagação da lesão isquêmica, pode submeter a zona de penumbra a mudanças na disponibilidade de substratos energéticos e na sua utilização como fonte de ATP.

Alguns grupos de pesquisa demonstraram que os astrócitos tem uma taxa metabólica oxidativa de glutamato elevada o suficiente para que o gasto energético com seu transporte para o meio intracelular seja compensado (Sonnewald *et al.*, 1993; Hertz and Hertz, 2003; McKenna, 2012). Uma vez transaminado, o α-cetoglutarato resultante seria metabolizado pelo ciclo do ácido cítrico, rendendo o equivalente a 9 moléculas de ATP. Segundo McKenna e Sonnewald (1996), quando as concentrações extracelulares de glutamato aumentam significativamente, a proporção de glutamato oxidado pelo ciclo do ácido cítrico nos astrócitos também aumenta, bem como a sua conversão em glutamina diminui (McKenna *et al.*, 1996a). Recentemente, um estudo comprovou que nenhum outro substrato energético pode diminuir efetivamente a oxidação de glutamato por competitividade em astrócitos de córtex de ratos (McKenna, 2012). Para completar, foi demonstrado que o destino metabólico do glutamato é, majoritariamente, a conversão em lactato nos astrócitos, sendo inclusive maior do que sua conversão em glutamina (Sonnewald *et al.*, 1993). Dessa forma, podemos observar que não só o sistema glutamatérgico está intimamente relacionado com a propagação da lesão isquêmica, bem como com o metabolismo energético cerebral, podendo participar das alterações metabólicas decorrentes da IC.

1.4. Participação do Astrócito

O SNC é composto por dois tipos predominantes de células: os neurônios e as células gliais. Enquanto os neurônios são a unidade básica funcional do SNC, responsáveis pela sinalização sináptica e pelo processamento de informação, as células gliais são conhecidas por sua função de suporte, tanto estrutural quanto metabólico. Entretanto, as células gliais não são elementos passivos no SNC. Diversos estudos demonstram que a neuroglia tem um papel ativo no processamento de informações e na função cerebral, tanto no desenvolvimento quanto na vida adulta. Em mamíferos, há três tipos mais conhecidos de células gliais: a microglia, os oligodendrócitos e os astrócitos (Allen and Barres, 2009).

O estudo das funções da glia em doenças neurodegenerativas tornou-se interessante quando várias pesquisas que visavam o entendimento de mecanismos de dano neurônio-específicos falharam. Complementarmente, diversos trabalhos mostram que os astrócitos desempenham funções não somente fisiológicas, mas também durante desordens do SNC (Zalc, 1997). Por serem abundantes no SNC, somado à importância de suas funções na homeostase cerebral, acredita-se que os astrócitos sejam importantes alvos terapêuticos.

Fisiologicamente, os astrócitos realizam processos essenciais à sobrevivência neuronal, como: (1) formação e manutenção da barreira hematoencefálica; (2) liberação de diversas moléculas sinalizadoras; (3) regulação da plasticidade sináptica; (4) regulação do acoplamento neurometabólico; (5) tamponamento do ambiente extracelular; (6) produção de antioxidantes; e (7) captação de neurotransmissores durante atividade sináptica (Gordon *et al.*, 2007; Clarke and Barres, 2013; Stobart and Anderson, 2013). Suas funções abrangentes podem ser realizadas devido ao posicionamento estratégico da astroglia no tecido cerebral: seus processos se mantêm em contato tanto com os vasos sanguíneos quanto com os neurônios. Isso permite a captação de substratos energéticos advindos do endotélio vascular e seu fornecimento às células neuronais para o suprimento da demanda energética (Stobart and Anderson, 2013), além de permitir que a

astroglia exerça controle local do fluxo sanguíneo no SNC por meio de moléculas vasoativas (Gordon *et al.*, 2007; Koehler *et al.*, 2009).

De acordo com a hipótese da lançadeira de lactato, durante a ativação neuronal pelo glutamato, os astrócitos captam esse neurotransmissor liberado do terminal pré-sináptico por meio dos transportadores dependentes de Na^+ GLAST e GLT-1. O aumento intracelular na concentração de Na^+ induz a atividade da Na^+/K^+ ATPase a bombear o excesso de Na^+ para fora da célula, conduzindo a uma maior demanda por ATP. A glicólise astrocitária é ativada e, assim, também é a produção de lactato. Quando os níveis deste aumentam, o lactato é transportado via MCT primeiro para o meio extracelular e, após, para dentro dos neurônios, onde é oxidado na mitocôndria (Pellerin and Magistretti, 1994) (Figura 2).

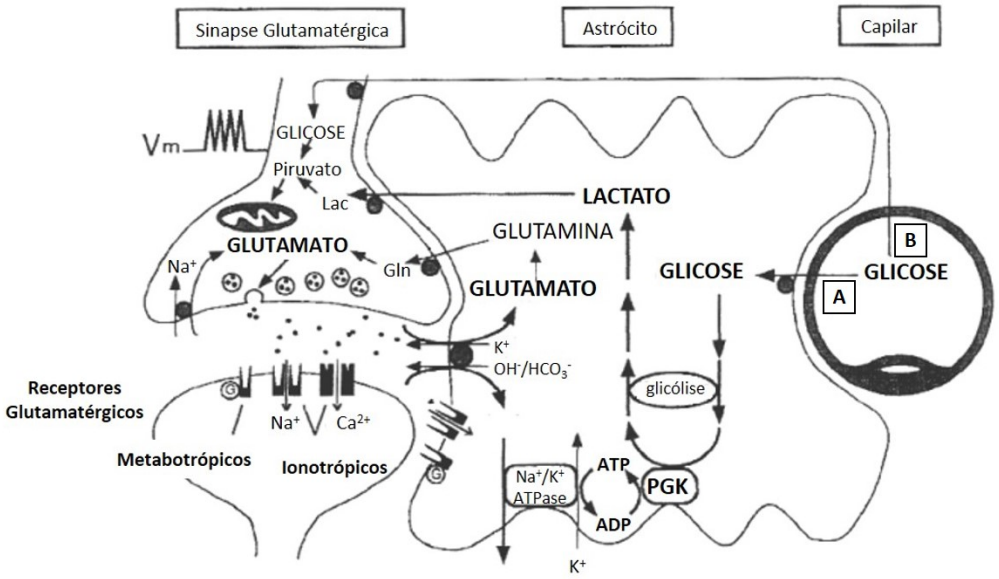

Figura 2. Primeiro esquema representativo da lançadeira de lactato astrócito-neurônio, mostrando a glicólise induzida pelo glutamato durante ativação neuronal fisiológica. Legenda: (A) captação de glicose induzida por glutamato; (B) captação de glicose neuronal basal; Gln, glutamina; Lac, lactato; PGK, fosfoglicerato cinase. Adaptado de Pellerin e Magistretti, 1994.

A relação astrócito-neurônio, bem como a função astrocitária, pode estar alterada após IC focal, considerando a baixa disponibilidade de substratos energéticos, o restrito fluxo sanguíneo na região da penumbra e a elevada demanda energética para responder às modificações patofisiológicas impostas pela propagação da lesão isquêmica. A investigação de como o metabolismo

dessas células pode estar sofrendo modulações é de grande importância para o desenvolvimento de novos mecanismos de neuroproteção.

1.4.1. Reatividade astrocitária

Além da morte celular no *core* isquêmico, a IC provoca uma série de alterações celulares e moleculares na zona de penumbra ao longo do tempo, incluindo sinalização de Ca^{2+}, proliferação celular, alterações morfológicas e regulação de expressão gênica (Panickar and Norenberg, 2005; Ding *et al.*, 2009; Zamanian *et al.*, 2012; Ding, 2013; Li *et al.*, 2013; Ding, 2014). Essas alterações são temporal e espacialmente dependentes com uma característica em comum: níveis de expressão elevados de proteína glial fibrilar ácida (GFAP, *glial fibrillary acidic protein*) em astrócitos reativos e a formação da cicatriz glial na zona de penumbra, que demarca o limite entre a região infartada e a região da penumbra (Haupt *et al.*, 2007; Hayakawa *et al.*, 2010; Barreto *et al.*, 2011b; Shimada *et al.*, 2011; Bao *et al.*, 2012).

Alterações astrocitárias estão entre as primeiras e mais impactantes respostas cerebrais à IC (Petito and Babiak, 1982). Sabe-se que a astroglia está viável na região da penumbra e que torna-se reativa, podendo esta reação ser causada diretamente pela dano isquêmico ou ser a resposta astrocitária às alterações em outros elementos do SNC (Panickar and Norenberg, 2005). A reatividade astrocitária (RA) é definida como uma resposta dos astrócitos à injúria cerebral, consistindo em mudanças que vão desde alterações reversíveis na expressão de proteínas e na hipertrofia celular com preservação estrutural, até uma cicatriz duradoura com rearranjo da arquitetura tecidual. A RA é considerada, tradicionalmente, prejudicial à recuperação do tecido pós-IC, uma vez que a cicatriz glial tem propriedades física e quimicamente inibitórias (Bidmon *et al.*, 1998; Yasuda *et al.*, 2004). Os astrócitos reativos apresentam diferenças marcantes, como aumento do núcleo celular, maior número de mitocôndrias e ribossomos, processos citoplasmáticos mais longos, grossos e numerosos e aumento do volume citoplasmático.

A astroglia presente na cicatriz glial apresenta processos com hipertrofia que formam uma barreira física, além de produzir moléculas inibitórias, citocinas pró-inflamatórias e permitir que fatores pró-apoptóticos se espalhem

no sinsítio astrocitário, expandindo a área infartada (Lin *et al.*, 1998). Apesar de alguns trabalhos sugerirem que tratamentos que diminuem o volume de infarto geralmente são acompanhados de uma menor resposta astrocitária (Fang *et al.*, 2006; Forslin Aronsson *et al.*, 2006; Ye *et al.*, 2007), é difícil determinar a causa e efeito, dado que a extensão de astrogliose provavelmente reflete a gravidade da lesão.

Em adição ao seu papel na formação de cicatrizes gliais, os astrócitos também respondem à IC com funções importantes para a neuroproteção e reparação tecidual. Estes incluem: a proteção de tecido viável contra novos danos (Nedergaard and Dirnagl, 2005), como os causados pela excitotoxicidade glutamatérgica; a reconstrução da barreira hemato-encefálica (Kaur and Ling, 2008; del Zoppo, 2009); e a produção de fatores neurotróficos (Swanson *et al.*, 2004).

Além disso, parece que a GFAP tem um papel importante na resposta astrocitária à IC. Camundongos *knockout* para GFAP exibem lesões maiores do que animais *wild type* após IC focal (Nawashiro *et al.*, 2000). Ainda, os ratos *knockout* tanto para GFAP quanto para vimentina têm o processo de ativação astrocitária prejudicado e a capacidade de captar glutamato diminuída (Li *et al.*, 2008). Além disso, os ratos *knockout* para a conexina 43, a proteína de *gap junction* formadora das redes de astrócitos necessária para neurotransmissão adequada e responsável pela regulação dos níveis de potássio, apresentam maior volume de infarto após MCAO (Nakase *et al.*, 2003). Desta forma, os astrócitos têm o potencial de ser tanto prejudiciais quanto benéficos após um insulto isquêmico, o que indica que a astroglia é um alvo promissor para manipulação (Barreto *et al.*, 2011a). Sabe-se que os astrócitos são mais resistentes do que os neurônios aos danos da IC, o que já é bem estabelecido em cultura de células (Panickar and Norenberg, 2005). Isso pode ser devido ao conteúdo astrocitário, rico em enzimas e proteínas envolvidas em mecanismos de defesa, e às reservas energéticas de glicogênio, que permitem a manutenção da demanda energética mesmo em ausência de glicose por 1-2h (Yu and Hertz, 1983), e, ainda, a outros fatores, como maior habilidade em utilizar ácidos graxos e corpos cetônicos como fonte energética (Guzman and Blazquez, 2004).

1.5. Mecanismos de reparo ao AVE no hemisfério contralateral

Na IC focal, a interação entre neurônios e glia no hemisfério lesionado (ipsilateral à lesão) não tem sido relacionada com a do hemisfério não lesionado (contralateral à lesão). Takatsuru, Nabekura e Koibuchi (2014) relatam a compensação funcional do hemisfério contralateral por meio de remodelamento sináptico específico uma semana após a indução do dano isquêmico focal. Durante esse período, os astrócitos tiveram um papel essencial na redução e na regulação das sinapses glutamatérgicas, evitando o dano excitotóxico. Outros estudos realizados em animais (Takatsuru *et al.*, 2014) também evidenciam que mudanças em circuitos neuronais podem ser induzidas no hemisfério contralateral durante recuperação funcional. Esse resultado mostra que é possível que o hemisfério cerebral intacto tenha potencial para exercer funções bilaterais em adultos. Entretanto, os mecanismos por trás dessas alterações ainda não são compreendidos (Takatsuru *et al.*, 2014). Além disso, o remodelamento sináptico, tendo os astrócitos e o sistema glutamatérgico como peças-chave, pode envolver também alterações bioenergéticas, como alterações na utilização e no fornecimento de substratos.

2. OBJETIVOS

2.1. OBJETIVO GERAL

Avaliar alterações relacionadas ao dano isquêmico focal em parâmetros bioquímicos relacionados ao metabolismo energético, ao sistema glutamatérgico e a alterações astrocitárias em um modelo animal de isquemia focal permanente, com ênfase no papel do lactato como substrato energético e na participação dos transportadores de ácidos monocarboxílicos.

2.2. OBJETIVOS ESPECÍFICOS

Os objetivos específicos desse estudo foram desenvolvidos comparando ambos os hemisférios cerebrais em 2 tempos diferentes (2 e 9 dias) após indução do dano isquêmico focal:

- Observar alterações motoras decorrentes do dano isquêmico focal nos animais do grupo isquemia;
- Medir o volume de infarto nos diferentes tempos;
- Avaliar alterações decorrentes da isquemia focal nos transportadores de glutamato: GLAST e GLT-1;
- Avaliar alterações decorrentes da isquemia focal nos transportadores de ácidos monocarboxílicos célula-específicos de neurônios e de astrócitos (MCT2 e MCT4, respectivamente);
- Avaliar alterações na captação e na oxidação de substratos energéticos em fatias de córtex próximo à região da lesão isquêmica;
- Avaliar alterações no metabolismo da glicose *in vivo*, comparando com os resultados obtidos *ex vivo* (em fatias);
- Avaliar expressão de GFAP e morfologia astrocitários nos diferentes tempos.

PARTE II

3. RESULTADOS

Os resultados estão descritos em um capítulo, o qual corresponde a um trabalho a ser submetido para publicação (Capítulo I).

3.1. CAPÍTULO I

Brain energy metabolism is modulated in both hemispheres after focal cerebral ischemia

Yasmine Nonose, Pedro E. Gewehr, Roberto F. Almeida, Jussemara S. da Silva, Bruna Bellaver, Leo A. M. Martins, Eduardo R. Zimmer, Samuel Greggio, Gianina T. Venturin, Jaderson C. da Costa, André Quincozes-Santos, Luc Pellerin, Diogo O. de Souza, Adriano M. de Assis.

Manuscrito a ser submetido ao periódico *Brain Journal*

Brain energy metabolism is modulated in both hemispheres after focal cerebral ischemia

Yasmine Nonose [1], Pedro E. Gewehr [1], Roberto F. Almeida [1], Jussemara S. da Silva [1], Bruna Bellaver [1], Leo A. M. Martins [1], Eduardo R. Zimmer [1,3], Samuel Greggio [3], Gianina T. Venturin [3], Jaderson C. Da Costa [3], André Quincozes-Santos [1,2], Luc Pellerin [4], Diogo O. de Souza [1,2], Adriano M. de Assis [1]

[1] Postgraduate Program in Biological Sciences: Biochemistry, ICBS, Federal University of Rio Grande do Sul, Porto Alegre, RS 90035-003, Brazil;

[2] Department of Biochemistry, Federal University of Rio Grande do Sul, Porto Alegre, RS 90035-003, Brazil;

[3] Brain Institute of Rio Grande do Sul, Pontifical Catholic University of Rio Grande do Sul (PUCRS), Porto Alegre, RS 90619-900, Brazil;

[4] Department of Physiology, University of Lausanne, Lausanne, 1005, Switzerland.

Correspondence to:

Adriano Martimbianco de Assis, Ph.D.

Programa de Pós-graduação em Ciências Biológicas: Bioquímica, Instituto de Ciências Básicas da Saúde, Universidade Federal do Rio Grande do Sul (UFRGS), Porto Alegre, Brazil

Ramiro Barcelos, 2600 - Anexo

Santa Cecília

90035-003 Porto Alegre, RS, Brazil

E-mail: deassisam@gmail.com

Key-words (< 5): Cerebral ischemia, energy metabolism, contralateral hemisphere, reactive astrocytes

Running title: Brain energy metabolism after focal ischemia

Abstract

Stroke is a chronically disabling disease for most of survivors. This fact means that, besides the understanding of pathophysiological mechanisms, we must look into pathways leading to brain repair and recovery. Considering that exhaustion of energy supplies is at the basis of this disorder, we hypothesized that ischemia-induced substrates availability and utilization in the brain might play a role in recovery. Accounting for the roles of astrocytic metabolism in excitotoxicity and brain energy metabolism, this study evaluated the effect of injury on the energy metabolism 2 and 9 days following focal permanent ischemia (FPI). The FPI injury was induced surgically by thermocoagulation in adult (90 days old) male Wistar rats. Animals were divided in two groups: sham and ischemia. The biochemical analyses were performed in both ipsi- and contralateral brain hemispheres separately, using tissue aside the lesion focus and an equivalent contralateral area. We noticed a significant increase in glutamate uptake 2 days post-FPI accompanied by increased lactate oxidation in both hemispheres, indicating that glutamate-derived lactate could be responsible for sustaining brain metabolism shortly after focal ischemia. Ipsilateral glutamate uptake and oxidation, together with lactate utilization, are still elevated 9 days post-FPI, which may account to support brain recovery. Two days post-FPI, we observed high levels of MCT4 in the contralateral hemisphere while MCT2 was downregulated in the same hemisphere. MCT4 high immunocontent were still present at 9 days, when it also appeared elevated in the ipsilateral side. GFAP overexpression was followed by diminished GLAST/GLT-1 mRNA expression and protein levels, contrasting with the elevated glutamate uptake rates found, indicating that elevated glutamate extracellular levels could be increasing glutamate transporters activity 2 days after FPI. Ischemia group GLAST expression was only lower in the ipsilateral hemisphere, but GLT-1 decreased in both ipsi- and contralateral sides, showing a different regulation and an important participation of this latter transporter. Also, diminished protein levels of GLAST in the contralateral hemisphere contributes to the hypothesis that GFAP may be important to retain this transporter on the plasma membrane. Astrocytes presented reactivity, showing a radial form accounted for numerous primary processes. Overall, in our study the FPI model showed to modulate brain energy metabolism, indicating that cell-specific changes in cellular transporters expression induced by cerebral ischemia may participate in metabolic adaptations and persist till medium term.

Introduction

Stroke is still a significant part of overall mortality and long-term disability worldwide (Kim and Johnston, 2011; Go *et al.*, 2013). Approximately, eight hundred thousand strokes occur each year in the U.S., being the majority primary (76%) and ischemic infarcts (87%) (Lloyd-Jones *et al.*, 2009; Demaerschalk *et al.*, 2010). More than 140 000 people die each year from stroke in the U.S. (www.strokecenter.org), while most survivors need to receive continuous care because of the stroke sequelae, and it represents more than a half of the annual cost of stroke (Dobkin, 2005; Di Carlo, 2009). Studies in both animal models and human patients showed that adult brain has the capability to self-repair in response to ischemic damage (Zhang *et al.*, 2013). Based on this, advances in the understanding of spontaneous brain repair mechanisms can expand the current therapeutic window, promoting restoration of function, and improving patient outcomes after stroke. Interestingly, some clinical evidences showed that not only the peri-infarct region play a crucial role in post-stroke recovery, but also the somatosensory cortex contralateral to the stroke region is determinant for post-stroke tissue reorganization and for compensation of impaired functions (Chollet *et al.*, 1991; Wittenberg *et al.*, 2003). Thereby, clarifying the mechanisms behind such compensation in the intact hemisphere is important for optimizing the functional recovery after stroke (Calautti and Baron, 2003).

It is clear that depletion of energy supplies and, thus, regulation of brain energy metabolism, plays a critical role in stroke pathophysiology and recovery (Schurr, 2002; Rosafio *et al.*, 2016), because brain tissue depends almost exclusively on oxidative phosphorylation for energy production. However, under ischemic conditions, anaerobic glycolysis keeps energy metabolism active at bare minimum, which causes accumulation of its end product lactate in the extracellular space (Hillered *et al.*, 1989; Walz and Harold, 1990; Dimlich and Nielsen, 1992; Allen and Attwell, 2002). Despite a long history of its negatively perceived role in ischemia, lactate has been shown to have neuroprotective properties in hypoxic conditions *in vitro* (Schurr *et al.*, 1997a, b; Berthet *et al.*, 2009; Castillo *et al.*, 2015) and *in vivo* (Schurr and Rigor, 1998; Schurr *et al.*, 2001; Berthet *et al.*, 2009; Berthet *et al.*, 2012). Lactate trafficking between cells is facilitated by a family of proton-dependent carriers named monocarboxylate transporters (MCTs). In the central nervous system (CNS), three MCTs were characterized as lactate transporters: MCT1, MCT2 and MCT4. MCT1 is the most

abundant glial transporter in the brain, being located in astrocytes, endothelial cells and neurons (Pierre *et al.*, 2000; Simpson *et al.*, 2007); while MCT2 is considered the main neuronal lactate transporter (Pierre *et al.*, 2002; Debernardi *et al.*, 2003), and MCT4 is exclusively expressed by astrocytes ((Rafiki *et al.*, 2003; Pellerin *et al.*, 2005; Rosafio and Pellerin, 2014). Recently, Rosafio and colleagues showed that cell-specific MCT expression may participate in the brain metabolic adaptations following transient ischemic insult (Rosafio *et al.*, 2016). Therefore, lactate is likely to play a beneficial role in the recovery phase, besides its participation on ischemia-induced adaptations on energy metabolism and substrate utilization.

Besides lactate, other substrates can be used as energy sources. Glutamate, the main excitatory neurotransmitter in the CNS, can be used as an energy fuel through entering the tricarboxylic acid cycle (TCA) after its conversion to α-ketoglutarate in astrocytes. Indeed, the astroglia is responsible for glutamate uptake from the synaptic cleft, regulating glutamatergic synapses and avoiding overstimulation (Danbolt, 2001). The tight control of extracellular glutamate levels is an energy-costly process, and it is controlled by astrocyte-specific transporters known as glutamate/aspartate transporter (GLAST) and glutamate transporter 1 (GLT-1) (Rothstein *et al.*, 1994). During cerebral ischemia, astrocytic glutamate uptake is impeded (Malarkey and Parpura, 2008), which combined with neurons depolarizations lead to a massive glutamate release, causing excitotoxicity, a major contributor to ischemic injury. It is well established that glutamate is oxidized by astroglial cells at a rate much higher than other substrates (McKenna, 2013), especially when exogenous glutamate concentration rises (McKenna *et al.*, 1996a).

In stroke, changes in astrocytes are among the earliest and most impressive responses to the ischemic injury. Surrounding the area of infarct, astroglial cells are viable and undergo reactive astroglyosis, which has been traditionally interpreted as a detrimental response for recovery due to its physical and chemical inhibitory properties (Bidmon *et al.*, 1998; Yasuda *et al.*, 2004). Nevertheless, astrocytes also respond to ischemia through neuroprotective and repairment functions, such as taking up excessive glutamate (Swanson *et al.*, 2004), promoting angiogenesis, neuronal plasticity and functional recovery (Rossi *et al.*, 2007; Carmichael, 2010; Zhao and Rempe, 2010). Therefore, astrocytes seem to be the link between energy metabolism, substrate utilization and possible mechanisms of post-stroke recovery.

Therefore, we hypothesized that focal ischemic damage might modulate substrate availability and utilization between brain hemispheres and induce adaptations. These changes may play a role in recovery after injury and the reactive astroglyosis may have a central role in this mechanism. To test our hypothesis, we combined different methodologies to examine how energy metabolism is modulated in the cerebral region surrounding the ischemic lesion in both brain hemispheres: (i) we performed the cylinder test to access the symmetry score of each animal; (ii) then, we measured the infarct volume induced by FPI to verify the extent of ischemic injury; (iii) we determined substrate uptake and oxidation rate *ex vivo* in slices and compared the results with microPET brain scan images (*in vivo*); (iv) we analyzed glutamate transporters expression and immunocontent; (v) we verified the MCTs immunocontent; and (vi) we analyzed some astrocytic parameters, such as GFAP expression and cell morphology by immunohistochemistry technique.

Materials and methods

Ethics

All animal experiments were performed in accordance with the National Institutes of Health "Guide for the Care and Use of Laboratory Animals" (NIH publication N°. 80-23, revised 1996) and were approved by the Federal University of Rio Grande do Sul Animal Care and Use Committee (process number 26674).

Reagents

2,3,5–Triphenyltetrazolium chloride (TTC) was purchased from Sigma-Aldrich (St. Louis, MO, USA). Electrophoresis reagents were from Bio-Rad Laboratories (Hercules, CA, USA) and immunoblotting reagents were from Amersham International (Little Chalfont, Bucks, UK). Polyclonal rabbit anti-rat MCT2 (#sc-50323), polyclonal rabbit anti-rat MCT4 (#sc-50329) and polyclonal rabbit anti-rat β-tubulin (#sc-9104) were purchased from Santa Cruz Biotechnology (Heidelberg, Germany). Polyclonal rabbit anti-rat GLT-1 (#GLT11-A) and anti-rat GLAST (#GLAST11-A) were purchased from Alpha Diagnostics Intl. Inc. (San Antonio, Texas, USA). Blots were revealed with Immobilon^{TM} Western Chemiluminescence kit (#P90720, Millipore Corp., Billerica, MA, USA). For substrate uptake experiments, 2-[U-^{14}C]-Deoxy-D-Glucose, Glutamic

Acid, L-[3,4-^{3}H] and Lactic Acid, L-[1-^{14}C] Na Salt were purchased from PerkinElmer (Boston, MA, USA). For substrate oxidation experiments, Glucose-D, [^{14}C(U)] (ARC0122H) and Lactic acid, L-[1-^{14}C] sodium salt were purchased from American Radiolabeled Chemicals, Inc. (St. Louis, MO, USA). Glutamic acid, L-[^{14}C(U)] (#NEC290E250UC) and Optiphase 'Hisafe' 3 (#1200-437) scintillation liquid were purchased from PerkinElmer (Boston, MA, USA). Protein quantification was performed with BCA Protein Assay kit from Thermo Fisher Scientific (#23227, Rockford, IL, USA), using bovine serum albumin as standard. All other reagents were analytical grade.

Animals

Animals were obtained from the Central Animal House of the Department of Biochemistry. Adult male Wistar rats (90–100 days old, weighing 300–350 g) were housed three to five per cage under controlled light and environmental conditions through the experiments (12 h light/12 h dark cycle at a constant temperature of 22±2 °C), with water and commercial food pellets available *ad libitum*.

Cylinder test

The cylinder test is based on the spontaneous exploratory behaviour of rodents, and it reveals forelimb preference when the animal rears to explore its environment by making forelimb contact with the cylinder walls (Schallert, 2006; Macrae, 2011). Animals were subjected to one trial 1 day before ischemia (pre-ischemia day), and again 2 and/or 9 days after ischemia. To prevent habituation to the cylinder, the number of movements recorded was limited to 20. The occurrences of ipsilateral (to the lesion), contralateral or simultaneous forelimb use were counted. The symmetry score for each animal was calculated on each day by the formula previously described (de Vasconcelos Dos Santos *et al.*, 2010).

Experimental Procedure and tissue preparation

The rats were divided into 2 groups: Sham and Ischemia. Animals were sacrificed by decapitation at 2 or 9 days following surgery and we evaluated the following parameters: *in vivo* (1) symmetry test, (2) [^{18}F]FDG uptake; *ex vivo* (3) lesion size measurement, (4) substrates uptake, (5) substrates oxidation to $^{14}CO_2$, (6) astrocytic reactivity; and *post mortem* (7) glutamate transporters expression and immunocontent,

(8) MCTs immunocontent. For the *ex vivo* experiments, the brain ipsi- and contralateral cortices were dissected and analyzed separately (Fig. 1A), while the tissue was still viable.

Induction of Focal Permanent Ischemia

The focal ischemic lesion was induced by blood thermocoagulation in the pial vessels over the motor and sensorimotor cortices, as previously described (Szele *et al.*, 1995; Giraldi-Guimardes *et al.*, 2009; Hansel *et al.*, 2014; Hansel *et al.*, 2015). Briefly, the animals were anesthetized with ketamine hydrochloride (70 mg/kg, i.p.) and xylazine hydrochloride (10 mg/kg, i.p.) and placed in a stereotaxic apparatus. The skull was surgically exposed, and a craniotomy was performed by exposing the left frontoparietal cortex (+2 to −6 mm A.P. and −2 to −4 mm M.L. from the bregma) (Paxinos and Watson, 2007). In Ischemia group, the blood inside the pial vessels was thermocoagulated transdurally by the approximation of a hot probe close to the dura mater. The rostrocaudal extent of the surface of the frontal and parietal cortices was lesioned. After the procedure, the skin was sutured, and the body temperature was maintained at 37 °C using a heating pad until recovery from the anesthesia. Animals from Sham group were only submitted to the aforementioned craniotomy.

Lesion Size Measurement

The brains were rapidly removed from the skull and sectioned in the coronal plane about 2 mm thick using a rat brain matrix. The slices were immersed for 30 min in 2 % of 2,3,5-triphenyltetrazolium chloride (TTC) (Sigma, St. Louis, MO, USA) solution at 37 °C followed by overnight fixation in 4 % paraformaldehyde (Sigma, St. Louis, MO, USA). After the TTC staining, slices were arranged in a frontal-occipital orientation, and digital images were taken. Brain slices were analyzed with Image J software (NIH, Bethesda, MD, USA). The infarct volume was calculated with the following formula: Infarct volume = [measured infarct area×slice thickness (2 mm)]+[area of contralateral corresponding structure×slice thickness]−[area of ipsilateral corresponding structure×slice thickness] (Swanson *et al.*, 1990; Liu *et al.*, 2009). The results are expressed as cubic millimeter.

MicroPET Brain Scan

The rats (n=6) were transported to the preclinical imaging facility 2 days before the microPET scans. At the three time points (1 day before surgery, 2 and 9 days post-FPI), the animals were individually anesthetized using a mixture of isoflurane and medical oxygen (3-4 % induction dose) and an intravenous bolus injection of [^{18}F]FDG (mean±s.d.:1.05±0.05 mCi) into the tail vein after overnight fasting. Then, the rat was returned to the home cage for a 40 min period of conscious (awake) uptake. After the uptake period, the rat was placed in a head-first prone position and scanned with the Triumph TM microPET/CT (LabPET-4, TriFoil Imaging, Northridge, CA, USA) under inhalatory anesthesia (2-3 % maintenance dose). Throughout these procedures, the animals were permanently kept on a pad heated to 36 ºC. For radiotracer readings, 30 min list mode static acquisitions were acquired with the field of view (FOV; 3.75 cm) centered on the rat's head. All data were reconstructed using maximum likelihood estimation method (MLEM-3D) algorithm with 20 iterations. Each reconstructed microPET image was spatially normalized into an [^{18}F]FDG template using brain normalization in PMOD v3.5 and the Fusion Toolbox (PMOD Technologies, Zurich, Switzerland). An MRI rat brain VOI template was used to overlay the normalized images, previously co-registered to the microPET image database. The glucose metabolism of 57 brain regions were expressed as standard uptake values (SUVs) (Wyckhuys *et al.*, 2014; Baptista *et al.*, 2015). For analyses at the voxel level, MINC tools (www.bic.mni.mcgill.ca/ServicesSoftware) were used for image processing and analysis.

Substrate Uptake

2-Deoxy-D-Glucose and L-Lactate Uptake

Slices (300 μm, 100-120 mg) of cerebral cortex were incubated at 37 °C with gentle shaking for 15 min in Dulbecco's buffer (in mM: 0.49 $MgCl_2$; 108.48 NaCl; 2.7 KCl; 17.68 NaH_2PO_4; 0.9 $CaCl_2$) at pH 7.4 containing one of the following: 5 mM D-glucose + 0.2 μCi 2-[U-^{14}C]-Deoxy-D-Glucose; or 10 mM L-Lactate + 0.2 μCi L-[^{14}C]-Lactate. The medium was oxygenated with 95% O_2 : 5% CO_2 throughout the incubation to prevent tissue hypoxia. After incubation, the reaction was stopped by putting the flasks on ice (4 °C). The slices were quickly washed 3 times with 1.0 mL of cold Dulbecco's buffer and 0.2 mL of 2 N NaOH solution was added to the pellet. After the tissue homogenization, 10 μL were aliquoted for protein quantification assay with BCA kit (Thermo Fisher Scientific, #23227, Rockford, IL, USA). Scintillation liquid was added

to the homogenate remaining, and the radioactivity incorporation was measured in a liquid scintillation counter (Hidex 300 SL, Mikrotek Laborsysteme, Overath, Germany) using MikroWin 300SL software (version 4.44). The radioactivity represents the uptake of 2-deoxy-glucose or L-lactate in 15 minutes/mg of protein.

L-Glutamate Uptake

Slices (300 μm, 100-120 mg) were rapidly obtained using a McIlwain Tissue Chopper and immersed in HBSS (in mM: 137 NaCl, 0.60 Na_2HPO_4, 3.0 $NaHCO_3$, 20 HEPES-Na^+, 5.0 KCl, 0.40 KH_2PO_4, 1.26 $CaCl_2$, 0.90 $MgSO_4$, and 5.55 glucose, pH 7.2) at 4 °C. Cortical slices were preincubated with HBSS at 37 °C for 15 min, followed by the addition of 0.33 μCi of L-[^{3}H]-Glutamate (Perkin Elmer, Boston, MA, USA). Incubation was stopped after 7 min with 2 ice-cold washes of 1 mL HBSS. After washing, 0.5 N NaOH was immediately added to the slices and kept over-night. Na^+ independent uptake was measured using the above-described protocol with alterations in the temperature (4 °C) and the composition of the medium (N-methyl-D-Glucamine instead of NaCl). Na^+ dependent uptake was measured as the difference between the total uptake and the Na^+-independent uptake (Thomazi *et al.*, 2004). Incorporated radioactivity was measured using a liquid scintillation counter (Hidex 300 SL, Mikrotek Laborsysteme, Overath, Germany).

Substrates Oxidation to $^{14}CO_2$

Cerebral cortex slices (300 μm, 100-120 mg) were obtained as described above, transferred into flasks and pre-incubated in Dulbecco's buffer for 30 min. Before incubation with substrates, the reaction medium was gassed with a 95% O_2: 5% CO_2 mixture for 30 seconds. Slices were incubated in 1 mL of Dulbecco's buffer containing either: (i) 5 mM D-Glucose + 0.2 μCi D-[^{14}C(U)]Glucose (American Radiolabeled Chemicals, Inc., St. Louis, MO, USA); (ii) 10 μM L-Glutamic Acid + 0.2 μCi L-[^{14}C(U)] Glutamate (PerkinElmer Boston, MA, USA); (iii) 10 μM sodium L-Lactate + 0.2 μCi L-[U-^{14}C]Lactate (American Radiolabeled Chemicals, Inc., St. Louis, MO, USA). Then, flasks containing the slices were sealed with rubber caps and parafilm, and incubated at 37 ºC for 1 hour in a Dubnoff metabolic shaker (60 cycles/min) as described previously (Dunlop *et al.*, 1975; Ferreira *et al.*, 2007). The incubation was stopped by adding 0.2 mL 50% tricarboxylic acid (TCA) through the rubber cap into the flask, while 0.1 mL of 2 N NaOH was injected into the central wells. Thereafter, flasks

were shaken for an additional 30 min at 37 ºC to trap CO_2. Afterwards, the content of the central well was transferred to vials and assayed for CO_2 radioactivity in a liquid-scintillation counter. All the results are expressed as nmol of substrate oxidized per mg of tissue and the initial specific activity of the incubation medium was considered for calculations (Muller *et al.*, 2013).

RNA extraction and quantitative RT-PCR

Total RNA was isolated from both ipsi- and contralateral cortices using TRIzol Reagent (Invitrogen, Carlsbad, CA). The concentration and purity of the RNA were determined spectrophotometrically at a ratio of 260/280. Then, 1 µg of total RNA was reverse transcribed using Applied Biosystems™ High-Capacity cDNA Reverse Transcription Kit (Applied Biosystems, Foster City, CA) in a 20 µL reaction, according to the manufacturer's instructions. GLAST (Rn00667869_m1), GLT-1 (Rn00691548_m1) and β-actin (Rn00570130_m1) mRNA levels were quantified by real-time RT-PCR using TaqMan primers and probes purchased from Applied Biosystems (#4331182, Foster City). Quantitative RT-PCR was performed in duplicate using the Applied Biosystems 7500 Fast system. As controls, a no-template and a no-reverse transcriptase were used in each assay, producing no detectable signal during 40 cycles of amplification. Therefore, target mRNA levels were normalized to β-actin levels using the $2^{-\Delta\Delta Ct}$ method (Livak and Schmittgen, 2001).

Western Blot

For protein immunocontent evaluation, cortical brain tissue from Sham and Ischemia groups were obtained 2 or 9 days after surgery. Total proteins were extracted by cellular lysis in ice-cold Lysis Buffer (4% SDS, 2 mM EDTA, 50 mM Tris-HCl pH 6.8) and standardized in SDS-PAGE sample buffer (62.5 mM Tris-HCl pH 6.8, 2% (w/v) SDS, 5% β-mercaptoethanol, 10% (v/v) glycerol, 0.002% (w/v) bromophenol blue). Samples were boiled at 95 ºC for 5 min before loading. Proteins (10 µg protein/well) were subjected to 10% acrylamide running gel and 4% acrylamide stacking gel using an Electrophoresis unit (Bio-Rad). After, proteins were transferred to a nitrocellulose membrane (GE Healthcare) and processed as follows: blocking with 5% (w/v) of skimmed milk overnight; incubation with primary polyclonal rabbit antibody overnight at 4 ºC [anti-rat MCT2 (#sc-50323, 1:200 dilution, Santa Cruz

Biotechnology); polyclonal rabbit anti-rat MCT4 (#sc-50329; 1:200 dilution, Santa Cruz Biotechnology); polyclonal rabbit anti-rat GLAST1 (#GLAST11-A, 1:5000 dilution, Alpha Diagnostics); polyclonal rabbit anti-rat GLT-1 (#GLT11-A, 1:5000 dilution, Alpha Diagnostics); and polyclonal rabbit anti-rat β-tubulin (#sc-9104, 1:1000 dilution, Santa Cruz Biotechnology)]; incubation with horseradish peroxidase-conjugated donkey anti-rabbit IgG (NA934V, 1:5000 dilution, GE Healthcare, UK) secondary antibody for 2 h; and, finally, (4) chemiluminescent bands were detected in an ImageQuant LAS4000 system (GE Healthcare) using Immobilon™ Western chemiluminescence kit (#P90720, Millipore). Both types of labeling were quantified with the ImageQuant TL software (Version 8.1, GE Healthcare). The results are expressed in percent of control levels.

Immunohistochemistry and Astrocyte Morphological Analysis

Immunohistochemistry for Glial Fibrillary Acidic Protein (GFAP) positive astrocyte was performed to evaluate morphological parameters. Briefly, brains (n=3) were divided into the following groups: Sham 2 days, Ischemia 2 days, Sham 9 days, and Ischemia 9 days. Brains were fixed for 24 h with 4% PFA diluted in phosphate buffer saline (PBS, pH 7.4), cryoprotected through immersion in sucrose solution (gradually, 15% to 30% until sank), and frozen at -20 ^{o}C. Coronal brain slices of 30 μm, approximately ranging (relative to bregma) from +2.20 mm (rostrally) to -0.80 mm (caudally), were obtained using a cryostat (MEV, SLEE Medical GMBH, Mainz, Germany). Brain slices were post-fixed with 4% PFA-PBS for 15 min, permeabilized in 0.1% triton X-100 diluted in PBS (PBS-Tx), and then blocked for 1h with 5% foetal goat serum also diluted in PBS-Tx. Histological samples were incubated for 24h at 4 ^{o}C with polyclonal rabbit anti-GFAP (Z0334, 1:500 in PBS-Tx, Dako, Glostrup, Denmark), followed by 2h incubation with goat anti-rabbit AlexaFluor® 555 secondary antibody (1:1000 in PBS-Tx, Invitrogen, Carlsbad, CA, USA). In addition, samples were stained for nuclear visualization with Hoescht 33258 (Invitrogen) accordingly to the manufacturer instructions. Images were obtained in Leica TCS SP5 II laser-scanning confocal microscopy and acquired at 8-bit gray-scale (256 gray levels) using the Leica Application Suite Advanced Fluorescence software (Leica Microsystems, Munich, Germany). The Sholl's mask creation (virtual concentric circles and orthogonal lines) and all analysis were performed using the imageJ software, a public domain Java Image processing programme (http://rsb.info.nih.gov/ij/).

All measurements were made in 3 regions of our interest (referred as Fig. 7 A, B, and C), approximately 300 μM surrounding the cortex lesion, at 2 days and 9 days post-surgery (Fig. 7A). Evaluation of cellular fluorescence intensity was performed as previously described (Mestriner *et al.*, 2015) with modifications (see supplementary data).

Statistics

In the microPET analysis, each parametric image was co-registered to a structural MRI template, images were blurred using a Gaussian kernel with a Full-Width Half-Maximum of 1.2 mm and t-statistical maps were generated (Statistical Parametric Mapping, Rminc, https://github.com/Mouse-Imaging-Centre/RMINC). In all *ex vivo* and *post mortem* analysis, brains from both Ischemia and Sham groups were separated into contra- and ipsilateral (left) hemispheres, the latter representing the ischemic side on the Ischemia group. Results from the ipsi- and contralateral hemispheres of Ischemia group were compared to the same brain hemispheres of Sham-operated controls, respectively. In addition, ischemic brains were also compared between the contra- and the ipsilateral hemisphere to determine whether the stroke had affected both brain sides. The data are expressed as mean $\pm$ S.E.M. All analyses were performed with Prism GraphPad (Version 6.01 for Windows, GraphPad Software, San Diego, CA, USA, www.graphpad.com). Differences among the groups were analyzed by *t* test, with levels of significance below $P<0.05$ indicated in the following section.

Results

FPI model decreased symmetry score and produced infarct volume

The cylinder test was performed to evaluate the sensorimotor performance of each animal and to verify the induction of the FPI model. The symmetry score decreased 2 days after FPI (Fig. 1B). On the Ischemia group, only animals with a symmetry score among 30% to 0% were selected for further analysis.

We used TTC to delineate the ischemic core region from the peri-infarct area and to assess the infarct volume. In agreement with a previous study (Hansel *et al.*, 2014), the brain infarct volume analysis by TTC staining, 2 days post-FPI, presented a large amount of tissue damage (visualized by pale staining, 119.18 ± 8.99 mm^3, n=5). Nevertheless, 9 days after the induction of ischemic injury, infarct volume measurement

was diminished when compared to the same group 2 days post-FPI, (32.0±6.42 mm^3, n=5). The Sham group did not present damage at any time point (Fig. 1C).

In vivo ^{18}F-FDG uptake is still impaired 9 days after FPI in the cortical ischemic cluster

Averaged SUV images showed consistent brain uptake of [^{18}F]FDG (Supplementary Fig. 1). Repeated measures One-way ANOVA demonstrated difference between time-points (pre, 2 and 9days) in the [^{18}F]FDG global uptake ($F_{(2, 10)}$=4.229, *P*=0.03) (Fig. 2 C, D, E). Tukey's correction revealed a reduction in the global [^{18}F]FDG uptake 2 days post-FPI if compared to pre-ischemia values ($P_{\text{-adjusted}}$=0.04). Anatomically delineated volumes of interest (VOIs) analyses, that we called Cortical Ischemic Cluster (Cortex regions: Auditory + Entorhinal + Somatosensory + Visual), demonstrated that 2 and 9 days post-FPI there is a decrease in [^{18}F]FDG uptake in ipsilateral hemisphere in relation to the contralateral (Fig. 2B, *P*=0.000 and *P*=0.010, respectively) (for a full description of VOIs, see Supplementary Fig. 2). A voxel-based analysis demonstrated a large unilateral cortico-hippocampal hypometabolic area in the 2 days post-FPI if compared with baseline values (peak $t_{(5)}$=7.9, *P*=0.0005, statistical cluster volume: 367.832 mm^3, Fig. 2C). We found a hypometabolic cortical region if compared pre-ischemia values, although smaller, 9 days post-FPI (peak $t_{(5)}$=4.8, *P*=0.005, statistical cluster volume: 41.184 mm^3, Fig. 2D). Additionally, a voxel-based analyses between 2 and 9 days [^{18}F]FDG values, demonstrated a significant recovery in the glucose metabolism (peak $t_{(5)}$=10.6, *P*=0.0001, Fig. 2E). But still, the lesioned hemisphere did not fully recover, as we observed a significant difference in the ipsilateral hemisphere 9 days post-FPI when compared to the same hemisphere baseline [^{18}F]FDG uptake measures (Fig. 2B, I: 3.00±0.09, n=6; Baseline: 3.44±0.12, n=6; *P*=0.0063).

Ex vivo substrate uptake is increased after FPI

To investigate the FPI-induced changes in substrate uptake, we performed an *ex vivo* assay for both experimental groups and analyzed ipsilateral and contralateral hemispheres separately. At 2 days post-FPI, slices from the ischemic ipsilateral cortex showed an increase in glucose uptake (Fig. 3A, I: 2.73±0.18, n=9; S: 1.70±0.13, n=5; *P*=0.002), lactate uptake (Fig. 3B, I: 8001±998.7, n=9; S: 5099±219.9, n=6; *P*=0.0373) and glutamate uptake (Fig. 3C, I: 21.14±3.17, n=5; S: 11.98±2.107, n=5; *P*=0.04) when

compared to the Sham group. In addition, lactate uptake was augmented in the ipsilateral hemisphere when compared to the contralateral at the same time point (Fig 3B, Ipsi-: 8001±998.7, n=9; Contra-: 4427±443.2, n=10; *P*=0.0035). Interestingly, glutamate uptake was also increased in the contralateral hemisphere of the Ischemia group (Fig 3C, I: 21.16±1.62, n=6; S: 13.90±1.45, n=6; *P*=0.0075), indicating that a focal ischemic insult triggers a synchronized regulation in glutamate transport between brain hemispheres in this time point. None of the aforementioned changes in substrate uptake was observed 9 days post-FPI, but we observed an increase in glutamate uptake in the ipsilateral hemisphere when compared to the contralateral in the Ischemia group (Fig. 3C, Ipsi-: 302.30±50.33, n=8; Contra-: 191.6±16.14, n=9; *P*=0.0437). Together, these findings demonstrate that FPI induced an increase in substrate uptake in the area surrounding the infarcted region in a short term after the ischemic injury and that substrate uptake changes undergo predominantly in the lesioned hemisphere.

Ex vivo substrate oxidation is augmented after FPI

To determine if the enhanced substrate uptake was correlated with increased substrate utilization for ATP production, we assayed cortical slices with radiolabeled substrates and measured $^{14}CO_2$ production. We observed that, 2 days post-FPI, all the three substrates analyzed showed an elevated oxidation rate in the cortex ipsilateral to the lesion in the Ischemia group when compared to the Sham group in the same brain hemisphere (Fig. 4A, Glucose I: 13.13±1.043, n=5; S: 8.527±1.219, n=5; *P*=0.0209; Fig. 4B, Lactate I: 0.077±0.006, n=8; S: 0.053±0.004, n=7; *P*=0.0057; Fig. 4C, Glutamate I: 5.52±0.67, n=7; 4.581±0.987, n=5; *P*=0.0065). Importantly, lactate oxidation in the Ischemia group was also augmented in the contralateral hemisphere when compared to Sham values (Fig. 4B, I: 0.050±0.004, n=6; S: 0.092±0.010, n=7; *P*=0.0053). Moreover, in the Ischemia group, glucose and glutamate metabolism were higher in the ipsilateral hemisphere when compared to the contralateral one (Fig. 4A, Glucose Ipsi-: 13.13±1.043, n=5; Contra-: 7.682±0.849, n=5; *P*=0.0037; Fig. 4C, Glutamate Ipsi-: 0.142±0.011, n=7; Contra-: 0.091±0.012, n=8; *P*=0.0089). Glucose metabolism returned to Sham levels 9 days after FPI, while glutamate and lactate utilization as energy substrate were still high in the ipsilateral hemisphere compared to the Sham group (Fig. 4C, Glutamate I: 3.666±0.270, n=7; S: 2.525±0.371, n=6; *P*=0.0279; Fig. 4B, Lactate I: 14.48±1.5, n=10; S: 9.79±0.632, n=7; *P*=0.0333). In addition, lactate and glutamate metabolism in the ipsilateral hemisphere is more

elevated than in the contralateral side (Fig. 4B, Lactate Ipsi-: 0.241±0.027, n=10; Contra-: 0.169±0.016, n=10; *P*=0.0315; Fig. 4C, Glutamate Ipsi-: 0.061±0.004, n=7; Contra-: 0.042±0.006, n=7; *P*=0.0273). As a whole, these results showed that increased oxidation of substrates can be related to increased uptake in the ipsilateral hemisphere 2 days post-FPI.

Changes in MCT and Glutamate transporters immunocontent

To verify if glutamate transporters mRNA expression matched cellular protein levels, and to evaluate MCTs immunocontent, the aforementioned brain regions were assessed through western blotting analysis. At 2 days post-FPI, MCT2 immunocontent was reduced in the contralateral hemisphere when compared to Sham animals (Fig. 5A, I: 70.97±6.42, n = 3; S: 100.0±4.40, n = 3; *P* = 0.0203), whilst it was not altered in the ipsilateral hemisphere. This alteration did not persisted to 9 days. In contrast, protein levels of MCT4 showed a tendency to increase 2 days post-FPI in the contralateral hemisphere (data not shown), with no alterations in the ipsilateral side. At 9 days post-FPI, both hemispheres presented a significant increase in MCT4 immunocontent (Fig. 5B, Ipsilateral I: 293.8±56.22, n=3; S: 100±25.8, n=3; *P*=0.0351; Contralateral I: 171.1±15.67, n=3; S: 100.0±10.81, n=3; *P*=0.0202). GLAST immunocontent was not significantly different from Sham levels at 2 days post-FPI, but showed a significant contralateral decrease at 9 days post-FPI when compared to the same hemisphere of the Sham and to the ipsi- in the same group (Fig 5C, Contralateral I: 79.21±1.75; S: 100.0±3.79, n=3; *P*=0.0076 ; Ipsilateral I: 102.40±8.54, n=3; *P*=0.056). GLT-1 presented less optical density in the ipsilateral hemisphere 2 days post-FPI (Fig. 5D, I: 65.22±3.55, n=3; S: 100.0±7.53, n=3; *P*=0.014). When analyzed at 9 days post-FPI, it still showed a decreased immunocontent tendency in the lesioned hemisphere, despite being not statistically significant (Fig. 5D). Therefore, western blot analysis also presented alterations not only in the ipsilateral hemisphere, but also in the contralateral hemisphere.

Decrease in GLAST and GLT-1 mRNA expression 2 and 9 days following FPI

To evaluate if GLAST and GLT-1 expression was related to increased glutamate uptake, real time RT-PCR was performed to quantify mRNA of these transporters. Both ipsilateral and contralateral cerebral cortices were analyzed in short (2 days) and

medium term (9 days). GLAST ipsilateral expression was decreased at 2 and 9 days post-FPI in the Ischemia group when compared to Sham (Fig. 6A, 2 days, ipsilateral I: 59.68±9.14, n=6; S: 100.0±16.09, n=6; *P*=0.05; 9 days, ipsilateral I: 59.37±9.57, n=3; S: 100.0±8.91, n=4; *P*=0.0278). Also, at 2 days post-FPI, GLAST expression was higher in the contralateral hemisphere when compared to the ipsi- in the Ischemia group (Ipsi-: 59.68±9.15, n=6; Contra-: 102.4±17.90, n=6; *P*=0.03).

GLT-1 mRNA content was also decreased in the ipsilateral (Fig. 6B, I: 51.11±11.29, n=6; S: 100.0±16.47, n=5; *P*=0.0328) and contralateral hemispheres (Fig. 6B, I: 64.25±11.41, n=6; S: 100.0±9.66; n=5; *P*=0.0379) 2 days after surgery. This decay in GLT-1 mRNA expression was also observed 9 days post-FPI in both hemispheres (ipsilateral I: 34.56±8.27, n=4; S: 100.0±18.77, n=5; *P*=0.0227; contralateral I: 47.98±11.84, n=4; S: 100.0±8.80, n=4; *P*=0.0124).

Ischemic injury promotes astroglial reactivity only in the ipsilateral hemisphere

In our study, it was analyzed the soma and processes of GFAP positive astrocytes that surround the cortical ischemic lesion in all the aforementioned regions. There was no morphological or quantitative differences between astrocytes from our 3 established regions of interest (Fig. 7A, regions: A, B, and C) within each cerebral hemisphere, *i.e.* in the ipsi- and contralateral cortices of Sham or Ischemia groups (data not shown). In a qualitative analysis, it was possible to observe a stronger GFAP immunoreactivity in the ipsilateral cortex in the 2-day and 9-day post-FPI. Primary processes that extend from astrocyte soma were more prominent in the ischemic cerebral hemisphere than the correspondent contralateral or both cerebral hemispheres of Sham group. It was also observed an increase number of ramification from primary processes (secondary processes) in these groups. In order to confirm our qualitative morphological findings, semi-quantitative and quantitative evaluations were performed to estimate the GFAP immunoreactivity and the astrocytic process changes. Indeed, the regional GFAP immunofluorescence was significantly increased in the ipsilateral cortex of 2 and 9 days post-surgical rats. (Fig 7B, 2 days, Ischemia Ipsi-: 13.22±2.054; Contra-: 33.37±1.693, n=3, *P*=0.0016; 9 days, Ischemia Ipsi-: 44.10±4.678; Contra-: 17.54±0.6448, n=3, *P*=0.0049). In the same way, cells inside attributed regions presented an increased immunoreactivity for GFAP (Fig 7C, 2 days, Ischemia Ipsi-: 118.6±3.33, n=3; Contra-:

82.45±9.74, *P*=0.0247; 9 days, Ischemia Ipsi-: 163.8±13.77; Contra-: 70.24±1.76, n=3, *P*=0.0025).

An increase in the number of total primary processes were also observed in both ipsilateral cortices of ischemic rats (Fig. 8B, 2days, Ischemia ipsi-: 5.19±0.12; Contra-: 3.28±0.24, n=3, *P*=0.0021; 9 days, Ischemia Ipsi-: 5.44±0.69; Contra-: 3.11±0.22, n=3, *P*=0.03). Consequentially, the number of total intersections in primary processes was increased in these groups (Fig. 8C, 2 days, Ischemia Ipsi-: 32.62±1.48; Contra-: 14.39±1.66, n=3, *P*=0.0012; 9 days, Ischemia Ipsi-: 35.39±5.91, n=3; Contra-: 12.61±0.49, *P*= 0.018). We also observed an increase in the number of total secondary processes in both ipsilateral cortices of ischemic rats (Fig 8D, 2 days, Ischemia Ipsi-: 3.22±0.72; Contra-: 0.55±0.05, n=3, *P*=0.0212; 9 days, Ischemia Ipsi-I: 4.33±0.92; Contra-: 1.00±0.19, n=3, *P*=0.0237). It is worthwhile to observe that the total number of primary processes and/or intersections is mainly due to an increase in the number of processes/intersections counted at central quadrants, *i.e.*, superior/inferior quadrants since no statistical significant differences were found in the number of processes/intersections counted at lateral quadrants, *i.e.*, left/right quadrants (Fig. 8E, 2 days, Ischemia Ipsi-: 2.69±0.14; Contra-: 1.33±0.19, n=3, *P*=0.0049; 9 days, Ischemia Ipsi-: 2.83±0.44; Contra-: 1.33±0.19, n=3, *P*= 0.0356; Fig 8F, 2 days, Ischemia Ipsi-: 18.53±1.51; Contra-: 5.61±0.91, n=3, *P*=0.0018; 9 days, Ischemia Ipsi-: 20.11±3.037; Contra-: 5.94±0.66, n=3, *P*=0.0103).

Discussion

Focal hypoperfusion triggers several neurochemical processes in the brain, including overproduction of lactate and excessive glutamate release. Surrounding the infarcted area, cerebral blood flow (CBF) reduction is less severe due to residual perfusion from collateral blood vessels and energy metabolism is partially preserved. This peripheral region might go through cellular changes to prevent infarct evolution. In addition, astrocytes are more resistant to the ischemic damage than neurons (Walz and Mukerji, 1990; Almeida *et al.*, 2002; Giffard and Swanson, 2005) and might be involved in recovery in both ipsi- and contralateral hemisphere (Takatsuru *et al.*, 2014). Our study provides evidence that brain energy metabolism and the glutamatergic system go through modulations somehow connected between brain hemispheres following FPI.

Importantly, we demonstrate that energy metabolism in the area around the lesion is ready to uptake and oxidize the substrates analyzed, despite the low perfusion, and that both lactate and glutamate are involved in the adaptations undergoing in the contralateral hemisphere.

The growth of the infarction at the cost of viable brain tissue is the 'natural' dynamic of permanent vessel occlusion. Nevertheless, some areas can spontaneously recover (Kunz *et al.*, 2010), as we observed *in vivo* in the microPET analysis and *ex vivo* TTC staining 9 days post-FPI. TTC is used to differentiate metabolically active from inactive tissue, being considerate a reliable and accessible marker. The colorless TTC is chemically reduced to red TPF (1.3.5-triphenylformazan) in the presence of dehydrogenases, which are most abundant in mitochondria (Altman, 1976; Kramer *et al.*, 2010). This result shows that, 9 days post-FPI induction, the infarcted area recuperated its metabolic activity. It could indicate ongoing angiogenesis or even migration of cellular progenitors and/or their proliferation (Carmichael, 2015). Meanwhile, metabolic recovery of infarcted zone does not reflect on motor improvement of the Ischemia group yet. The Ischemia group animals did not presented significant motor recovery in the cylinder test 9 days post-FPI (data not shown). The role of the intact hemisphere after focal ischemia, reviewed elsewhere (Takatsuru *et al.*, 2014), showed that functional compensation by the contralateral cortex is still occurring 1 week after injury. Only after this period, the animals can use the news synapses to present motor improvement.

Experiments in brain slices to measure uptake and oxidation demonstrated that, in the analyzed cerebral regions, 2 days post-FPI, the machinery responsible for these metabolic functions is active and able to take up substrates and produce energy. Interestingly, the metabolic rate of the ipsilateral hemisphere is augmented when compared to the contralateral side, which is the opposite of the microPET results at the same time point. The explanation for this is that *ex vivo* uptakes takes places in controlled conditions and substrate is applied directly on the slice, in contrast with the MicroPET, an *in vivo* assessment, that shows a decrease in [^{18}F]FDG uptake and metabolism because of impaired local circulation. In addition, the microPET showed that [^{18}F]FDG uptake in the cortical ischemic cluster was not fully restored 9 days post-FPI when compared to baseline measures, while glucose uptake and utilization measured in Ischemia group slices exhibit no differences from Sham group. The results

were similar among ischemia group ipsi- and contralateral hemispheres, as well. It indicates that, *in vivo*, substrate is still not available for energy production in that brain region due to constrained blood flow.

Interestingly, 2 days post-FPI, enhanced glutamate uptake coincides with increased lactate oxidation in both ipsi- and contralateral hemispheres, suggesting that glutamate-originated lactate is being used as energy source in the brain (McKenna, 2013). It is known that glutamate has an oxidation rate in astrocytes much higher than any other substrate (McKenna *et al.*, 1993; McKenna *et al.*, 1996b). In addition, a previous *in vitro* study from Sonnewald and colleagues (Sonnewald *et al.*, 1993) reported that radiolabel from glutamate metabolism was more incorporated into lactate by astrocytes than was converted to glutamine. This finding was confirmed by another work by demonstrating that when exogenous glutamate concentration was increased, the proportion of glutamate oxidized by the TCA cycle in astrocytes also increased, while conversion to glutamine decreased (McKenna *et al.*, 1996a). In our work, 9 days after induction of focal ischemic damage, glutamate and lactate oxidation rate is still elevated in the ipsilateral hemisphere, which may indicate that these substrates have a role in brain recovery. No significant changes were found in the contralateral hemisphere in this time point (9 days).

The MCT protein contents are regulated at the transcriptional level, but more markedly at the translational level (Halestrap, 2013). Under hypoxic conditions, MCT4 expression is upregulated through, most likely, the transcription factor hypoxia-inducible factor-1α (HIF-1α), since its expression was linked to oxygen tension (Singh *et al.*, 2012; Rosafio and Pellerin, 2014; Bergersen, 2015). In our work, 2 days post-FPI the MCT4 expression was increased only in the contralateral hemisphere, showing that the ipsilateral cortex could not respond to the extended damage so fast with changes in MCT4 expression. Also, seems that HIF-1α is a component of recovery by the intact hemisphere. Wiener and colleagues (Wiener *et al.*, 1996) reported that brain FPI increases mRNA encoding for HIF-1α in the penumbra region (Bergeron *et al.*, 1999). Our results may indicate that HIF-1α could have a more prolonged signaling effect in permanent ischemia.

In contrast, MCT2 expression is not influenced by HIF-1α and is mostly expressed in neurons, notably in neutrophil associated with neuronal processes and spines (Pierre *et al.*, 2002; Bergersen, 2015). We observed a decrease in MCT2 immunocontent 2 days

post-FPI in the contralateral hemisphere, but not in the ipsilateral, thus arguing for a specific decrease in protein levels. Interestingly, it was reported that, in a transient model of cerebral ischemia, MCT4 was found in neurons 24h after reperfusion, although it was considered an exclusive astrocytic transporter under physiological conditions (Bergersen *et al.*, 2002; Rafiki *et al.*, 2003; Pellerin *et al.*, 2005). It is know that MCT4 present an elevated Km (30 mmol/L), while MCT2 does not (1 mmol/L), suggesting that MCT4 transport would increase with substrate availability. Thus, the hypothesis that MCT4 expression might play an important role for neurons to achieve a new metabolic state following ischemia in the contralateral hemisphere, while MCT2 is not available, is interesting and worth investigating.

One of the most essential roles of astrocytes in the brain is removal of glutamate from the synaptic cleft by performing its uptake, which is an energetically expensive process (Danbolt, 2001; McKenna, 2007; Kreft *et al.*, 2012). Here, we observed a paradoxal decrease in glutamate transporters expression and protein levels, accompanied by increased activity (uptake). These results reveal that increased glutamate uptake is not necessarily followed by an increase in transporter expression after focal ischemia. Moreover, the loss of glutamate transporters may not account for the loss in their functional activity and, besides, cortical slices stabilized in proper buffering can have its uptake capability restored, since glutamate uptake is dependent on Na^+/K^+ gradient (Anderson and Swanson, 2000; Danbolt, 2001). It is also important to consider that increased glutamate availability in the extracellular space, like expected in a short term after FPI, might potentiate GLT-1 function, since glutamate is a very effective agonist (Takatsuru *et al.*, 2014). Previous studies have shown that neurons are directly involved in regulating the expression of both GLT-1 and GLAST (Gegelashvili *et al.*, 1997; Swanson *et al.*, 1997; Schlag *et al.*, 1998). Thus, downregulation of these transporters can be a consequence of glutamate-induced neuronal death or the reduction of synaptic activity in both brain hemispheres in the areas analyzed. Our results showed that FPI alters not only GLT-1 expression in the lesioned hemisphere, but the intact one as well at 2 and 9 days following injury. Interestingly, GLT-1 immunocontent remained similar to Sham controls in the contralateral side in these time points, indicating a more complex mechanism to regulate both mRNA expression and protein levels of this latter transporter, with needs to be further investigated. Furthermore, our data indicate that regulation at expression levels are connected between brain hemispheres and GLT-1

might play a role in response to ischemic damage in the intact hemisphere. On the other hand, GLAST mRNA expression was diminished in the ipsilateral hemisphere, while its protein levels was similar to Sham control in both time points, pointing for a distinct regulation mechanism for this transporter. A study by Sullivan and colleagues (Sullivan *et al.*, 2007) suggested an essential role for GFAP in regulating glutamate transporter trafficking and function by retaining GLAST in the plasma-membrane after an hypoxic insult (Middeldorp and Hol, 2011; Nijboer *et al.*, 2013), which could explain the conservation of its immunocontent between experimental groups found 2 and 9 days post-surgery, since our data indicated overexpression of GFAP in the lesioned hemisphere of Ischemia group in both time points. At 9 days post-FPI, we observed decreased GLAST immunocontent in the contralateral side when compared to the other brain hemisphere or to the same area of the Sham. That may indicate that, after cerebral ischemia, greater expression of GFAP is needed to keep GLAST anchored in the plasma membrane. Further investigation should clarify the mechanism behind such findings.

GFAP has been shown to be involved in astrocyte functions, which are important during regeneration, synaptic plasticity and reactive gliosis (Middeldorp and Hol, 2011). Tanaka et al. (Tanaka *et al.*, 2002) suggested that neuronal death is increased when GFAP is absent in injury conditions. Therefore, GFAP may play a crucial role in neuronal survival after injury and astrocytes normally have a protective function in the progress of ischemic brain damage (Middeldorp and Hol, 2011). Our data showed that (i) astrocytes overexpressed GFAP; and (ii) the number of primary processes of astrocytes account for the significant changes observed in cell morphology, thus showing a more radial symmetry on the ipsilateral astroglia of the Ischemia group. Together, this reflects reactivity in astrocytes from the Ischemia group and an important morphological change when compared to that observed in astrocytes from the correspondent contralateral hemisphere or both cerebral hemispheres of Sham rats. Another work involving experimental ischemic stroke in adult mice showed the development of larger infarcts in GFAP-/-Vim-/- mice when compared to wild-type mice (Li *et al.*, 2008). This suggests that, in the adult, reactive astrocytes are important for the protection of the ischemic penumbral region, mostly through effective elimination of glutamate and reactive oxygen species (Li *et al.*, 2008; de Pablo *et al.*, 2013) or by effective regulatory volume decrease that in brain ischemia counteracts the development of edema (Ding *et al.*, 1998). Nevertheless, the mechanisms linking GFAP

to the response of reactive astrocytes in pathological situations remain understood. Despite many reports of a deleterious role, reactive astrocytes might also contribute to neuroprotection (Barreto *et al.*, 2011). Our data suggest that overexpressing GFAP, increasing glutamate transporters activity and transport of energy substrates might be the mechanisms behind such pro-recovery role of astroglia.

Experimental models of transient ischemia can be very useful, especially to assess cellular and molecular mechanisms behind reperfusion damage. However, in the clinic, cerebral ischemia in humans is most likely permanent (Yu *et al.*, 2015), which reduces the time window for treatment and salvage of the penumbral region. Despite significant progress in patient care, therapeutic options for stroke victims are limited, and only a small percentage of patients are treated with thrombolysis or by an endovascular approach (Krzyzanowska *et al.*, 2016), making the usage of permanent occlusion models more similar to the human pathology. In this work, our results presented new evidence that the whole brain is affected by focal ischemic damage, causing modulations mostly through cellular protein expression, substrates availability and utilization, astrocytic parameters and the glutamate transporters. Some changes persist or appear only latter after FPI injury. Also, we observed a connection between the glutamatergic system and lactate metabolism through the connectivity between the ipsi- and contralateral hemispheres. These significant changes support the hypothesis of metabolic reprogramming occurring after ischemic injury and appear to promote recovery and adaptation, offering a therapeutic target to reduce adverse outcomes of stroke in human patients.

Funding

This work was supported by the Science Without Borders Program (88881.030387/2013-1), Conselho Nacional de Desenvolvimento Científico e Tecnológico (CNPq), Coordenação de Aperfeiçoamento de Pessoal de Nível Superior (CAPES), Fundação de Amparo à Pesquisa do Estado do Rio Grande do Sul (FAPERGS) e Instituto Nacional de Ciência e Tecnologia para Excitotoxicidade e Neuroproteção (573577/2008-5).

Conflict of Interest None.

References

Allen NJ, Attwell D. Modulation of ASIC channels in rat cerebellar Purkinje neurons by ischaemia-related signals. The Journal of physiology 2002; 543(Pt 2): 521-9.

Almeida A, Delgado-Esteban M, Bolanos JP, Medina JM. Oxygen and glucose deprivation induces mitochondrial dysfunction and oxidative stress in neurones but not in astrocytes in primary culture. Journal of neurochemistry 2002; 81(2): 207-17.

Altman FP. Tetrazolium salts and formazans. Progress in histochemistry and cytochemistry 1976; 9(3): 1-56.

Anderson CM, Swanson RA. Astrocyte glutamate transport: review of properties, regulation, and physiological functions. Glia 2000; 32(1): 1-14.

Baptista PP, Saur L, Bagatini PB, Greggio S, Venturin GT, Vaz SP, *et al.* Antidepressant Effects of Ketamine Are Not Related to (1)(8)F-FDG Metabolism or Tyrosine Hydroxylase Immunoreactivity in the Ventral Tegmental Area of Wistar Rats. Neurochemical research 2015; 40(6): 1153-64.

Barreto G, White RE, Ouyang Y, Xu L, Giffard RG. Astrocytes: targets for neuroprotection in stroke. Central nervous system agents in medicinal chemistry 2011; 11(2): 164-73.

Bergeron M, Yu AY, Solway KE, Semenza GL, Sharp FR. Induction of hypoxia-inducible factor-1 (HIF-1) and its target genes following focal ischaemia in rat brain. The European journal of neuroscience 1999; 11(12): 4159-70.

Bergersen L, Rafiki A, Ottersen OP. Immunogold cytochemistry identifies specialized membrane domains for monocarboxylate transport in the central nervous system. Neurochemical research 2002; 27(1-2): 89-96.

Bergersen LH. Lactate transport and signaling in the brain: potential therapeutic targets and roles in body-brain interaction. Journal of cerebral blood flow and metabolism : official journal of the International Society of Cerebral Blood Flow and Metabolism 2015; 35(2): 176-85.

Berthet C, Castillo X, Magistretti PJ, Hirt L. New evidence of neuroprotection by lactate after transient focal cerebral ischaemia: extended benefit after intracerebroventricular injection and efficacy of intravenous administration. Cerebrovascular diseases (Basel, Switzerland) 2012; 34(5-6): 329-35.

Berthet C, Lei H, Thevenet J, Gruetter R, Magistretti PJ, Hirt L. Neuroprotective role of lactate after cerebral ischemia. Journal of cerebral blood flow and metabolism : official journal of the International Society of Cerebral Blood Flow and Metabolism 2009; 29(11): 1780-9.

Bidmon HJ, Jancsik V, Schleicher A, Hagemann G, Witte OW, Woodhams P*, et al.* Structural alterations and changes in cytoskeletal proteins and proteoglycans after focal cortical ischemia. Neuroscience 1998; 82(2): 397-420.

Calautti C, Baron JC. Functional neuroimaging studies of motor recovery after stroke in adults: a review. Stroke; a journal of cerebral circulation 2003; 34(6): 1553-66.

Carmichael ST. Targets for neural repair therapies after stroke. Stroke; a journal of cerebral circulation 2010; 41(10 Suppl): S124-6.

Carmichael ST. The 3 Rs of Stroke Biology: Radial, Relayed, and Regenerative. Neurotherapeutics : the journal of the American Society for Experimental NeuroTherapeutics 2015.

Castillo X, Rosafio K, Wyss MT, Drandarov K, Buck A, Pellerin L*, et al.* A probable dual mode of action for both L- and D-lactate neuroprotection in cerebral ischemia. Journal of cerebral blood flow and metabolism : official journal of the International Society of Cerebral Blood Flow and Metabolism 2015; 35(10): 1561-9.

Chollet F, DiPiero V, Wise RJ, Brooks DJ, Dolan RJ, Frackowiak RS. The functional anatomy of motor recovery after stroke in humans: a study with positron emission tomography. Annals of neurology 1991; 29(1): 63-71.

Danbolt NC. Glutamate uptake. Progress in neurobiology 2001; 65(1): 1-105.

de Pablo Y, Nilsson M, Pekna M, Pekny M. Intermediate filaments are important for astrocyte response to oxidative stress induced by oxygen-glucose deprivation and reperfusion. Histochemistry and cell biology 2013; 140(1): 81-91.

de Vasconcelos Dos Santos A, da Costa Reis J, Diaz Paredes B, Moraes L, Jasmin, Giraldi-Guimaraes A*, et al.* Therapeutic window for treatment of cortical ischemia with bone marrow-derived cells in rats. Brain research 2010; 1306: 149-58.

Debernardi R, Pierre K, Lengacher S, Magistretti PJ, Pellerin L. Cell-specific expression pattern of monocarboxylate transporters in astrocytes and neurons observed in different mouse brain cortical cell cultures. Journal of neuroscience research 2003; 73(2): 141-55.

Demaerschalk BM, Hwang HM, Leung G. US cost burden of ischemic stroke: a systematic literature review. The American journal of managed care 2010; 16(7): 525-33.

Di Carlo A. Human and economic burden of stroke. Age and Ageing 2009; 38(1): 4-5.

Dimlich RV, Nielsen MM. Facilitating postischemic reduction of cerebral lactate in rats. Stroke; a journal of cerebral circulation 1992; 23(8): 1145-52; discussion 52-3.

Ding M, Eliasson C, Betsholtz C, Hamberger A, Pekny M. Altered taurine release following hypotonic stress in astrocytes from mice deficient for GFAP and vimentin. Brain research Molecular brain research 1998; 62(1): 77-81.

Dobkin B. Rehabilitation after stroke. New England Journal of Medicine; 2005. p. 1677-84.

Dunlop DS, van Elden W, Lajtha A. Optimal conditions for protein synthesis in incubated slices of rat brain. Brain Res 1975; 99(2): 303-18.

Ferreira GC, Tonin A, Schuck PF, Viegas CM, Ceolato PC, Latini A*, et al.* Evidence for a synergistic action of glutaric and 3-hydroxyglutaric acids disturbing rat brain energy metabolism. International journal of developmental neuroscience : the official journal of the International Society for Developmental Neuroscience 2007; 25(6): 391-8.

Gegelashvili G, Danbolt NC, Schousboe A. Neuronal soluble factors differentially regulate the expression of the GLT1 and GLAST glutamate transporters in cultured astroglia. Journal of neurochemistry 1997; 69(6): 2612-5.

Giffard RG, Swanson RA. Ischemia-induced programmed cell death in astrocytes. Glia 2005; 50(4): 299-306.

Giraldi-Guimardes A, Rezende-Lima M, Bruno FP, Mendez-Otero R. Treatment with bone marrow mononuclear cells induces functional recovery and decreases neurodegeneration after sensorimotor cortical ischemia in rats. Brain research 2009; 1266: 108-20.

Go AS, Mozaffarian D, Roger VL, Benjamin EJ, Berry JD, Blaha MJ*, et al.* Executive summary: heart disease and stroke statistics--2014 update: a report from the American Heart Association. Circulation 2014; 129(3): 399-410.

Go AS, Mozaffarian D, Roger VL, Benjamin EJ, Berry JD, Blaha MJ*, et al.* Heart Disease and Stroke Statistics—2014 Update: A Report From the American Heart Association. Circulation 2013.

Halestrap AP. The SLC16 gene family - structure, role and regulation in health and disease. Molecular aspects of medicine 2013; 34(2-3): 337-49.

Hansel G, Ramos DB, Delgado CA, Souza DG, Almeida RF, Portela LV*, et al.* The potential therapeutic effect of guanosine after cortical focal ischemia in rats. PLoS One 2014; 9(2): e90693.

Hansel G, Tonon AC, Guella FL, Pettenuzzo LF, Duarte T, Duarte MM*, et al.* Guanosine Protects Against Cortical Focal Ischemia. Involvement of Inflammatory Response. Molecular neurobiology 2015; 52(3): 1791-803.

Hillered L, Hallstrom A, Segersvard S, Persson L, Ungerstedt U. Dynamics of extracellular metabolites in the striatum after middle cerebral artery occlusion in the rat monitored by intracerebral microdialysis. Journal of cerebral blood flow and metabolism : official journal of the International Society of Cerebral Blood Flow and Metabolism 1989; 9(5): 607-16.

Kim AS, Johnston SC. Global Variation in the Relative Burden of Stroke and Ischemic Heart Disease. Circulation 2011; 124(3): 314-23.

Kramer M, Dang J, Baertling F, Denecke B, Clarner T, Kirsch C*, et al.* TTC staining of damaged brain areas after MCA occlusion in the rat does not constrict quantitative gene and protein analyses. Journal of neuroscience methods 2010; 187(1): 84-9.

Kreft M, Bak LK, Waagepetersen HS, Schousboe A. Aspects of astrocyte energy metabolism, amino acid neurotransmitter homoeostasis and metabolic compartmentation. ASN NEURO 2012; 4(3): e00086.

Krzyzanowska W, Pomierny B, Budziszewska B, Filip M, Pera J. N-Acetylcysteine and Ceftriaxone as Preconditioning Strategies in Focal Brain Ischemia: Influence on Glutamate Transporters Expression. Neurotoxicity research 2016.

Kunz A, Dirnagl U, Mergenthaler P. Acute pathophysiological processes after ischaemic and traumatic brain injury. Best practice & research Clinical anaesthesiology 2010; 24(4): 495-509.

Li L, Lundkvist A, Andersson D, Wilhelmsson U, Nagai N, Pardo AC*, et al.* Protective role of reactive astrocytes in brain ischemia. Journal of cerebral blood flow and metabolism : official journal of the International Society of Cerebral Blood Flow and Metabolism 2008; 28(3): 468-81.

Liu S, Zhen G, Meloni BP, Campbell K, Winn HR. RODENT STROKE MODEL GUIDELINES FOR PRECLINICAL STROKE TRIALS (1ST EDITION). Journal of experimental stroke & translational medicine 2009; 2(2): 2-27.

Livak KJ, Schmittgen TD. Analysis of relative gene expression data using real-time quantitative PCR and the 2(-Delta Delta C(T)) Method. Methods (San Diego, Calif) 2001; 25(4): 402-8.

Lloyd-Jones D, Adams R, Carnethon M, De Simone G, Ferguson TB, Flegal K*, et al.* Heart Disease and Stroke Statistics—2009 Update: A Report From the American Heart Association Statistics Committee and Stroke Statistics Subcommittee. Circulation 2009; 119(3): e21-e181.

Macrae IM. Preclinical stroke research--advantages and disadvantages of the most common rodent models of focal ischaemia. British journal of pharmacology 2011; 164(4): 1062-78.

Malarkey EB, Parpura V. Mechanisms of glutamate release from astrocytes. Neurochemistry international 2008; 52(1-2): 142-54.

McKenna MC. The glutamate-glutamine cycle is not stoichiometric: fates of glutamate in brain. Journal of neuroscience research 2007; 85(15): 3347-58.

McKenna MC. Glutamate pays its own way in astrocytes. Front Endocrinol (Lausanne) 2013; 4: 191.

McKenna MC, Sonnewald U, Huang X, Stevenson J, Zielke HR. Exogenous glutamate concentration regulates the metabolic fate of glutamate in astrocytes. Journal of neurochemistry 1996a; 66(1): 386-93.

McKenna MC, Tildon JT, Stevenson JH, Boatright R, Huang S. Regulation of energy metabolism in synaptic terminals and cultured rat brain astrocytes: differences revealed using aminooxyacetate. Developmental neuroscience 1993; 15(3-5): 320-9.

McKenna MC, Tildon JT, Stevenson JH, Huang X. New insights into the compartmentation of glutamate and glutamine in cultured rat brain astrocytes. Developmental neuroscience 1996b; 18(5-6): 380-90.

Mestriner RG, Saur L, Bagatini PB, Baptista PP, Vaz SP, Ferreira K*, et al.* Astrocyte morphology after ischemic and hemorrhagic experimental stroke has no influence on the different recovery patterns. Behavioural brain research 2015; 278: 257-61.

Middeldorp J, Hol EM. GFAP in health and disease. Progress in neurobiology 2011; 93(3): 421-43.

Muller AP, Longoni A, Farina M, da Silveira CK, Souza DO, Perry ML*, et al.* Propylthiouracil-induced hypothyroidism during lactation alters leucine and mannose metabolism in rat cerebellar slices. Experimental biology and medicine (Maywood, NJ) 2013; 238(1): 31-6.

Nijboer CH, Heijnen CJ, Degos V, Willemen HL, Gressens P, Kavelaars A. Astrocyte GRK2 as a novel regulator of glutamate transport and brain damage. Neurobiology of disease 2013; 54: 206-15.

Paxinos G, Watson C. The rat brain in stereotaxic coordinates. 6th ed. Amsterdam ; Oxford: Elsevier Academic; 2007.

Pellerin L, Bergersen LH, Halestrap AP, Pierre K. Cellular and subcellular distribution of monocarboxylate transporters in cultured brain cells and in the adult brain. Journal of neuroscience research 2005; 79(1-2): 55-64.

Pierre K, Magistretti PJ, Pellerin L. MCT2 is a major neuronal monocarboxylate transporter in the adult mouse brain. J Cereb Blood Flow Metab 2002; 22(5): 586-95.

Pierre K, Pellerin L, Debernardi R, Riederer BM, Magistretti PJ. Cell-specific localization of monocarboxylate transporters, MCT1 and MCT2, in the adult mouse brain revealed by double immunohistochemical labeling and confocal microscopy. Neuroscience 2000; 100(3): 617-27.

Rafiki A, Boulland JL, Halestrap AP, Ottersen OP, Bergersen L. Highly differential expression of the monocarboxylate transporters MCT2 and MCT4 in the developing rat brain. Neuroscience 2003; 122(3): 677-88.

Rosafio K, Castillo X, Hirt L, Pellerin L. Cell-specific modulation of monocarboxylate transporter expression contributes to the metabolic reprograming taking place following cerebral ischemia. Neuroscience 2016; 317: 108-20.

Rosafio K, Pellerin L. Oxygen tension controls the expression of the monocarboxylate transporter MCT4 in cultured mouse cortical astrocytes via a hypoxia-inducible factor-1alpha-mediated transcriptional regulation. Glia 2014; 62(3): 477-90.

Rossi DJ, Brady JD, Mohr C. Astrocyte metabolism and signaling during brain ischemia. Nature neuroscience 2007; 10(11): 1377-86.

Rothstein JD, Martin L, Levey AI, Dykes-Hoberg M, Jin L, Wu D*, et al.* Localization of neuronal and glial glutamate transporters. Neuron 1994; 13(3): 713-25.

Schallert T. Behavioral tests for preclinical intervention assessment. NeuroRx : the journal of the American Society for Experimental NeuroTherapeutics 2006; 3(4): 497-504.

Schlag BD, Vondrasek JR, Munir M, Kalandadze A, Zelenaia OA, Rothstein JD*, et al.* Regulation of the glial Na+-dependent glutamate transporters by cyclic AMP analogs and neurons. Molecular pharmacology 1998; 53(3): 355-69.

Schurr A. Energy metabolism, stress hormones and neural recovery from cerebral ischemia/hypoxia. Neurochemistry international 2002; 41(1): 1-8.

Schurr A, Payne RS, Miller JJ, Rigor BM. Brain lactate is an obligatory aerobic energy substrate for functional recovery after hypoxia: further in vitro validation. Journal of neurochemistry 1997a; 69(1): 423-6.

Schurr A, Payne RS, Miller JJ, Rigor BM. Brain lactate, not glucose, fuels the recovery of synaptic function from hypoxia upon reoxygenation: an in vitro study. Brain research 1997b; 744(1): 105-11.

Schurr A, Payne RS, Miller JJ, Tseng MT, Rigor BM. Blockade of lactate transport exacerbates delayed neuronal damage in a rat model of cerebral ischemia. Brain research 2001; 895(1-2): 268-72.

Schurr A, Rigor BM. Brain anaerobic lactate production: a suicide note or a survival kit? Developmental neuroscience 1998; 20(4-5): 348-57.

Sholl DA. Dendritic organization in the neurons of the visual and motor cortices of the cat. Journal of anatomy 1953; 87(4): 387-406.

Simpson IA, Carruthers A, Vannucci SJ. Supply and demand in cerebral energy metabolism: the role of nutrient transporters. Journal of cerebral blood flow and metabolism : official journal of the International Society of Cerebral Blood Flow and Metabolism 2007; 27(11): 1766-91.

Singh N, Sharma G, Mishra V. Hypoxia inducible factor-1: its potential role in cerebral ischemia. Cellular and molecular neurobiology 2012; 32(4): 491-507.

Sonnewald U, Westergaard N, Petersen SB, Unsgard G, Schousboe A. Metabolism of [U-13C]glutamate in astrocytes studied by 13C NMR spectroscopy: incorporation of more label into lactate than into glutamine demonstrates the importance of the tricarboxylic acid cycle. Journal of neurochemistry 1993; 61(3): 1179-82.

Sullivan SM, Lee A, Bjorkman ST, Miller SM, Sullivan RK, Poronnik P*, et al.* Cytoskeletal anchoring of GLAST determines susceptibility to brain damage: an identified role for GFAP. The Journal of biological chemistry 2007; 282(40): 29414-23.

Swanson RA, Liu J, Miller JW, Rothstein JD, Farrell K, Stein BA*, et al.* Neuronal regulation of glutamate transporter subtype expression in astrocytes. The Journal of neuroscience : the official journal of the Society for Neuroscience 1997; 17(3): 932-40.

Swanson RA, Morton MT, Tsao-Wu G, Savalos RA, Davidson C, Sharp FR. A semiautomated method for measuring brain infarct volume. Journal of cerebral blood flow and metabolism : official journal of the International Society of Cerebral Blood Flow and Metabolism 1990; 10(2): 290-3.

Swanson RA, Ying W, Kauppinen TM. Astrocyte influences on ischemic neuronal death. Current molecular medicine 2004; 4(2): 193-205.

Szele FG, Alexander C, Chesselet MF. Expression of molecules associated with neuronal plasticity in the striatum after aspiration and thermocoagulatory lesions of the cerebral cortex in adult rats. The Journal of neuroscience : the official journal of the Society for Neuroscience 1995; 15(6): 4429-48.

Takatsuru Y, Nabekura J, Koibuchi N. Contribution of neuronal and glial circuit in intact hemisphere for functional remodeling after focal ischemia. Neuroscience research 2014; 78: 38-44.

Tanaka H, Katoh A, Oguro K, Shimazaki K, Gomi H, Itohara S*, et al.* Disturbance of hippocampal long-term potentiation after transient ischemia in GFAP deficient mice. Journal of neuroscience research 2002; 67(1): 11-20.

Thomazi AP, Godinho GF, Rodrigues JM, Schwalm FD, Frizzo ME, Moriguchi E*, et al.* Ontogenetic profile of glutamate uptake in brain structures slices from rats: sensitivity to guanosine. Mech Ageing Dev 2004; 125(7): 475-81.

Walz W, Harold DE. Brain lactic acidosis and synaptic function. Canadian journal of physiology and pharmacology 1990; 68(2): 164-9.

Walz W, Mukerji S. Simulation of aspects of ischemia in cell culture: changes in lactate compartmentation. Glia 1990; 3(6): 522-8.

Wiener CM, Booth G, Semenza GL. In vivo expression of mRNAs encoding hypoxia-inducible factor 1. Biochemical and biophysical research communications 1996; 225(2): 485-8.

Wittenberg GF, Chen R, Ishii K, Bushara KO, Eckloff S, Croarkin E*, et al.* Constraint-induced therapy in stroke: magnetic-stimulation motor maps and cerebral activation. Neurorehabil Neural Repair 2003; 17(1): 48-57.

Wyckhuys T, Wyffels L, Langlois X, Schmidt M, Stroobants S, Staelens S. The [18F]FDG muPET readout of a brain activation model to evaluate the metabotropic glutamate receptor 2 positive allosteric modulator JNJ-42153605. The Journal of pharmacology and experimental therapeutics 2014; 350(2): 375-86.

Yasuda Y, Tateishi N, Shimoda T, Satoh S, Ogitani E, Fujita S. Relationship between S100beta and GFAP expression in astrocytes during infarction and glial scar formation after mild transient ischemia. Brain research 2004; 1021(1): 20-31.

Yu M, Xue Y, Liang W, Zhang Y, Zhang Z. Protection mechanism of early hyperbaric oxygen therapy in rats with permanent cerebral ischemia. Journal of physical therapy science 2015; 27(10): 3271-4.

Zhang R, Chopp M, Zhang ZG. Oligodendrogenesis after cerebral ischemia. Frontiers in cellular neuroscience 2013; 7: 201.

Zhao Y, Rempe DA. Targeting astrocytes for stroke therapy. Neurotherapeutics : the journal of the American Society for Experimental NeuroTherapeutics 2010; 7(4): 439-51.

Figure legends

Fig. 1. FPI model reduced symmetry score and produced infarct volume in TTC stain. (A) Timeline indicating the experimental design. (B) Symmetry score differences between groups 2 and 9 days post-FPI; *** representing $P<0.001$ (t test, n=10 per group). Data expressed as mean±S.E.M. (C) Representative TTC-stained FPI-injuried brain at 2 and 9 days post-ischemia compared to a Sham control. The corresponding position mapped to the bregma is showed taken from Paxinos and Watson, 2007.

Fig. 2. MicroPET [^{18}F]FDG uptake presented decreased ipsilateral activity 2 and 9 days post-FPI in the cortical ischemic cluster compared to baseline. (A) Schematic illustration of anesthesia and measurement schedule of each animal. (B) Cortical Ischemic Cluster representing the *ex vivo* analyzed area in all time points., *** representing $P<0.001$, (t test). (C) Comparison between baseline and 2 days post-FPI measurements on [^{18}F]FDG uptake. Red color representing bigger statistical significance, $P=0.0005$ (t-statistical map). (D) 9 days post-FPI [^{18}F]FDG uptake, showing a hypometabolic cortical region when compared baseline values, $P=0.005$ (t-statistical map). (E) Voxel-based analyses between 2 and 9 days [^{18}F]FDG uptake values, demonstrating a significant recovery in the glucose metabolism accounting for the whole brain, $P=0.0001$ (t-statistical map).

Fig. 3. *Ex vivo* substrate uptake is modulated by focal ischemic damage mostly in the ipsilateral hemisphere. (A) Short term increase in glucose uptake in the ipsilateral hemisphere. ** representing $P<0.01$ (t test). (B) Enhanced lactate uptake in the ipsilateral hemisphere when compared to the same hemisphere of Sham, * representing $P<0.05$ (t test); and when compared to the contralateral in the same group ** representing $P<0.01$ (t test). (C) Glutamate uptake increased in both ischemic brain hemispheres 2 days post-FPI, while only in the ipsilateral this alteration persisted till 9 days. * representing $P<0.05$ (t test). All data expressed as mean±S.E.M.

Fig. 4. Enhanced substrate oxidation to $^{14}CO_2$ after FPI mostly in the ischemic hemisphere. (A) 2 days post-FPI, glucose utilization is higher in the ipsilateral hemisphere when compared to the same hemisphere of the Sham, * representing $P<0.05$ (t test); and to the contralateral on the same group, ** representing $P<0.01$ (t test). (B) Increased lactate oxidation in both brain hemispheres 2 days post-FPI. Latter, at 9 days, there is still ipsilateral hypermetabolism. * representing $P<0.05$ (t test). **

representing $P<0.01$ (t test). (C) Enhanced ipsilateral glutamate oxidation that continued till 9 days post-FPI when compared to Sham and to the contralateral hemisphere in the same group. * representing $P<0.05$ (t test). ** representing $P<0.01$ (t test).

Fig. 5. Western blot analysis on transporters immunocontent. (A) Reduced contralateral MCT2 immunocontent in ischemia group at 2 days post-FPI. * representing $P<0.05$ (t test). (B) Increased contralateral MCT4 immunocontent 2 days post-FPI. At 9 days, protein levels were still high in the contralateral, but also elevated in the ipsilateral hemisphere when compared to the same hemisphere of the Sham * representing $P<0.05$ (t test). (C) GLAST protein levels diminished contralateraly in ischemia group at 9 days post-FPI. * representing $P<0.05$ (t test). ** representing $P<0.01$ (t test). (D) Lower levels of GLT-1 immunocontent were found in the ipsilateral hemisphere of Ischemia group in both time points when compared to the same hemisphere of the Sham (2 and 9 days) and when compared to the contralateral hemisphere in the same group (9 days). * representing $P<0.05$ (t test). Data expressed as mean$\pm$S.E.M. (percentage of control).

Fig. 6. Decreased mRNA expression of astrocytic glutamate transporters GLAST and GLT-1 at 2 and 9 days post-FPI. (A) Ipsilateral GLAST expression was diminished when compared to the same hemisphere of sham group in both time points. * representing $P<0.05$ (t test). (B) GLT-1 expression in both brain hemispheres was decreased when compared to Sham, and this alteration persisted to 9 days post-FPI. * representing $P<0.05$ (t test). All data expressed as mean$\pm$S.E.M (percentage of control).

Fig. 7. GFAP is overexpressed in ipsilateral astrocytes post-FPI. (A) Brain slice amplified field demonstrating our regions of interest (adapted from Paxinos and Watson, 2007) in the ipsi- (*blue*) and contralateral (*red*) hemispheres. (B) Regional immunofluorescence for GFAP (gray values). ** representing $P<0.01$ (t test). (C) Cellular immunofluorescence of GFAP (gray values). * representing $P<0.05$ (t test). ** representing $P<0.01$ (t test). (D) Representative morphological changes were evident in ipsilateral astrocytes in the 2-day and 9-day post-surgical rats. All data expressed as mean$\pm$S.E.M. Scale bar: 20 μm.

Fig. 8. Primary and secondary astrocytic processes analysis. Evaluation of cell morphology by Sholl's analysis (Sholl, 1953), (A) Example of astrocyte with overlaid virtual concentric circles and lines used to Sholl's analysis. (B) Number of total primary

processes and (C) total number of intersections counted for primary processes. * representing $P<0.05$ (t test). ** representing $P<0.01$ (t test). (D) Total number of secondary processes. * representing $P<0.05$ (t test). (E) Number of central and lateral primary processes of astrocytes and (F) intersections.* representing $P<0.05$, ** representing $P<0.01$ (t test). All data expressed as mean±S.E.M.

Supplementary Fig. 1. Averaged SUV images showing consistent [^{18}F]FDG uptake in (A) 1 day before surgery, (B) 2 days and (C) 9 days post-FPI .

Supplementary Fig. 2. All brain regions analyzed assessed by MicroPET statistics (A-L). All data expressed as mean±S.E.M.

Fig. 1.

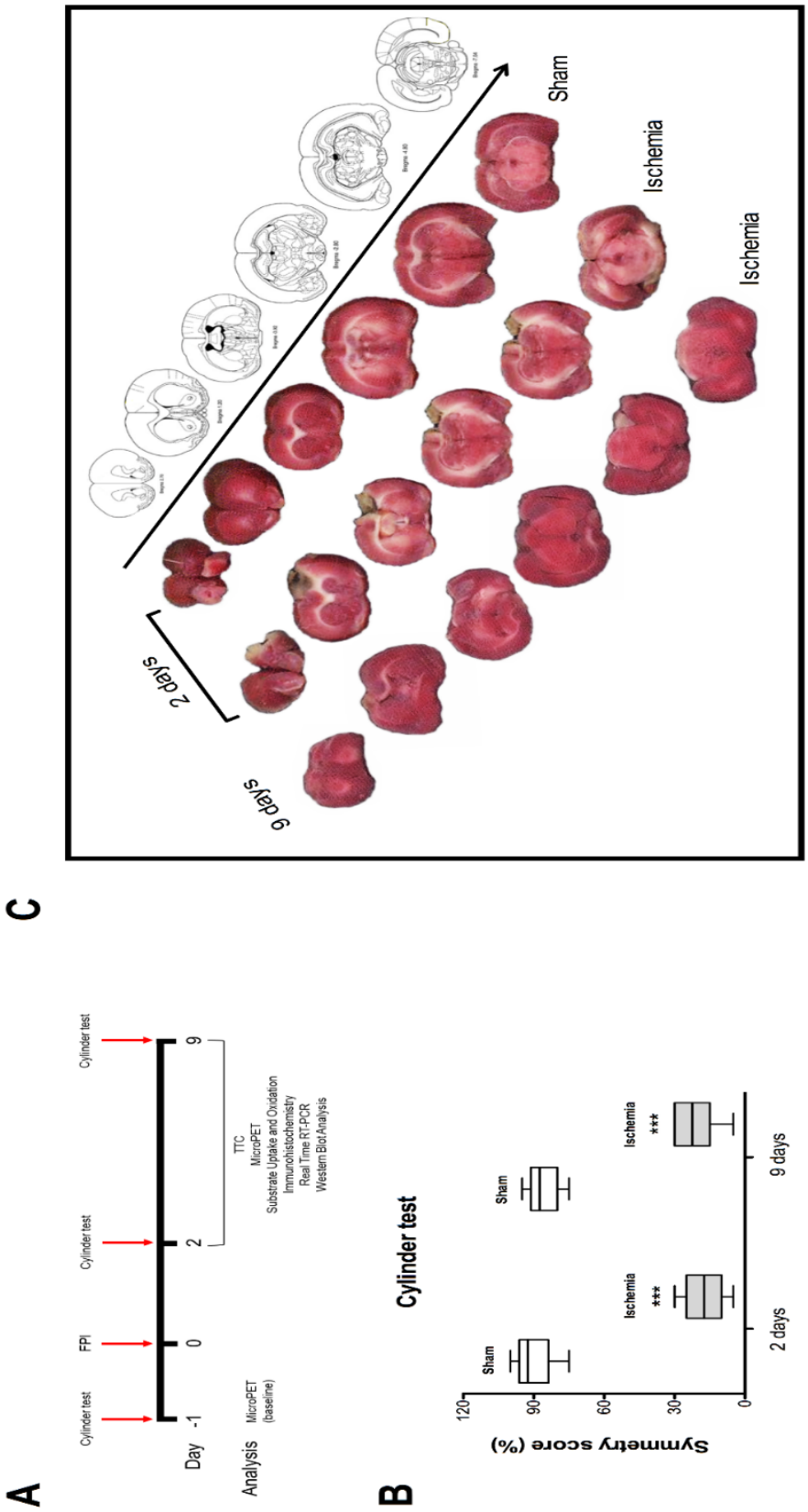
A
Cylinder test
FPI
Cylinder test
Cylinder test
Day -1 0 2 9
Analysis
MicroPET (baseline)
TTC
MicroPET
Substrate Uptake and Oxidation
Immunohistochemistry
Real Time RT-PCR
Western Blot Analysis
B
Cylinder test
Symmetry score (%)
120
90
60
30
0
Sham
Ischemia
***
Sham
Ischemia
***
2 days
9 days
C
2 days
9 days
Sham
Ischemia
Ischemia

Fig. 2.

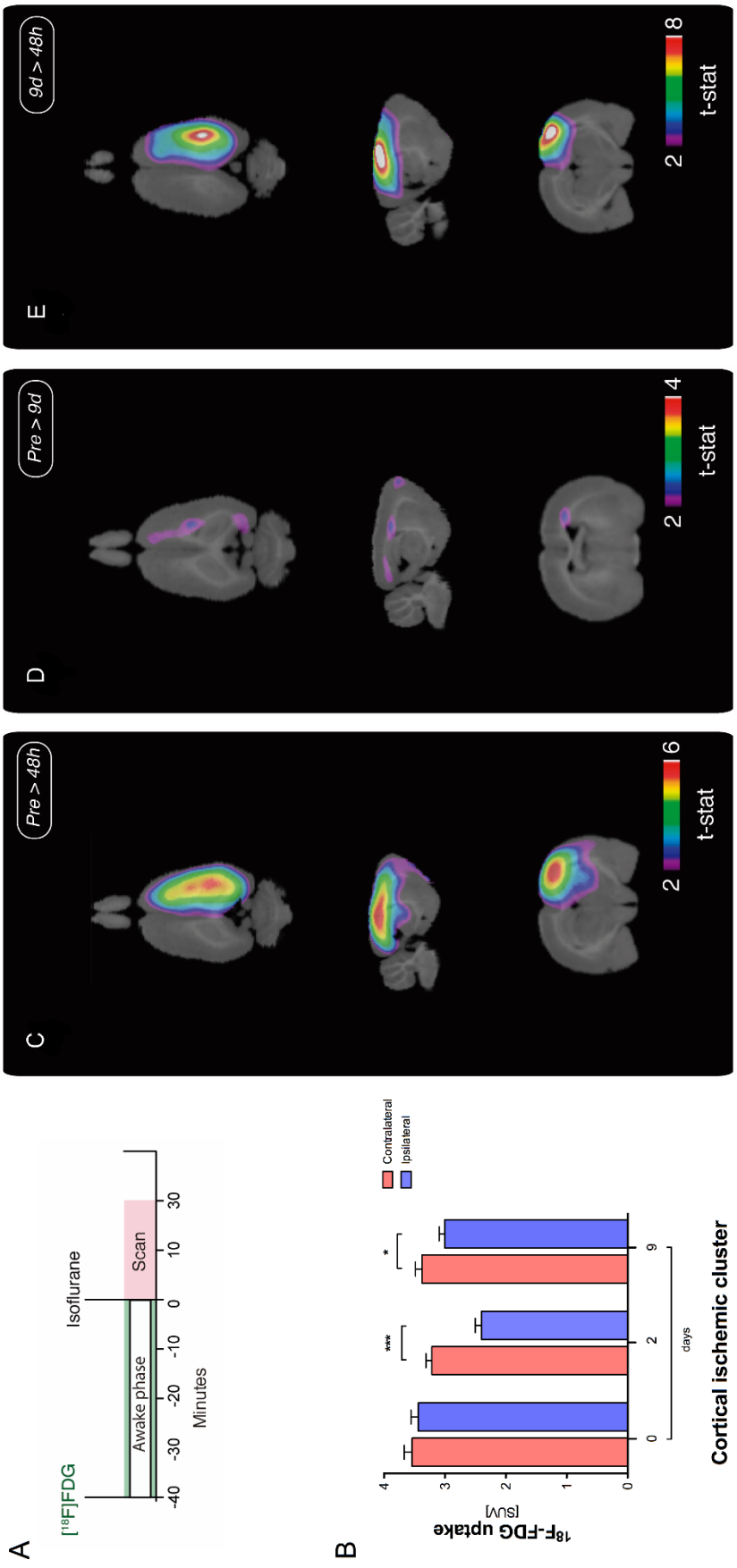
A
[18F]FDG
Awake phase
Isoflurane
Scan
-40
-30
-20
-10
0
10
30
Minutes
B
Contralateral
Ipsilateral
18F-FDG uptake
[SUV]
4
3
2
1
0
***
*
0
2
9
days
Cortical ischemic cluster
C
Pre > 48h
2
6
t-stat
D
Pre > 9d
2
4
t-stat
E
9d > 48h
2
8
t-stat

Fig. 3.

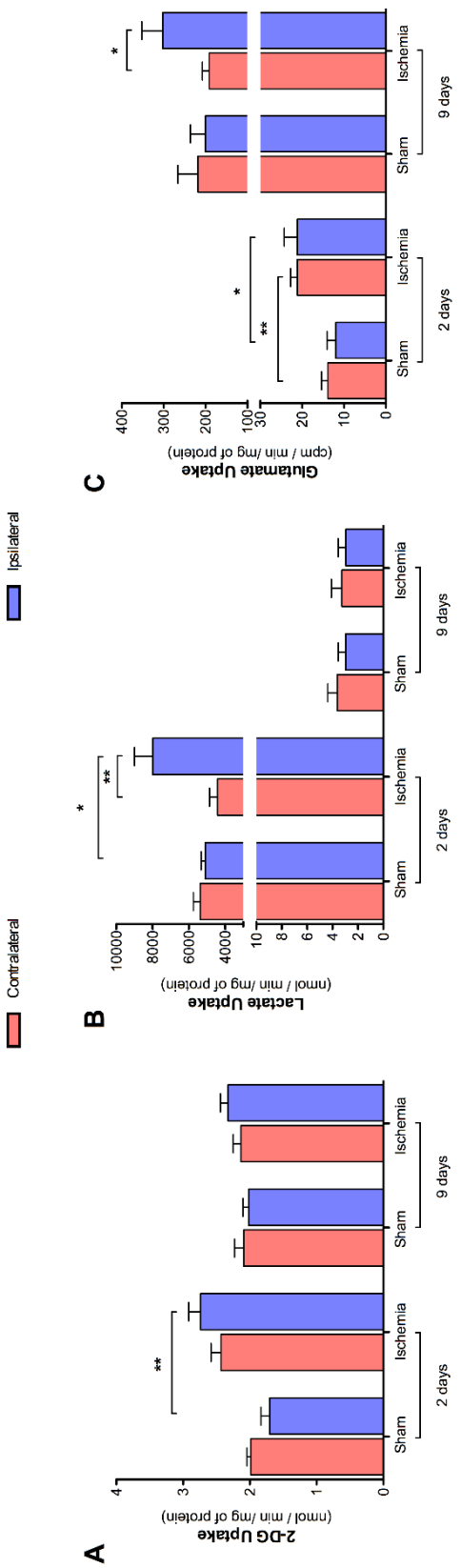
A
2-DG Uptake
(nmol / min /mg of protein)
B
Lactate Uptake
(nmol / min /mg of protein)
C
Glutamate Uptake
(cpm / min /mg of protein)
Contralateral
Ipsilateral
Sham
Ischemia
2 days
9 days
*
**

Fig. 4.

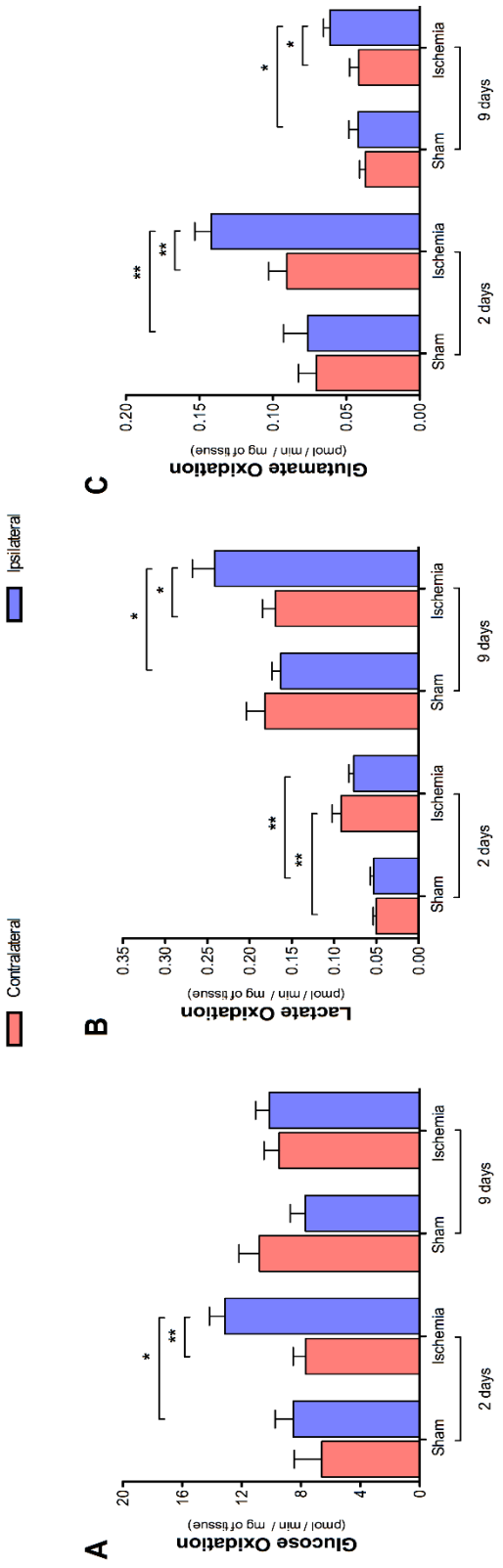
A
Glucose Oxidation
(pmol / min / mg of tissue)
B
Lactate Oxidation
(pmol / min / mg of tissue)
C
Glutamate Oxidation
(pmol / min / mg of tissue)
Contralateral
Ipsilateral
Sham
Ischemia
2 days
9 days

Fig. 5.

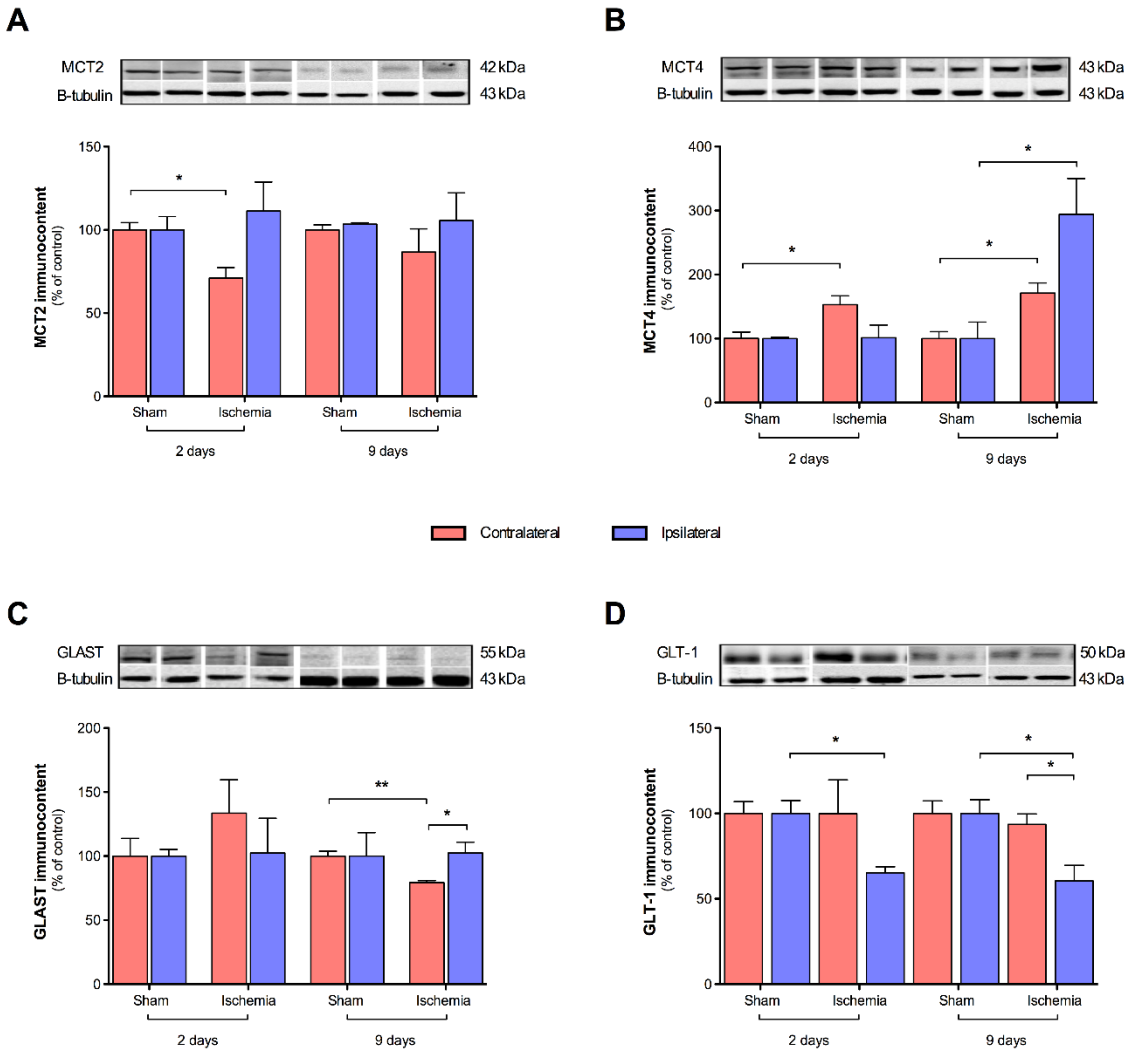
A
MCT2
B-tubulin
42 kDa
43 kDa
MCT2 immunocontent
(% of control)
150
100
50
0
*
Sham
Ischemia
Sham
Ischemia
2 days
9 days
B
MCT4
B-tubulin
43 kDa
43 kDa
MCT4 immunocontent
(% of control)
400
300
200
100
0
*
*
*
Sham
Ischemia
Sham
Ischemia
2 days
9 days
Contralateral
Ipsilateral
C
GLAST
B-tubulin
55 kDa
43 kDa
GLAST immunocontent
(% of control)
200
150
100
50
0
**
*
Sham
Ischemia
Sham
Ischemia
2 days
9 days
D
GLT-1
B-tubulin
50 kDa
43 kDa
GLT-1 immunocontent
(% of control)
150
100
50
0
*
*
*
Sham
Ischemia
Sham
Ischemia
2 days
9 days

Fig. 6.

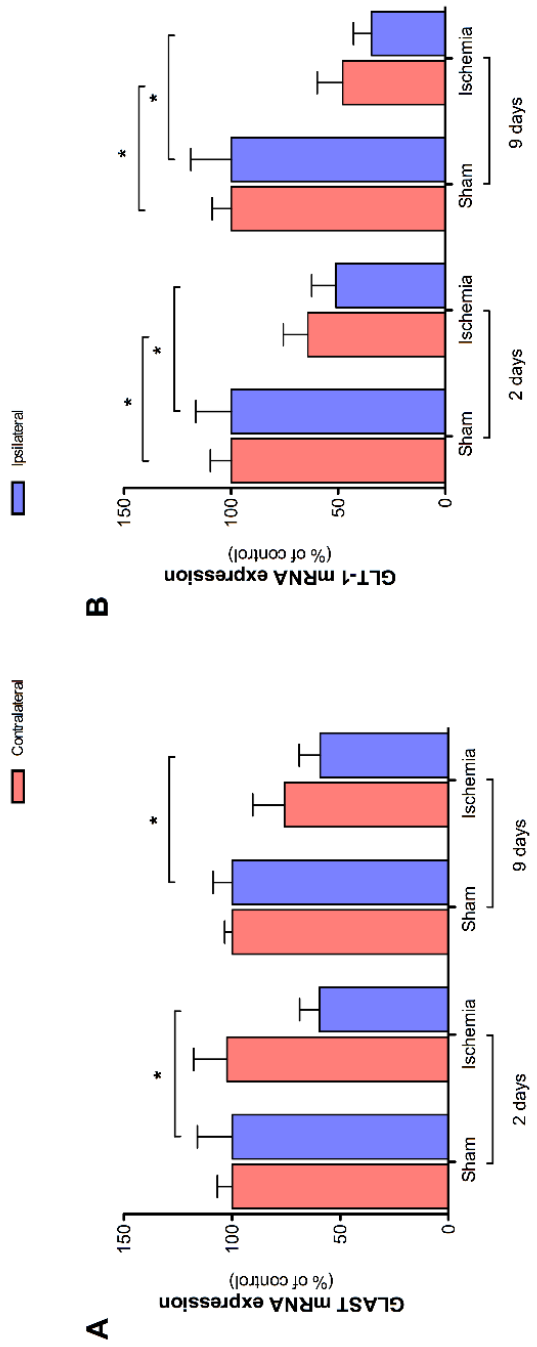
A
GLAST mRNA expression
(% of control)
150
100
50
0
Sham
Ischemia
2 days
9 days
Contralateral
Ipsilateral
B
GLT-1 mRNA expression
(% of control)
*

Fig. 7.

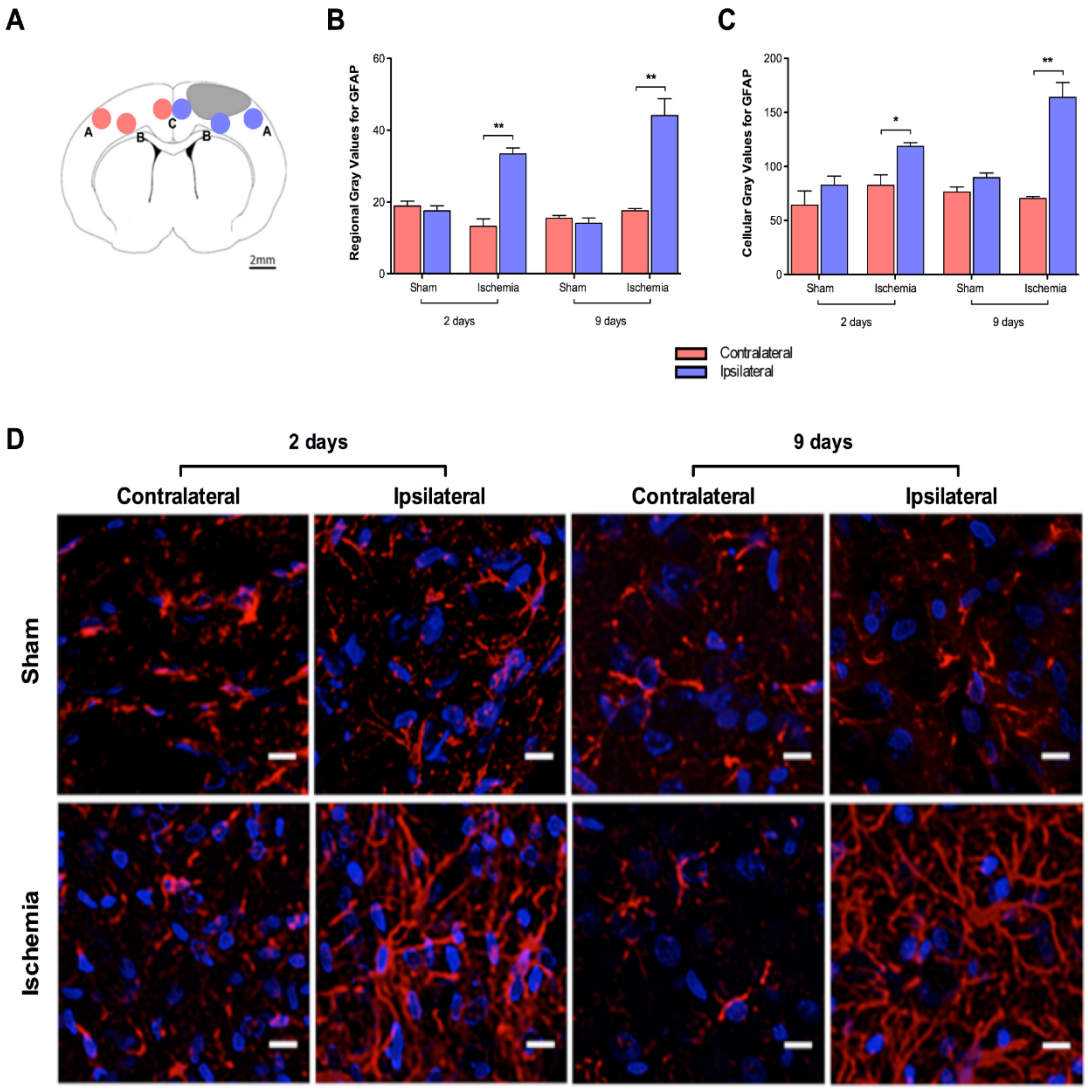
A
B
C
D
A
B
C
B
A
2mm
Regional Gray Values for GFAP
Cellular Gray Values for GFAP
Sham
Ischemia
Sham
Ischemia
2 days
9 days
Contralateral
Ipsilateral
2 days
9 days
Contralateral
Ipsilateral
Contralateral
Ipsilateral
Sham
Ischemia

Fig. 8.

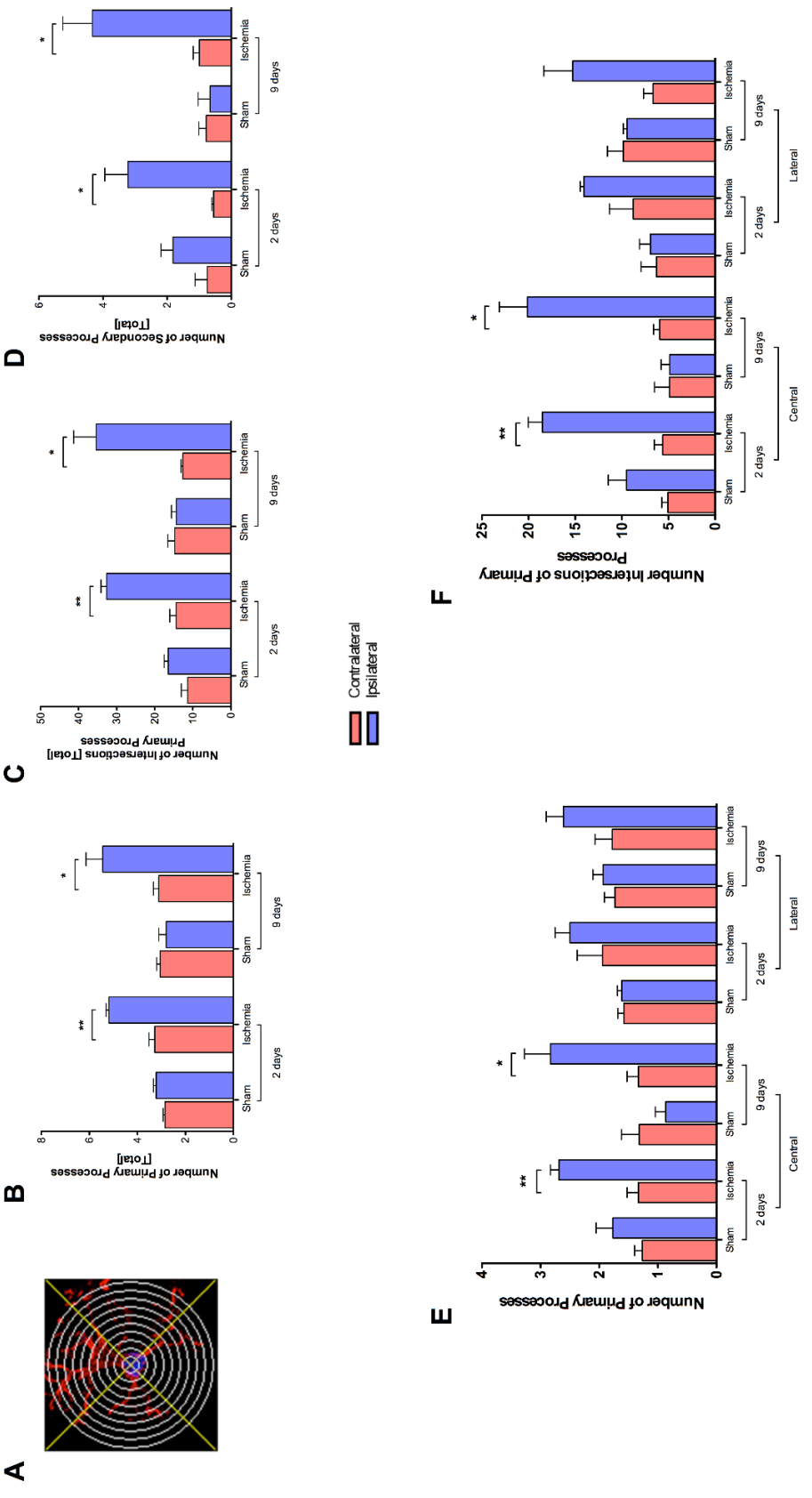
A
B
Number of Primary Processes [Total]
C
Number of Intersections [Total] Primary Processes
D
Number of Secondary Processes [Total]
Contralateral
Ipsilateral
E
Number of Primary Processes
F
Number Intersections of Primary Processes
Sham
Ischemia
2 days
9 days
Central
Lateral

Supplementary Fig. 1

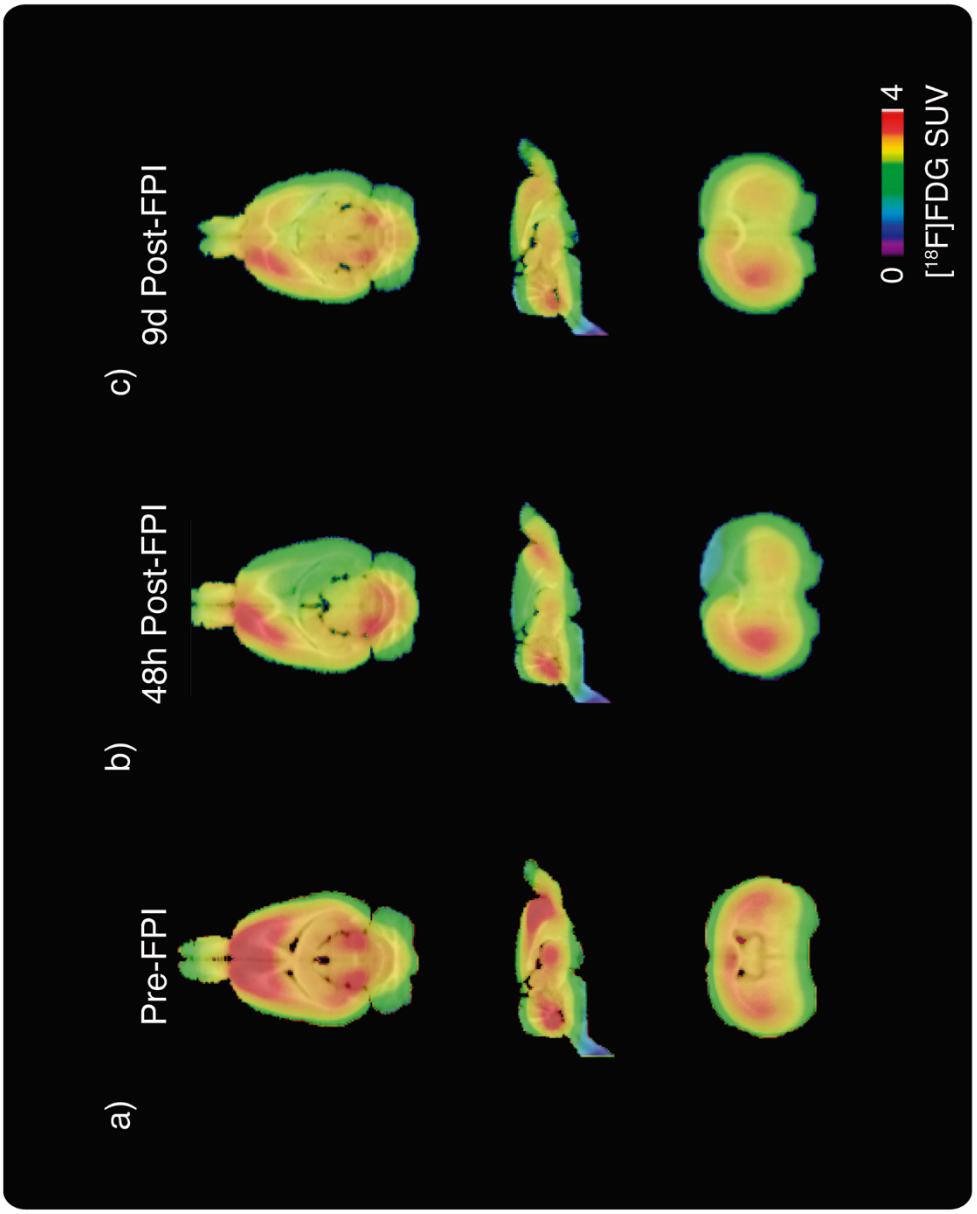

Supplementary Fig. 2

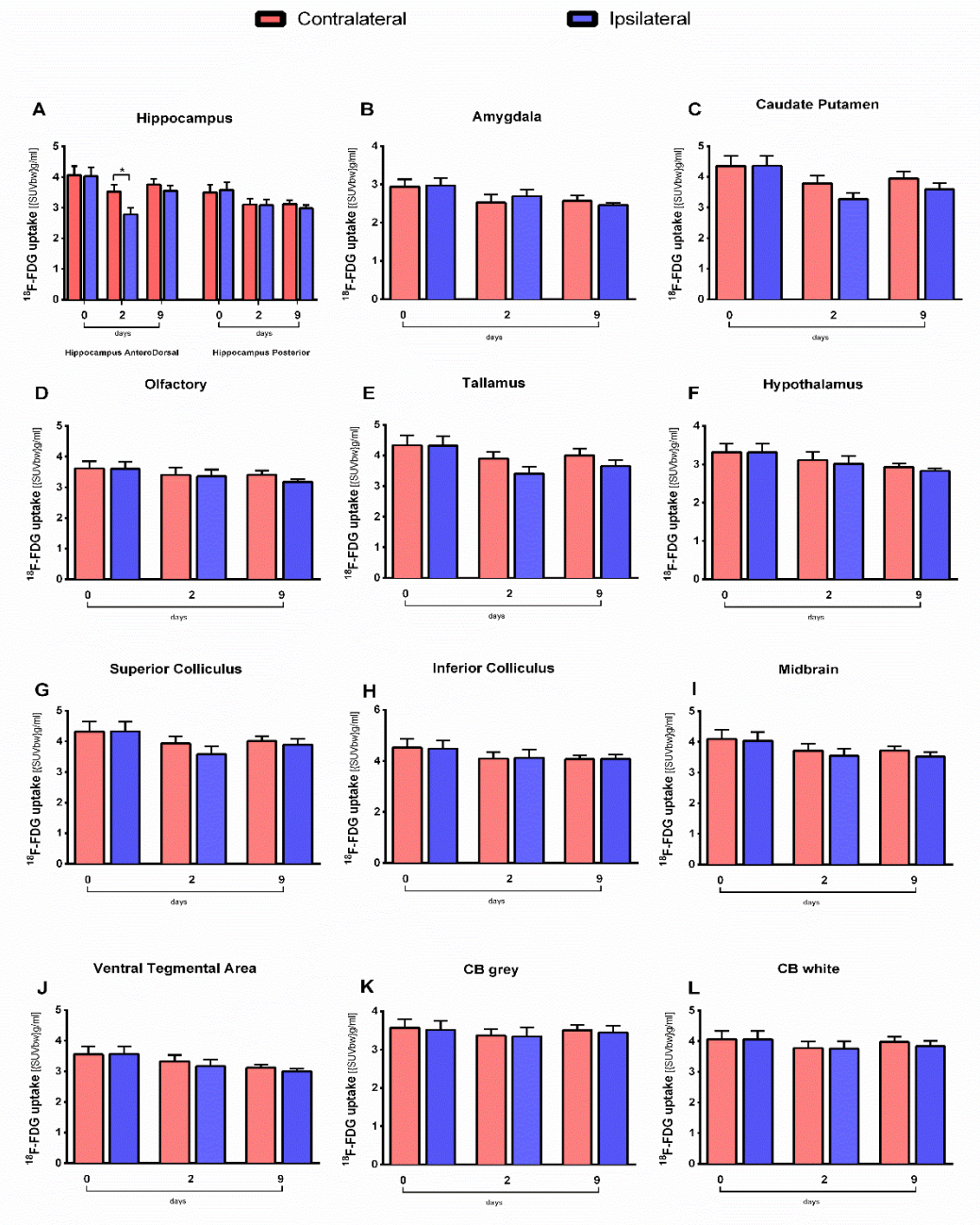

PARTE III

4. DISCUSSÃO

O AVE é uma das maiores causas de morte e deficiência adquirida em adultos, representando uma doença crônica incapacitante para a maioria dos sobreviventes. Mesmo com o desenvolvimento de políticas de prevenção e controle dos fatores de risco (i.e. hipertensão, tabagismo, doenças cardiovasculares, diabetes), o índice de mortalidade dos pacientes tende a decair mais rapidamente do que a incidência da IC (Dyken, 1991; Koton *et al.*, 2014; Carmichael, 2015). Assim sendo, além da compreensão dos mecanismos patofisiológicos, devemos buscar o entendimento dos processos que levam à reparação e à recuperação do cérebro. Considerando que a insuficiência bioenergética constitui a base patofisiológica dessa desordem, a disponibilidade de substratos, bem como sua utilização, pode sofrer modificações e representar um alvo terapêutico promissor para manipulação farmacológica.

Diversos processos neuroquímicos são desencadeados no cérebro após o início do evento isquêmico, causando morte celular na zona de infarto. Entretanto, em torno dessa área, a redução do fluxo sanguíneo cerebral é atenuada devido à perfusão dos vasos sanguíneos colaterais, permitindo que o metabolismo energético seja parcialmente preservado. Dessa forma, a região periférica pode passar por alterações celulares e moleculares para evitar a evolução do infarto. Os astrócitos, células gliais responsáveis por diversas funções na homeostase neuronal, são mais resistentes ao dano isquêmico do que os neurônios (Almeida *et al.*, 2002; Giffard and Swanson, 2005) e podem estar envolvidos na recuperação tanto no hemisfério ipsilateral quanto no contralateral (Takatsuru *et al.*, 2014). Nossos resultados demonstram que o metabolismo energético cerebral e o sistema glutamatérgico sofrem alterações que, de alguma forma, estão conectadas entre os hemisférios cerebrais pós-FPI. É importante ressaltar que os resultados mostram que, na área ao redor da lesão (incluindo a zona de penumbra), as células estão prontas para captar e oxidar os substratos avaliados, apesar da baixa perfusão, e tanto o lactato quanto o glutamato estão envolvidos nas adaptações que ocorrem no hemisfério contralateral.

O crescimento do *core* isquêmico às custas da zona de penumbra é a dinâmica 'natural' após a oclusão permanente da circulação sanguínea. No entanto, algumas áreas podem se recuperar espontaneamente (Kunz *et al.*, 2010), como foi observado *in vivo* no MicroPET e *ex vivo* na coloração de TTC 9 dias após a lesão. A coloração de TTC é utilizada para diferenciar tecido metabolicamente ativo de inativo, sendo considerada um marcador confiável e acessível na medição de volume de infarto. Originalmente incolor, o cloridrato de TTC é quimicamente reduzido a TPF vermelho (1,3,5-trifenil formazan) na presença de desidrogenases, as quais são mais abundantes na mitocôndria (Altman, 1976; Kramer *et al.*, 2010). Esse resultado mostra que, 9 dias pós-FPI, a área infartada recuperou uma parte significativa de sua atividade metabólica. Isso pode indicar angiogênese em curso ou mesmo a migração de células progenitoras e/ou a sua proliferação no local da lesão (Carmichael, 2015). Nossos resultados também evidenciaram que, nesse período, a recuperação metabólica da zona infartada ainda não reflete melhoria motora no grupo isquemia. Os animais desse grupo experimental não apresentaram recuperação motora significativa no teste do cilindro 9 dias pós-FPI em comparação com sua performance aos 2 dias pós-FPI. Takatsuru e colegas (Takatsuru *et al.*, 2014) analisaram o papel do hemisfério intacto na compensação das funções motoras no membro anterior contralateral após isquemia cerebral focal e mostraram que essa compensação funcional ainda está ocorrendo durante uma semana após a lesão. Somente após este período, os animais poderiam usar as novas sinapses formadas no hemisfério contralateral para apresentar melhora motora significativa.

A avaliação da captação e da oxidação de substratos em fatias de córtex cerebral demonstrou que, nas regiões cerebrais analisadas, 2 dias após FPI, a maquinaria responsável por estas funções metabólicas está funcionalmente ativa, sendo capaz de utilizar os substratos analisados para produzir energia. Curiosamente, a taxa metabólica do hemisfério ipsilateral é aumentada quando em comparação com o lado contralateral, o que contrasta com os resultados obtidos com o MicroPET no mesmo período. A explicação para isto é que os ensaios *ex vivo* são realizados em condições controladas e o substrato é aplicado diretamente sobre a fatia. De maneira contrária, o MicroPET, análise

in vivo, mostra uma diminuição da captação de [^{18}F]FDG e do seu metabolismo devido à ausência de fluxo sanguíneo local. Além disso, 9 dias após a FPI, as análises em microPET mostraram que a captação de [^{18}F]FDG foi semelhante aos níveis basais, enquanto a captação de glicose e utilização medidas em fatias do grupo isquemia não apresentaram diferenças em relação ao grupo Sham.

De maneira interessante, 2 dias pós-FPI, o aumento na captação de glutamato coincide com aumento da oxidação de lactato em ambos os hemisférios ipsi- e contralateral, sugerindo que o lactato derivado do glutamato está sendo utilizado como fonte de energia no cérebro (McKenna, 2013) (Figura 3). Essa pode ser a primeira participação do hemisfério contralateral na tentativa de conter a evolução do infarto; entretanto, mais estudos são necessários para reforçar esta hipótese. Ainda assim, sabe-se que o glutamato tem uma taxa de oxidação em astrócitos muito mais elevada do que qualquer outro substrato (McKenna *et al.*, 1993; McKenna *et al.*, 1996b), e que a incorporação de carbonos advindos do metabolismo do glutamato na molécula de lactato em astrócitos ocorre em maior proporção do que a conversão em glutamina (Sonnewald *et al.*, 1993). Essa última descoberta foi confirmada pela demonstração de que a proporção de glutamato oxidado pelo ciclo do TCA é diretamente dependente de sua concentração extracelular, ao mesmo tempo que é inversamente proporcional à sua conversão em glutamina (McKenna *et al.*, 1996a). A elevada disponibilidade de glutamato no meio extracelular, como esperado após a indução de dano isquêmico, pode estar contribuindo para que haja uma maior utilização desse substrato para produção de ATP em ambos os hemisférios, enquanto que sua conversão em lactato pode estar sendo destinada ao suporte energético neuronal. Além disso, nossos dados demonstram que, 9 dias pós-FPI, as taxas de oxidação tanto do lactato quanto do glutamato ainda estão elevadas no hemisfério ipsilateral, o que pode indicar que esses substratos têm um papel importante na recuperação do cérebro. Nenhuma mudança significativa foi encontrada no hemisfério contralateral do grupo isquemia em relação ao mesmo hemisfério do grupo Sham nesse mesmo período de tempo.

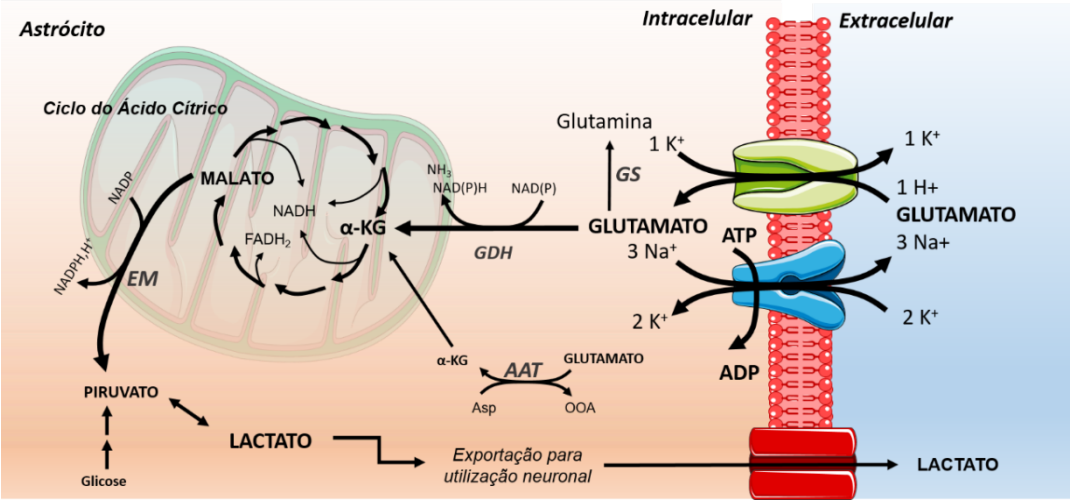

Figura 3. Hipótese para a conversão do glutamato em lactato. Após sua captação pelos transportadores astrocitários, o glutamato é convertido em α-cetoglutarato e entra no ciclo do ácido cítrico (TCA). O excesso de glutamato ocasiona o desvio de malato para o citoplasma, onde é convertido primeiro em piruvato e, depois, em lactato, o qual é exportado do astrócito para utilização neuronal. *AAT*: aspartato aminotransferase; α-*KG*: alfa-cetoglutarato; *Asp*: aspartato; *EM:* enzima málica; *GDH*: gutamato desidrogenase; *GS*: glutamina sintetase; *OAA*: oxaloacetato.

Os resultados obtidos em fatias de córtex *ex vivo* indicam, no geral, uma maior ativação do metabolismo energético para compensação do dano isquêmico focal. Assim, para investigar o envolvimento dos MCTs e dos transportadores de glutamato nas modulações descritas até agora neste trabalho, foram realizadas análises de imunoconteúdo por *western blot*. Além disso, a expressão de mRNA dos transportadores astrocitários de glutamato foi avaliada por RT-qPCR. Nosso trabalho indica que, 2 dias pós-FPI, há uma diminuição dos níveis protéicos de MCT2 no hemisfério contralateral, acompanhada por um aumento dos níveis de MCT4 nesse mesmo hemisfério. Sabe-se que os MCTs são regulados de forma mais acentuada ao nível de tradução (Halestrap, 2013). O MCT4 parece ser o principal MCT em astrócitos em roedores (Bergersen *et al.*, 2001; Rafiki *et al.*, 2003) e, sob condições de hipóxia, sua expressão é regulada através do fator de transcrição HIF-1α (*hypoxia-inducible fator* 1α, Fator Induzido por Hipóxia 1α), uma vez que a sua expressão está ligada a tensão de oxigênio (Singh *et al.*, 2012; Rosafio and Pellerin, 2014; Bergersen, 2015). Após 2 dias da lesão, o imunoconteúdo de

MCT4 mostrou-se aumentado apenas no hemisfério contralateral, indicando que o córtex ipsilateral não conseguiu responder ao dano isquêmico tão rapidamente. Além disso, já foi sugerido que o HIF-1α é um componente de recuperação pelo hemisfério intacto. Estudos anteriores relataram que o dano isquêmico focal permanente aumenta o mRNA que codifica o HIF-1α na região de penumbra (Wiener *et al.*, 1996; Bergeron *et al.*, 1999). Os nossos resultados podem indicar que o HIF-1α poderia ter um efeito de sinalização mais prolongada na lesão isquêmica permanente, uma vez que seus efeitos nos níveis de MCT4 ainda puderam ser observados após 9 dias de FPI.

Em contraste, o MCT2 é principalmente encontrado em neurônios, associado com processos e espinhos dendríticos neuronais, e sua expressão não é influenciada pelo HIF-1α (Pierre *et al.*, 2002; Bergersen, 2015). Observou-se uma diminuição no imunoconteúdo de MCT2 após 2 dias da lesão no hemisfério contralateral, mas não no ipsilateral. Tal alteração pode ser devido à morte neuronal. Os nossos dados também mostram que a expressão de MCT4 está aumentada no mesmo hemisfério cerebral no mesmo período de tempo. Recentemente, Rosafio e colegas (Rosafio *et al.*, 2016) observaram a expressão de MCT4 em neurônios em MCAO 24h pós-reperfusão, embora esse transportador seja considerado exclusivo de astrócitos sob condições fisiológicas (Bergersen *et al.*, 2002; Rafiki *et al.*, 2003; Pellerin *et al.*, 2005). É importante observar que o Km do MCT4 (30 mmol/L) é considerado elevado, enquanto que o Km do MCT2 (menos que 1 mmol/L) sugere que este último estará geralmente saturado. A hipótese de que os neurônios possam expressar MCT4 em condições de hipóxia é interessante, pois dessa forma o transporte de lactato teria uma tendência a aumentar conforme a disponibilidade de substrato (Bergersen, 2015). Assim, a expressão de MCT4 exerceria um papel importante para os neurônios, possibilitando um novo estado metabólico pós-isquemia no hemisfério contralateral, enquanto MCT2 não está disponível.

Um dos papéis mais importantes da astroglia no cérebro é a captação de glutamato na fenda sináptica, o que é um processo energeticamente custoso por depender do gradiente de Na^+ (Danbolt, 2001; McKenna, 2013). Nesse trabalho, observamos uma diminuição na expressão e no imunoconteúdo de transportadores de glutamato acompanhados, paradoxalmente, por aumento

de atividade (captação). Esses resultados revelam que o aumento da captação de glutamato não é necessariamente acompanhado por um aumento na expressão dos transportadores após isquemia cerebral focal, sugerindo que a diminuição dos níveis de transportadores de glutamato não está relacionada com sua atividade. Além disso, os experimentos de captação foram realizados em fatias de córtex estabilizadas em solução tampão, o que pode ter restaurado a sua capacidade funcional, uma vez que o transporte de glutamato é dependente do gradiente Na^+ / K^+ (Anderson and Swanson, 2000; Danbolt, 2001). É também importante considerar que o aumento da disponibilidade de glutamato no meio extracelular, como esperado após IC, pode aumentar a capacidade de transporte do GLT-1, uma vez que o glutamato é um agonista muito eficaz (Takatsuru *et al.*, 2014). Além disso, a diminuição da expressão gênica dos transportadores de glutamato pode ser uma consequência da morte neuronal induzida pelo dano isquêmico. Estudos anteriores demonstraram que os neurônios estão diretamente envolvidos na regulação da expressão de ambos GLT-1 e GLAST (Gegelashvili *et al.*, 1997; Swanson *et al.*, 1997; Schlag *et al.*, 1998), bem como a atividade sináptica. Os nossos resultados mostram que a lesão induzida por FPI altera a expressão de GLT-1 não só no hemisfério lesionado, mas também no hemisfério intacto nos dois tempos analisados. Curiosamente, o imunoconteúdo de GLT-1 no grupo isquemia permaneceu semelhante ao do grupo Sham no hemisfério contralateral nesses mesmos tempos, o que indica um mecanismo mais complexo envolvendo a regulação da expressão gênica e do imunoconteúdo desse transportador e indicando uma necessidade de investigar melhor essa questão. Além disso, os nossos dados indicam que a regulação a nível de expressão gênica estão conectados inter-hemisférios cerebrais e que o GLT-1 pode desempenhar um papel na resposta a danos isquêmicos no hemisfério intacto. Por outro lado, um declínio na expressão de GLAST no hemisfério ipsilateral foi observada 2 e 9 dias pós-FPI. De maneira interessante, essa diminuição de expressão não é acompanhada por diminuição do imunoconteúdo de GLAST no hemisfério lesionado (ipsi) em nenhum dos tempos analisados. Um estudo realizado por Sullivan e colegas (Sullivan *et al.*, 2007) sugere um papel essencial da GFAP na regulação do tráfego dos transportadores de glutamato, bem como na sua função. Ainda, a

GFAP seria responsável por reter o GLAST na membrana plasmática após dano hipóxico (Middeldorp and Hol, 2011; Nijboer *et al.*, 2013). Tais achados poderiam explicar a manutenção no imunoconteúdo de GLAST entre os grupos experimentais encontrada 2 e 9 dias pós-FPI no hemisfério lesionado (ipsi), uma vez que nossos dados mostram que os astrócitos apresentam sinais de reatividade (vide a seguir), i.e. maior expressão de GFAP no hemisfério ipsilateral a partir do segundo dia após FPI. Em contraste, 9 dias pós-FPI, observamos um declínio nos níveis proteicos de GLAST no hemisfério contralateral se comparado com o hemisfério oposto (ipsi) do grupo isquemia e com o mesmo hemisfério do Sham. Isso poderia indicar que, após evento isquêmico, a maior expressão de GFAP é necessária para a manutenção dos níveis de GLAST. De qualquer forma, faz-se necessário a investigação do mecanismo de regulação deste transportador para entender sua participação no hemisfério intacto (contra-) pós-IC.

Os resultados supracitados descrevem algumas alterações em parâmetros astrocitários (i.e. captação de glutamato, expressão de transportadores de glutamato), confirmando o papel essencial dessa célula glial em resposta à injúria cerebral. Além desses parâmetros, analisamos a expressão de GFAP no modelo de FPI devido ao seu envolvimento em funções astrocitárias importantes durante a regeneração cerebral e RA (Middeldorp and Hol, 2011). Sabe-se que o aumento da expressão de GFAP já foi correlacionado com uma diminuição na atividade de glutamina sintetase (Weir and Thomas, 1984) e, consequentemente, a diminuição tanto nos níveis de glutamina quanto nas taxas de conversão de glutamato-glutamina (Lieth *et al.*, 1998). Outros grupos de pesquisa já demonstraram maior suscetibilidade ao dano isquêmico na ausência de GFAP (Nawashiro *et al.*, 1998; Nawashiro *et al.*, 2000; Tanaka *et al.*, 2002; Li *et al.*, 2008; de Pablo *et al.*, 2013), sugerindo que a RA é importante para a proteção da zona de penumbra - supostamente por meio da eliminação eficaz do glutamato e das espécies reativas de oxigênio. Ainda, uma função vascular, como a regulação do fluxo sanguíneo, já foi sugerida para a GFAP, uma vez que camundongos *knockout* para essa proteína são hipersensíveis à oclusão arterial, apresentando uma grande queda do fluxo sanguíneo (Carmignoto and Gomez-Gonzalo, 2010). Isso poderia indicar uma

associação alterada dos pés astrocíticos com os vasos sanguíneo, uma vez que o aumento de cálcio no local de contato astrócito-vasculatura é crítico para a sinalização (Gordon *et al.*, 2007; Gordon *et al.*, 2008). Além disso, em algumas regiões do SNC, tanto o número quanto o diâmetro dos processos astrocíticos estão reduzidos em camundongos *knockout* para GFAP. No entanto, os mecanismos que ligam essa proteína às respostas da RA permanecem incompreendidos (Brenner, 2014; Hol and Pekny, 2015). Resultados conflitantes entre diferentes estudos refletem a grande complexidade na funcionalidade da GFAP, sugerindo, ainda, diferenças regionais nas atividades dessa proteína no cérebro (Brenner, 2014).

Quanto à morfologia astrocitária, nossos resultados mostram que a alteração mais marcante foi o aumento do número de processos centrais primários no hemisfério ipsilateral do grupo isquemia em ambos os tempos analisados, atribuindo uma simetria mais radial à astroglia. Isso indica uma maior RA no grupo isquêmico e uma alteração morfológica importante quando comparada com a observada em astrócitos do hemisfério contralateral correspondente ou ambos os hemisférios cerebrais de ratos Sham.

Na presente dissertação empregamos um modelo animal de IC permanente (sem reperfusão). Modelos experimentais de IC envolvendo reperfusão são bastante empregados na literatura, porém, na prática clínica, a isquemia cerebral em humanos é majoritariamente permanente (Yu *et al.*, 2015), o que reduz a janela temporal para a recuperação da zona de penumbra. Apesar dos progressos significativos na assistência ao paciente, as opções terapêuticas para vítimas de AVE são limitadas, e apenas uma pequena porcentagem de pacientes são tratados com rt-PA ou com abordagem endovascular (Krzyzanowska *et al.*, 2016), fazendo com que o uso de modelos de oclusão permanente se assemelhe mais à patologia observada em humanos.

Em resumo, nossos resultados apresentaram provas de que o cérebro como um todo é afetado pelo dano isquêmico focal, causando modulações principalmente através de expressão celular de proteínas, disponibilidade e utilização de substratos e parâmetros astrocitários (i.e. super-expressão, de GFAP, aumento da atividade dos transportadores de glutamato e o transporte

de substratos) (Figura 4). Algumas mudanças persistem ou aparecem apenas 9 dias pós-FPI. Além disso, observou-se uma ligação entre o sistema glutamatérgico e metabolismo do lactato através da conectividade entre os hemisférios ipsi- e contralateral. Estas mudanças significativas suportam a hipótese de que há uma reprogramação metabólica após a lesão isquêmica para promover a recuperação e a adaptação do tecido cerebral, oferecendo novos alvos terapêuticos para auxiliar o tratamento do AVE em pacientes humanos

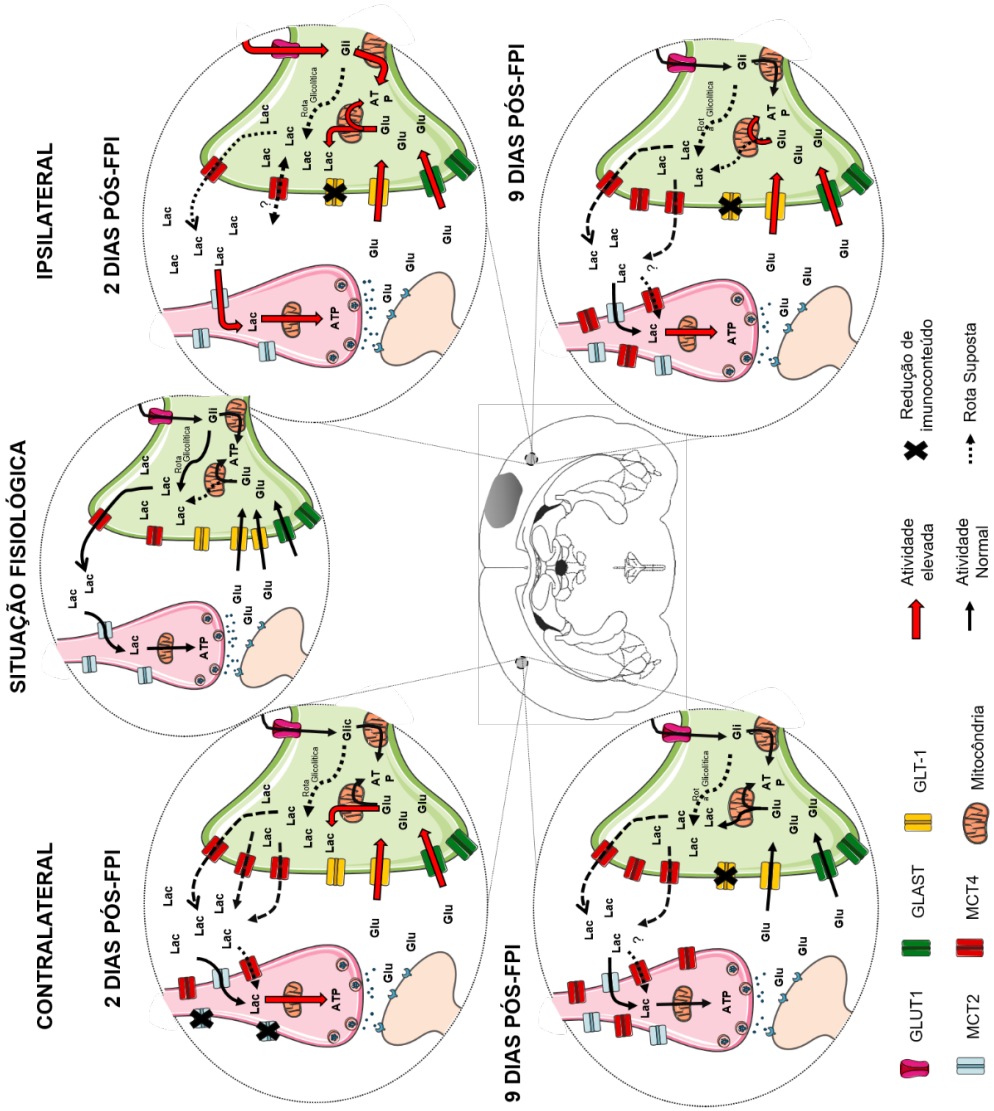

Figura 4. Resumo gráfico dos resultados obtidos referente às alterações no metabolismo energético cerebral pelo modelo de FPI. As rotas que não foram contempladas pelos experimentos desse trabalho estão traçadas com linhas pontilhadas.

5. CONCLUSÕES

Nesse trabalho, evidenciamos que: (i) o modelo utilizado diminui a taxa de simetria dos animais 2 e 9 dias após FPI; (ii) houve retorno parcial de atividade metabólica aos 9 dias em grande parte da área infartada corada pelo TTC; (iii) a captação e a oxidação de substratos aumentaram substancialmente no hemisfério ipsilateral 2 dias após FPI; (iv) o microPET evidenciou que a captação de [^{18}F]FDG é diminuída *in vivo*, contrastando os resultados obtidos *ex vivo*; (v) o aumento da atividade dos transportadores de glutamato não é necessariamente acompanhado por maiores níveis de expressão e/ou imunoconteúdo. Além disso, nosso trabalho mostrou pela primeira vez que o aumento da captação de glutamato parece estar relacionado ao aumento da oxidação de lactato em ambos os hemisférios cerebrais em um modelo de isquemia cerebral focal.

Acreditamos que a RA exerce grande influência sobre as mudanças supracitadas, uma vez que os astrócitos são o tipo glial mais abundante no córtex cerebral e responsáveis por diversas funções fisiológicas e de reparo. Além disso, os astrócitos constituem um elo entre a vasculatura cerebral e os neurônios. Mais estudos são necessários para elucidar os mecanismos responsáveis pelo impacto da astroglia na recuperação pós-isquemia e seu papel no hemisfério contralateral.

6. PERSPECTIVAS

Pretendemos dar continuidade a esse trabalho, investigando os mecanismos que regulam a ativação do metabolismo energético, principalmente astrocitário, em ambos os hemisférios pós-FPI. Antes da submissão do manuscrito relacionado a esta dissertação, pretendemos realizar a expressão de HIF-1 alfa e dos GLUTs (1 e 3). Além disso, pretendemos também aplicar um protocolo de tratamento com uma substância neuroprotetora (guanosina) para verificar o possível papel benéfico dessa purina em parâmetros energéticos, glutamatérgicos e astrocitários.

7. REFERÊNCIAS

Guidelines for management of ischaemic stroke and transient ischaemic attack 2008. Cerebrovascular diseases (Basel, Switzerland) 2008; 25(5): 457-507.

Alle H, Roth A, Geiger JR. Energy-efficient action potentials in hippocampal mossy fibers. Science (New York, NY) 2009; 325(5946): 1405-8.

Allen NJ, Barres BA. Neuroscience: Glia - more than just brain glue. Nature 2009; 457(7230): 675-7.

Almeida A, Delgado-Esteban M, Bolanos JP, Medina JM. Oxygen and glucose deprivation induces mitochondrial dysfunction and oxidative stress in neurones but not in astrocytes in primary culture. Journal of neurochemistry 2002; 81(2): 207-17.

Altman FP. Tetrazolium salts and formazans. Progress in histochemistry and cytochemistry 1976; 9(3): 1-56.

American Stroke Association. Types of Stroke. 2012 Acesso em 14 de novembro de 2015.]; Disponível em: http://www.strokeassociation.org/STROKEORG/AboutStroke/TypesofStroke/IschemicClots/Ischemic-Strokes-Clots_UCM_310939_Article.jsp#.VtMXNJwrLIV

Anderson CM, Swanson RA. Astrocyte glutamate transport: review of properties, regulation, and physiological functions. Glia 2000; 32(1): 1-14.

Astrup J, Siesjo BK, Symon L. Thresholds in cerebral ischemia - the ischemic penumbra. Stroke; a journal of cerebral circulation 1981; 12(6): 723-5.

Bandera E, Botteri M, Minelli C, Sutton A, Abrams KR, Latronico N. Cerebral blood flow threshold of ischemic penumbra and infarct core in acute ischemic stroke: a systematic review. Stroke; a journal of cerebral circulation 2006; 37(5): 1334-9.

Bao Y, Qin L, Kim E, Bhosle S, Guo H, Febbraio M*, et al.* CD36 is involved in astrocyte activation and astroglial scar formation. Journal of cerebral blood flow and metabolism : official journal of the International Society of Cerebral Blood Flow and Metabolism 2012; 32(8): 1567-77.

Barreto G, White RE, Ouyang Y, Xu L, Giffard RG. Astrocytes: targets for neuroprotection in stroke. Central nervous system agents in medicinal chemistry 2011a; 11(2): 164-73.

Barreto GE, Sun X, Xu L, Giffard RG. Astrocyte proliferation following stroke in the mouse depends on distance from the infarct. PloS one 2011b; 6(11): e27881.

Baud O, Fayol L, Gressens P, Pellerin L, Magistretti P, Evrard P*, et al.* Perinatal and early postnatal changes in the expression of monocarboxylate transporters MCT1 and MCT2 in the rat forebrain. The Journal of comparative neurology 2003; 465(3): 445-54.

Belanger M, Allaman I, Magistretti PJ. Brain energy metabolism: focus on astrocyte-neuron metabolic cooperation. Cell metabolism 2011; 14(6): 724-38.

Bergeron M, Yu AY, Solway KE, Semenza GL, Sharp FR. Induction of hypoxia-inducible factor-1 (HIF-1) and its target genes following focal ischaemia in rat brain. The European journal of neuroscience 1999; 11(12): 4159-70.

Bergersen L, Rafiki A, Ottersen OP. Immunogold cytochemistry identifies specialized membrane domains for monocarboxylate transport in the central nervous system. Neurochemical research 2002; 27(1-2): 89-96.

Bergersen L, Waerhaug O, Helm J, Thomas M, Laake P, Davies AJ*, et al.* A novel postsynaptic density protein: the monocarboxylate transporter MCT2 is co-localized with delta-glutamate receptors in postsynaptic densities of parallel fiber-Purkinje cell synapses. Experimental brain research 2001; 136(4): 523-34.

Bergersen LH. Lactate transport and signaling in the brain: potential therapeutic targets and roles in body-brain interaction. Journal of cerebral blood flow and metabolism : official journal of the International Society of Cerebral Blood Flow and Metabolism 2015; 35(2): 176-85.

Bidmon HJ, Jancsik V, Schleicher A, Hagemann G, Witte OW, Woodhams P*, et al.* Structural alterations and changes in cytoskeletal proteins and proteoglycans after focal cortical ischemia. Neuroscience 1998; 82(2): 397-420.

Bogousslavsky J, Van Melle G, Regli F. The Lausanne Stroke Registry: analysis of 1,000 consecutive patients with first stroke. Stroke; a journal of cerebral circulation 1988; 19(9): 1083-92.

Bonde C, Sarup A, Schousboe A, Gegelashvili G, Zimmer J, Noraberg J. Neurotoxic and neuroprotective effects of the glutamate transporter inhibitor DL-threo-beta-benzyloxyaspartate (DL-TBOA) during physiological and ischemia-like conditions. Neurochemistry international 2003; 43(4-5): 371-80.

Brenner M. Role of GFAP in CNS injuries. Neuroscience letters 2014; 565: 7-13.

Broughton BR, Reutens DC, Sobey CG. Apoptotic mechanisms after cerebral ischemia. Stroke; a journal of cerebral circulation 2009; 40(5): e331-9.

Brouns R, De Deyn PP. The complexity of neurobiological processes in acute ischemic stroke. Clinical neurology and neurosurgery 2009; 111(6): 483-95.

Brouns R, Sheorajpanday R, Wauters A, De Surgeloose D, Marien P, De Deyn PP. Evaluation of lactate as a marker of metabolic stress and cause of secondary damage in acute ischemic stroke or TIA. Clinica chimica acta; international journal of clinical chemistry 2008; 397(1-2): 27-31.

Calabresi P, Centonze D, Bernardi G. Cellular factors controlling neuronal vulnerability in the brain: a lesson from the striatum. Neurology 2000; 55(9): 1249-55.

Carmichael ST. The 3 Rs of Stroke Biology: Radial, Relayed, and Regenerative. Neurotherapeutics : the journal of the American Society for Experimental NeuroTherapeutics 2015.

Carmignoto G, Gomez-Gonzalo M. The contribution of astrocyte signalling to neurovascular coupling. Brain research reviews 2010; 63(1-2): 138-48.

Castillo J, Alvarez-Sabin J, Davalos A, Diez-Tejedor E, Lizasoain I, Martinez-Vila E*, et al.* [Consensus review. Pharmacological neuroprotection in cerebral ischemia: is it still a therapeutic option?]. Neurologia (Barcelona, Spain) 2003; 18(7): 368-84.

Clarke LE, Barres BA. Emerging roles of astrocytes in neural circuit development. Nature reviews Neuroscience 2013; 14(5): 311-21.

Danbolt NC. Glutamate uptake. Progress in neurobiology 2001; 65(1): 1-105.

de Pablo Y, Nilsson M, Pekna M, Pekny M. Intermediate filaments are important for astrocyte response to oxidative stress induced by oxygen-glucose deprivation and reperfusion. Histochemistry and cell biology 2013; 140(1): 81-91.

del Zoppo GJ. Inflammation and the neurovascular unit in the setting of focal cerebral ischemia. Neuroscience 2009; 158(3): 972-82.

Dimmer KS, Friedrich B, Lang F, Deitmer JW, Broer S. The low-affinity monocarboxylate transporter MCT4 is adapted to the export of lactate in highly glycolytic cells. The Biochemical journal 2000; 350 Pt 1: 219-27.

Ding S. astrocytic Ca signaling in health and brain disorders. Future neurology 2013; 8(5): 529-54.

Ding S. Dynamic reactive astrocytes after focal ischemia. Neural regeneration research 2014; 9(23): 2048-52.

Ding S, Wang T, Cui W, Haydon PG. Photothrombosis ischemia stimulates a sustained astrocytic Ca2+ signaling in vivo. Glia 2009; 57(7): 767-76.

Dirnagl U, Iadecola C, Moskowitz MA. Pathobiology of ischaemic stroke: an integrated view. Trends in neurosciences 1999; 22(9): 391-7.

Donnan GA, Baron J-C, Davis SM, Sharp FR, editors. The Ischemic Penumbra: Pathophysiology, Imaging and Therapy; 2007.

Duehrkop C, Rieben R. Ischemia/reperfusion injury: effect of simultaneous inhibition of plasma cascade systems versus specific complement inhibition. Biochemical pharmacology 2014; 88(1): 12-22.

Dugan L, Choi D. Hypoxia-ischemia and Brain Infarction. In: GJ S, BW A, RW A, editors. Basic Neurochemistry: Molecular, Cellular and Medical Aspects. Philadelphia: Lippincott-Raven; 1999.

Dyken ML. Stroke Risk Factors. In: Norris JW, Hachinski VC, editors. Prevention of Stroke. New York, NY: Springer New York; 1991. p. 83-101.

Eltzschig HK, Eckle T. Ischemia and reperfusion[mdash]from mechanism to translation. Nat Med 2011; 17(11): 1391-401.

Fang SH, Wei EQ, Zhou Y, Wang ML, Zhang WP, Yu GL*, et al.* Increased expression of cysteinyl leukotriene receptor-1 in the brain mediates neuronal damage and astrogliosis after focal cerebral ischemia in rats. Neuroscience 2006; 140(3): 969-79.

Fluri F, Schuhmann MK, Kleinschnitz C. Animal models of ischemic stroke and their application in clinical research. Drug design, development and therapy 2015; 9: 3445-54.

Fonarow GC, Smith EE, Saver JL, Reeves MJ, Bhatt DL, Grau-Sepulveda MV*, et al.* Timeliness of tissue-type plasminogen activator therapy in acute ischemic

stroke: patient characteristics, hospital factors, and outcomes associated with door-to-needle times within 60 minutes. Circulation 2011; 123(7): 750-8.

Forslin Aronsson S, Spulber S, Popescu LM, Winblad B, Post C, Oprica M*, et al.* alpha-Melanocyte-stimulating hormone is neuroprotective in rat global cerebral ischemia. Neuropeptides 2006; 40(1): 65-75.

Garcia JH. Experimental ischemic stroke: a review. Stroke; a journal of cerebral circulation 1984; 15(1): 5-14.

Gegelashvili G, Danbolt NC, Schousboe A. Neuronal soluble factors differentially regulate the expression of the GLT1 and GLAST glutamate transporters in cultured astroglia. Journal of neurochemistry 1997; 69(6): 2612-5.

Giffard RG, Swanson RA. Ischemia-induced programmed cell death in astrocytes. Glia 2005; 50(4): 299-306.

Go AS, Mozaffarian D, Roger VL, Benjamin EJ, Berry JD, Blaha MJ*, et al.* Executive summary: heart disease and stroke statistics--2014 update: a report from the American Heart Association. Circulation 2014; 129(3): 399-410.

Gordon GR, Choi HB, Rungta RL, Ellis-Davies GC, MacVicar BA. Brain metabolism dictates the polarity of astrocyte control over arterioles. Nature 2008; 456(7223): 745-9.

Gordon GR, Mulligan SJ, MacVicar BA. Astrocyte control of the cerebrovasculature. Glia 2007; 55(12): 1214-21.

Group TNIONDASR-PSS. Tissue plasminogen activator for acute ischemic stroke. . The New England journal of medicine 1995; 333(24): 1581-7.

Guzman M, Blazquez C. Ketone body synthesis in the brain: possible neuroprotective effects. Prostaglandins, leukotrienes, and essential fatty acids 2004; 70(3): 287-92.

Had-Aissouni L. Toward a new role for plasma membrane sodium-dependent glutamate transporters of astrocytes: maintenance of antioxidant defenses beyond extracellular glutamate clearance. Amino acids 2012; 42(1): 181-97.

Halestrap AP. The SLC16 gene family - structure, role and regulation in health and disease. Molecular aspects of medicine 2013; 34(2-3): 337-49.

Hamprecht B, Verleysdonk S, Wiesinger H. Enzymes of carbohydrate and energy metabolism. In: Kettenmann H, Ransom B, editors. Neuroglia. Oxford: Oxford University Press; 2005. p. 202-15.

Hansel G. Efeitos neuroprotetores da guanosina e da inosina frente às ações neurotóxicas da isquemia cerebral in vivo. Porto Alegre: Universidade Federal do Rio Grande do Sul - UFRGS; 2014.

Haupt C, Witte OW, Frahm C. Up-regulation of Connexin43 in the glial scar following photothrombotic ischemic injury. Molecular and cellular neurosciences 2007; 35(1): 89-99.

Hayakawa K, Nakano T, Irie K, Higuchi S, Fujioka M, Orito K*, et al.* Inhibition of reactive astrocytes with fluorocitrate retards neurovascular remodeling and recovery after focal cerebral ischemia in mice. Journal of cerebral blood flow and metabolism : official journal of the International Society of Cerebral Blood Flow and Metabolism 2010; 30(4): 871-82.

Hertz L, Hertz E. Cataplerotic TCA cycle flux determined as glutamate-sustained oxygen consumption in primary cultures of astrocytes. Neurochemistry international 2003; 43(4-5): 355-61.

Hol EM, Pekny M. Glial fibrillary acidic protein (GFAP) and the astrocyte intermediate filament system in diseases of the central nervous system. Current opinion in cell biology 2015; 32: 121-30.

Hossmann KA. Animal Models of Cerebral Ischemia. 1. Review of Literature. Cerebrovascular Diseases 1991; 1(suppl 1)(Suppl. 1): 2-15.

Howells DW, Porritt MJ, Rewell SSJ, O'Collins V, Sena ES, van der Worp HB*, et al.* Different strokes for different folks: the rich diversity of animal models of focal cerebral ischemia. Journal of cerebral blood flow and metabolism : official journal of the International Society of Cerebral Blood Flow and Metabolism 2010; 30(8): 1412-31.

Ibrahim MZ. Glycogen and its related enzymes of metabolism in the central nervous system. Advances in anatomy, embryology, and cell biology 1975; 52(1): 3-89.

Katsura K, Kristian T, Siesjo BK. Energy metabolism, ion homeostasis, and cell damage in the brain. Biochemical Society transactions 1994; 22(4): 991-6.

Kaur C, Ling EA. Blood brain barrier in hypoxic-ischemic conditions. Current neurovascular research 2008; 5(1): 71-81.

Koehler RC, Roman RJ, Harder DR. Astrocytes and the regulation of cerebral blood flow. Trends in neurosciences 2009; 32(3): 160-9.

Koton S, Schneider AL, Rosamond WD, Shahar E, Sang Y, Gottesman RF*, et al.* Stroke incidence and mortality trends in US communities, 1987 to 2011. Jama 2014; 312(3): 259-68.

Kramer M, Dang J, Baertling F, Denecke B, Clarner T, Kirsch C*, et al.* TTC staining of damaged brain areas after MCA occlusion in the rat does not constrict quantitative gene and protein analyses. Journal of neuroscience methods 2010; 187(1): 84-9.

Krzyzanowska W, Pomierny B, Budziszewska B, Filip M, Pera J. N-Acetylcysteine and Ceftriaxone as Preconditioning Strategies in Focal Brain Ischemia: Influence on Glutamate Transporters Expression. Neurotoxicity research 2016.

Kunz A, Dirnagl U, Mergenthaler P. Acute pathophysiological processes after ischaemic and traumatic brain injury. Best practice & research Clinical anaesthesiology 2010; 24(4): 495-509.

Li H, Zhang N, Sun G, Ding S. Inhibition of the group I mGluRs reduces acute brain damage and improves long-term histological outcomes after photothrombosis-induced ischaemia. ASN neuro 2013; 5(3): 195-207.

Li L, Lundkvist A, Andersson D, Wilhelmsson U, Nagai N, Pardo AC*, et al.* Protective role of reactive astrocytes in brain ischemia. Journal of cerebral blood flow and metabolism : official journal of the International Society of Cerebral Blood Flow and Metabolism 2008; 28(3): 468-81.

Lieth E, Barber AJ, Xu B, Dice C, Ratz MJ, Tanase D*, et al.* Glial reactivity and impaired glutamate metabolism in short-term experimental diabetic retinopathy. Penn State Retina Research Group. Diabetes 1998; 47(5): 815-20.

Lin JH, Weigel H, Cotrina ML, Liu S, Bueno E, Hansen AJ*, et al.* Gap-junction-mediated propagation and amplification of cell injury. Nature neuroscience 1998; 1(6): 494-500.

Lipton P. Ischemic cell death in brain neurons. Physiological reviews 1999; 79(4): 1431-568.

Magistretti PJ. Energy Metabolism. In: MJ Z, FE B, SC L, JL R, LR S, editors. Fundamental Neuroscience. San Diego: Academic Press; 1999. p. 389-413.

Malarkey EB, Parpura V. Mechanisms of glutamate release from astrocytes. Neurochemistry international 2008; 52(1-2): 142-54.

Martin RL, Lloyd HG, Cowan AI. The early events of oxygen and glucose deprivation: setting the scene for neuronal death? Trends in neurosciences 1994; 17(6): 251-7.

McIlwain H. Electrical influences and speed of chemical change in the brain. Physiological reviews 1956; 36(3): 355-75.

McKenna MC. Substrate competition studies demonstrate oxidative metabolism of glucose, glutamate, glutamine, lactate and 3-hydroxybutyrate in cortical astrocytes from rat brain. Neurochemical research 2012; 37(11): 2613-26.

McKenna MC. Glutamate pays its own way in astrocytes. Frontiers in endocrinology 2013; 4: 191.

McKenna MC, Sonnewald U, Huang X, Stevenson J, Zielke HR. Exogenous glutamate concentration regulates the metabolic fate of glutamate in astrocytes. Journal of neurochemistry 1996a; 66(1): 386-93.

McKenna MC, Tildon JT, Stevenson JH, Boatright R, Huang S. Regulation of energy metabolism in synaptic terminals and cultured rat brain astrocytes: differences revealed using aminooxyacetate. Developmental neuroscience 1993; 15(3-5): 320-9.

McKenna MC, Tildon JT, Stevenson JH, Huang X. New insights into the compartmentation of glutamate and glutamine in cultured rat brain astrocytes. Developmental neuroscience 1996b; 18(5-6): 380-90.

Middeldorp J, Hol EM. GFAP in health and disease. Progress in neurobiology 2011; 93(3): 421-43.

Ministério Da Saúde. Acidente Vascular Cerebral (AVC). 2012 Disponível em: http://www.brasil.gov.br/saude/2012/04/acidente-vascular-cerebral-avc:. Acesso em 21 de fevereiro de 2016.

Nakase T, Fushiki S, Naus CC. Astrocytic gap junctions composed of connexin 43 reduce apoptotic neuronal damage in cerebral ischemia. Stroke; a journal of cerebral circulation 2003; 34(8): 1987-93.

Nawashiro H, Brenner M, Fukui S, Shima K, Hallenbeck JM. High susceptibility to cerebral ischemia in GFAP-null mice. Journal of cerebral blood flow and metabolism : official journal of the International Society of Cerebral Blood Flow and Metabolism 2000; 20(7): 1040-4.

Nawashiro H, Messing A, Azzam N, Brenner M. Mice lacking GFAP are hypersensitive to traumatic cerebrospinal injury. Neuroreport 1998; 9(8): 1691-6.

Nedergaard M, Dirnagl U. Role of glial cells in cerebral ischemia. Glia 2005; 50(4): 281-6.

Nedergaard M, Takano T, Hansen AJ. Beyond the role of glutamate as a neurotransmitter. Nature reviews Neuroscience 2002; 3(9): 748-55.

Nicoli F, Lefur Y, Denis B, Ranjeva JP, Confort-Gouny S, Cozzone PJ. Metabolic Counterpart of Decreased Apparent Diffusion Coefficient During Hyperacute Ischemic Stroke: A Brain Proton Magnetic Resonance Spectroscopic Imaging Study. Stroke; a journal of cerebral circulation 2003; 34(7): e82-e7.

Nijboer CH, Heijnen CJ, Degos V, Willemen HL, Gressens P, Kavelaars A. Astrocyte GRK2 as a novel regulator of glutamate transport and brain damage. Neurobiology of disease 2013; 54: 206-15.

OMS. World Health Report; 2002. Disponível em: http://www.who.int/whr/2002/en/. Acesso em 21 de janeiro de 2016.

OMS. The top ten causes of death. 2010 Disponível em: http://www.who.int/mediacentre/factsheets/fs310/en/. Acesso em 03 de setembro de 2015.

Orrenius S, Ankarcrona M, Nicotera P. Mechanisms of calcium-related cell death. Advances in neurology 1996; 71: 137-49; discussion 49-51.

Panickar KS, Norenberg MD. Astrocytes in cerebral ischemic injury: morphological and general considerations. Glia 2005; 50(4): 287-98.

Parnham M, Sies H. Ebselen: prospective therapy for cerebral ischaemia. Expert opinion on investigational drugs 2000; 9(3): 607-19.

Pellerin L. Lactate as a pivotal element in neuron-glia metabolic cooperation. Neurochemistry international 2003; 43(4-5): 331-8.

Pellerin L, Bergersen LH, Halestrap AP, Pierre K. Cellular and subcellular distribution of monocarboxylate transporters in cultured brain cells and in the adult brain. Journal of neuroscience research 2005; 79(1-2): 55-64.

Pellerin L, Magistretti PJ. Glutamate uptake into astrocytes stimulates aerobic glycolysis: a mechanism coupling neuronal activity to glucose utilization. Proceedings of the National Academy of Sciences of the United States of America 1994; 91(22): 10625-9.

Petito CK, Babiak T. Early proliferative changes in astrocytes in postischemic noninfarcted rat brain. Annals of neurology 1982; 11(5): 510-8.

Phillis JW, O'Regan MH, Estevez AY, Song D, VanderHeide SJ. Cerebral energy metabolism during severe ischemia of varying duration and following reperfusion. Journal of neurochemistry 1996; 67(4): 1525-31.

Phillis JW, Ren J, O'Regan MH. Transporter reversal as a mechanism of glutamate release from the ischemic rat cerebral cortex: studies with DL-threo-beta-benzyloxyaspartate. Brain research 2000; 880(1-2): 224.

Phillis JW, Ren J, O'Regan MH. Studies on the effects of lactate transport inhibition, pyruvate, glucose and glutamine on amino acid, lactate and glucose release from the ischemic rat cerebral cortex. Journal of neurochemistry 2001; 76(1): 247-57.

Philp NJ, Yoon H, Grollman EF. Monocarboxylate transporter MCT1 is located in the apical membrane and MCT3 in the basal membrane of rat RPE. The American journal of physiology 1998; 274(6 Pt 2): R1824-8.

Philp NJ, Yoon H, Lombardi L. Mouse MCT3 gene is expressed preferentially in retinal pigment and choroid plexus epithelia. American journal of physiology Cell physiology 2001; 280(5): C1319-26.

Pierre K, Magistretti PJ, Pellerin L. MCT2 is a major neuronal monocarboxylate transporter in the adult mouse brain. J Cereb Blood Flow Metab 2002; 22(5): 586-95.

Pierre K, Pellerin L. Monocarboxylate transporters in the central nervous system: distribution, regulation and function. Journal of neurochemistry 2005; 94(1): 1-14.

Rafiki A, Boulland JL, Halestrap AP, Ottersen OP, Bergersen L. Highly differential expression of the monocarboxylate transporters MCT2 and MCT4 in the developing rat brain. Neuroscience 2003; 122(3): 677-88.

Rosafio K, Castillo X, Hirt L, Pellerin L. Cell-specific modulation of monocarboxylate transporter expression contributes to the metabolic reprograming taking place following cerebral ischemia. Neuroscience 2016; 317: 108-20.

Rosafio K, Pellerin L. Oxygen tension controls the expression of the monocarboxylate transporter MCT4 in cultured mouse cortical astrocytes via a hypoxia-inducible factor-1alpha-mediated transcriptional regulation. Glia 2014; 62(3): 477-90.

Rothstein JD, Martin L, Levey AI, Dykes-Hoberg M, Jin L, Wu D*, et al.* Localization of neuronal and glial glutamate transporters. Neuron 1994; 13(3): 713-25.

Schlag BD, Vondrasek JR, Munir M, Kalandadze A, Zelenaia OA, Rothstein JD*, et al.* Regulation of the glial Na+-dependent glutamate transporters by cyclic AMP analogs and neurons. Molecular pharmacology 1998; 53(3): 355-69.

Shimada IS, Borders A, Aronshtam A, Spees JL. Proliferating reactive astrocytes are regulated by Notch-1 in the peri-infarct area after stroke. Stroke; a journal of cerebral circulation 2011; 42(11): 3231-7.

Singh N, Sharma G, Mishra V. Hypoxia inducible factor-1: its potential role in cerebral ischemia. Cellular and molecular neurobiology 2012; 32(4): 491-507.

Sonnewald U, Westergaard N, Petersen SB, Unsgard G, Schousboe A. Metabolism of [U-13C]glutamate in astrocytes studied by 13C NMR spectroscopy: incorporation of more label into lactate than into glutamine demonstrates the importance of the tricarboxylic acid cycle. Journal of neurochemistry 1993; 61(3): 1179-82.

Stobart JL, Anderson CM. Multifunctional role of astrocytes as gatekeepers of neuronal energy supply. Frontiers in cellular neuroscience 2013; 7: 38.

Strom JO, Ingberg E, Theodorsson A, Theodorsson E. Method parameters' impact on mortality and variability in rat stroke experiments: a meta-analysis. BMC neuroscience 2013; 14: 41.

Sullivan SM, Lee A, Bjorkman ST, Miller SM, Sullivan RK, Poronnik P*, et al.* Cytoskeletal anchoring of GLAST determines susceptibility to brain damage: an identified role for GFAP. The Journal of biological chemistry 2007; 282(40): 29414-23.

Swanson RA, Liu J, Miller JW, Rothstein JD, Farrell K, Stein BA*, et al.* Neuronal regulation of glutamate transporter subtype expression in astrocytes. The Journal of neuroscience : the official journal of the Society for Neuroscience 1997; 17(3): 932-40.

Swanson RA, Ying W, Kauppinen TM. Astrocyte influences on ischemic neuronal death. Current molecular medicine 2004; 4(2): 193-205.

Szele FG, Alexander C, Chesselet MF. Expression of molecules associated with neuronal plasticity in the striatum after aspiration and thermocoagulatory lesions of the cerebral cortex in adult rats. The Journal of neuroscience : the official journal of the Society for Neuroscience 1995; 15(6): 4429-48.

Takatsuru Y, Nabekura J, Koibuchi N. Contribution of neuronal and glial circuit in intact hemisphere for functional remodeling after focal ischemia. Neuroscience research 2014; 78: 38-44.

Takizawa S, Hakim AM. Animal Models of Cerebral Ischemia. 2. Rat Models. Cerebrovascular Diseases 1991; 1(suppl 1)(Suppl. 1): 16-21.

Tanaka H, Katoh A, Oguro K, Shimazaki K, Gomi H, Itohara S*, et al.* Disturbance of hippocampal long-term potentiation after transient ischemia in GFAP deficient mice. Journal of neuroscience research 2002; 67(1): 11-20.

Weir MD, Thomas DG. Effect of dexamethasone on glutamine synthetase and glial fibrillary acidic protein in normal and transformed astrocytes. Clinical neuropharmacology 1984; 7(4): 303-6.

Wiener CM, Booth G, Semenza GL. In vivo expression of mRNAs encoding hypoxia-inducible factor 1. Biochemical and biophysical research communications 1996; 225(2): 485-8.

Yao H, Ginsberg MD, Eveleth DD, LaManna JC, Watson BD, Alonso OF*, et al.* Local cerebral glucose utilization and cytoskeletal proteolysis as indices of evolving focal ischemic injury in core and penumbra. Journal of cerebral blood flow and metabolism : official journal of the International Society of Cerebral Blood Flow and Metabolism 1995; 15(3): 398-408.

Yasuda Y, Tateishi N, Shimoda T, Satoh S, Ogitani E, Fujita S. Relationship between S100beta and GFAP expression in astrocytes during infarction and glial scar formation after mild transient ischemia. Brain research 2004; 1021(1): 20-31.

Ye YL, Shi WZ, Zhang WP, Wang ML, Zhou Y, Fang SH*, et al.* Cilostazol, a phosphodiesterase 3 inhibitor, protects mice against acute and late ischemic brain injuries. European journal of pharmacology 2007; 557(1): 23-31.

Yu A, Hertz L. Metabolic sources of energy in astrocytes. In: Hertz L, Kvamme E, McGeer E, Schousboe A, editors. Glutamine, Glutamate and GABA in the Central Nervous System. New York: Alan R. Liss; 1983. p. 431-9.

Yu M, Xue Y, Liang W, Zhang Y, Zhang Z. Protection mechanism of early hyperbaric oxygen therapy in rats with permanent cerebral ischemia. Journal of physical therapy science 2015; 27(10): 3271-4.

Zalc B. Neuroglia edited by H. Kettenmann and B. R. Ransom. Oxford University Press, Oxford/New York, 1995, ISBN 0-19-507847-0, 1,104 pp., $195.00. Journal of neurochemistry 1997; 68(6): 2625-.

Zamanian JL, Xu L, Foo LC, Nouri N, Zhou L, Giffard RG*, et al.* Genomic analysis of reactive astrogliosis. The Journal of neuroscience : the official journal of the Society for Neuroscience 2012; 32(18): 6391-410.

Zivin JA. Factors determining the therapeutic window for stroke. Neurology 1998; 50(3): 599-603.

8. ANEXOS

8.1. INSTRUÇÕES PARA AUTORES – *BRAIN OXFORD JOURNAL*

Manuscript categories

Original Articles published in *Brain* address neurological diseases and their mechanisms, and should contain no more than eight display items (figures and/or tables). Animal studies are considered but must demonstrate novel signalling pathways underlying disease or describe novel therapeutic interventions, and have significant clinical relevance. Papers that are predominantly methodological or that present hypotheses or models unsupported by original data are not suitable. **Studies of normal subjects (including the aged) and normal signalling mechanisms in animals are not considered** and will be returned to authors without peer review. **Preliminary reports of work in progress or single case studies are not considered.** More detailed studies of single cases may in rare instances be considered as Reports (see below) only when they resolve definitively an important problem in the field or when the data lead to a significant conceptual advance. Studies of single cases that can be readily performed on groups of patients will not be considered. The ARRIVE guidelines for animal research should be followed where possible.

Authorship and ethical guidelines

Declaration of Authorship

All persons designated as authors should qualify for authorship. The order in which names appear should be a joint decision by the co-authors. Each author must have participated sufficiently in the work to take public responsibility for the content. Authorship credit should be based on substantial contribution to conception and design, execution, or analysis and interpretation of data. All authors should be involved in drafting the article or revising it critically for intellectual content and must have read and approved the final version of the manuscript. Assurance that all authors of the paper have fulfilled these criteria for authorship should be given in the covering letter. Authors must list their names at the top of the paper and should comply with the International

Committee of Medical Journal Editors (ICMJE) criteria for authorship. Consortia or working group authors will be listed on PubMed as collaborators rather than authors. Collaborator names are searchable on PubMed in the same way as authors. PubMed rules for this can be found here.

A Declaration of Authorship must be signed by all authors to confirm that they consent to take public responsibility for the content of the paper and that consent from patients has been obtained. This form is required to conform to good editorial practice and to avoid disputes and must be signed by all participating authors. To reduce the time from submission to the receipt of the declaration forms, during the submission process the corresponding author will be asked, as a prerequisite to submission to Brain, to take full responsibility for all authors listed on the paper. If authors are not at the same venue, separate forms may be used for each author.

The Declaration of Authorship is available to download here or from the online submission site, where it can be found in the top right hand corner of the login page under 'instructions and forms'.

Once signed, you can return your form to us in one of three ways:
(i) Upload with your manuscript
(ii) E-mail to the editorial office (brain@ucl.ac.uk)
(iii) Post to the address given on the contacts page

Please note that the Declaration of Authorship differs from the License to Publish which is sent by our publishers after a paper has been accepted. Both forms must be completed prior to publication.

Conflicts of interest

Potential financial interests of any authors must be disclosed to the Editor by filling in the appropriate section on Manuscript Central during submission of the manuscript. This statement will be published at the Editor's discretion. A conflict of interest would ensue if: there is anything that would embarrass you or any of your co-authors if it was to emerge after publication and had not been declared, e.g. shareholding in or receipt of a grant or consultancy fee from a

pharmaceutical company or a contract from a medical devices manufacturer. Financial concessions on purchasing equipment in return for publicity of that item should be declared. All sources of funding must be disclosed at the end of the main text under a separate heading 'Funding'.

Ethical guidelines

Confidentiality

All material submitted to *Brain* remains confidential and we operate a peer review system in which the identity of the referees is protected.

Duplicate publication

Duplicate publication is the publication of the same paper or substantially similar papers in more than one journal. Authors must explain in the submission letter any prior publication of the same or a substantially similar paper, and should explain any circumstances that might lead the Editor or reviewers to believe that the paper may have been published elsewhere (for example, when the title of a submitted paper is the same as or similar to the title of a previously published article).

If work that makes up more than 10% of the manuscript submitted to *Brain* has been published elsewhere, please provide a copy of the published article in order that we can make a judgement on the amount of overlap without delay.

If a member of the editorial board learns that work under consideration has previously been published in whole or in part, the Editor may return the paper without review, reject the paper, announce the duplication publicly in an editorial and/or contact the authors' employers.

Submission of manuscripts to more than one journal

Authors may not send the same manuscript to more than one journal concurrently. If this occurs, the Editor may return the paper without review, reject the paper, contact the Editor of the other journal(s) in question and/or contact the authors' employers.

Plagiarism and scientific misconduct

Plagiarism is the use of others' published and unpublished ideas or words (or other intellectual property) without due reference or permission and/or their presentation as new and original points. Plagiarism is serious scientific misconduct and will be dealt with accordingly. Text may be checked for passages plagiarized from other publications at the Editor's discretion. The Editor reserves the right to inspect raw data.

Data auditing

The journal reserves the right to view original figures and data and may make periodic requests to see these.

COPE

Brain is a member of the Committee On Publication Ethics, COPE. Please visit their websitewww.publicationethics.org for guidance on good editorial conduct. Links to further information on research ethics can be found here.

Consent from patients

Papers reporting experiments on patients or healthy volunteers must record the fact that the subjects' consent was obtained according to the Declaration of Helsinki and that it has been approved by the ethical committee of the institution in which the work was performed. Consent must be also recorded when photographs of patients are shown or other details are given that could lead to identification of these individuals.

Animal research: reporting in vivo experiments

The ARRIVE guidelines must be followed when preparing manuscripts for *Brain*. Experiments with animals should be performed in accordance with the legal requirements of the relevant local or national authority and the name of the authorizing body should be stated in the paper. Procedures should be such that experimental animals do not suffer unnecessarily. The text of the paper should include experimental details of the procedure and of anaesthetics used. The journal reserves the right to reject papers where the ethical aspects are, in the Editor's opinion, open to doubt.

Drug disclaimer

The mention of trade names, commercial products or organizations, and the inclusion of advertisements in the journal does not imply endorsement by the Guarantors of *Brain*, the Editor, the Editorial Board, Oxford University Press or the organization to which the authors are affiliated. The editors and publishers have taken all reasonable precautions to verify drug names and doses, the results of experimental work and clinical findings published in the journal. The ultimate responsibility for the use and dosage of drugs mentioned in the journal and in interpretation of published material lies with the medical practitioner, and the editors and publishers cannot accept liability for damages arising from any errors or omissions in the journal. Please inform the editors of any errors.

Disclaimer

Statements of fact and opinion in published articles are those of the respective authors and contributors and not of *Brain* or Oxford University Press. Neither Oxford University Press nor *Brain* make any representations, express or implied, in respect of the accuracy of the material in this journal and cannot accept any legal responsibility or liability for any errors or omissions that may be made. The reader should make his/her own evaluation as to the appropriateness or otherwise of any experimental technique described.

Preparing a manuscript

Brain style

Brain has specific style criteria and using these in preparing your manuscript will speed up the production process should your article be accepted for publication.

Title page

(i) Full title of the paper (maximum of 100 characters). Please note we do not allow any abbreviations in titles except for current accepted gene symbols.
(ii) Author names and affiliations.
(iii) Full postal and email address of the corresponding author.
(iv) Running title (maximum of 40 characters).

Abstract

For Original Articles and Reviews please include an abstract containing up to 400 words. For Updates and Reports the abstract should be no longer 200 words. The abstract must summarize the paper in full, including background, methods, results and conclusion, although these subtitles should not be included. Details such as the number of subjects, number of controls, the age range of patients and their gender should be included if appropriate. Statistical evidence to support your main conclusions should also be included here if space permits. No abbreviations should appear in the abstract, except for current accepted gene symbols. Grey Matter articles and Letters to the Editor do not have an abstract.

Keywords

Keywords of the authors' choice up to a maximum of five should be provided below the abstract.

Abbreviations

Aim to make your paper reader-friendly to those outside your field, avoiding all abbreviations where possible. The Scientific Editor reserves the right to replace abbreviations with their full meaning.

Do not abbreviate the name of a disease unless it is unwieldy and complicated: Parkinson's disease, Alzheimer's disease, multiple sclerosis and Huntington's disease etc. are not abbreviated in *Brain*, but hereditary motor and sensory neuropathies may be abbreviated to HMSN.
The following abbreviations do not need to be defined or listed. AIDS; ANOVA; ATP; A,T,C,G; CNS; CSF; CT; DNA; ECG; EEG; EMG; GABA; HIV; MRI; PET; PCR; RNA.
Any other abbreviation used in the paper must be defined. Abbreviations used in the text should be provided in an alphabetized list below the keywords and do not need defining elsewhere in the manuscript. Abbreviations used only once in the text or those better known by their abbreviated form, can be written as e.g. NADH (reduced nicotinamide-adenine dinucleotide).

Abbreviations for scientific units should conform to the Système Internationale (SI units). The statistical guidelines advocated by the International Committee of Medical Journal Editors (Ann Intern Med 1988; 108: 266-73) should be followed.

Numbers

The numbers one to nine are written in full, unless followed by a unit, e.g. five mice, 6 days, seven patients with Parkinson's disease, 8 ml.

Main text

Sections should include, in order: Introduction, Materials and methods, Results, Discussion, Acknowledgements, Funding, Supplementary material, References. Reviews and Grey Matter articles can contain subheadings of your choice.

Manuscripts should be 1.5 or double-spaced, including text, tables, legends and references. Justified text in Times New Roman font size 12 is used, with main headings in font size 14 and sub-headings in 13 pt. Headings and subheadings should be no more than 100 characters in length. A guide to in-text citations is given below.

The main text should be saved as a DOC or RTF file. PDF files are not acceptable. Please do not prepare your manuscript as a LaTeX file, as these do not convert correctly for review. Legends for figures should be listed at the end of the main body of the manuscript.

Gene nomenclature

Authors should use approved gene nomenclature where this is available. Authors proposing a new gene nomenclature should contact the HUGO Gene Nomenclature Committee.

For human genes, please use symbols approved by the HUGO Gene Nomenclature Committee (HGNC). HGNC nomenclature can be queried. The species listed below all have gene nomenclature committees. Please use the nomenclature they have approved by searching for gene symbols at the following links:

Mouse

Rat

Gene symbols and names in all other mammals (and usually all vertebrates) should follow the same nomenclature as the human gene.

It can be difficult for readers to determine whether authors are referring to a gene or its corresponding protein, therefore it is important to use accepted conventions for gene and protein symbols. Symbols for genes should be italicized (*IGF1*), whereas symbols for proteins are not italicized (IGF1). Gene names that are written out in full are not italicized (insulin-like growth factor 1).

Authors should check each gene/protein name and symbol in their paper even if it has been published previously. Genes and their corresponding proteins often have different names and symbols and sometimes you may find that the approved gene/protein name or symbol has been updated. Brain prefers that the same symbol is used for genes and proteins; however, where proteins are more widely known by an alternative name/symbol, then the encoding gene, where possible, should be referred to e.g. 'TRAIL (encoded by *TNFSF10*)'. Synonyms can be referred to using 'also known as' or 'previously known as' e.g. TARDBP (previously known as TDP-43). Thereafter, use the current approved symbol and not the previous designation.

Brain allows the use of gene symbols in the abstract and headings. Gene symbols do not need defining in the Abbreviations list. For clarity it is best to be consistent in the use of either the full gene name, or the symbol throughout the text, but use of either is acceptable.

Statistics

Authors are expected to apply the most appropriate statistical tools for data analysis, and it is acceptable to present results from frequentist, information-theory, and Bayesian approaches in the same manuscript. Authors should include a section at the end of the 'Materials and methods' section, with the heading 'Statistical analysis'. Describe procedures used to evaluate fit of the model to the data, such as goodness-of-fit tests, inspection of residuals, or tests of model assumptions. For results of statistical tests, report the statistical test

that was applied (e.g. two-sample *t*-test, analysis of covariance), the test statistic (e.g. t, U, F, r), degrees of freedom as subscripts to the test statistic (Lazic, 2010), and the exact probability value (*P*). Indicate whether statistical tests were one- or two-tailed, and the alpha-level that was used to determine significance (e.g. $P < 0.05$). A 95% confidence interval for the size of each effect is encouraged (Halsey *et al*., 2015). *Post hoc* power tests are discouraged.

Authors should include a section in the 'Materials and methods' section titled 'Experimental design'. In line with the ARRIVE guidelines, authors should specify how blinding was performed (e.g. third party concealment of treatments with individually uniquely coded vials) and how randomization was performed (e.g. the order of treatments was randomized by drawing vial code numbers from a hat without replacement using a randomized block design). If either blinding or randomization was not performed, justification should be given. Details of a *priori* sample size calculations should be presented (including power to be achieved, alpha, the source of means and standard deviations involved in the calculation, and effect size). This is important because a statistical result is more likely to be a false positive or false negative result when the study has low power (Button *et al*., 2013). Pseudoreplication should be minimized at the design stage (Lazic, 2010).

References

Button KS, Ioannidis JP, Mokrysz C, Nosek BA, Flint J, Robinson ES, *et al*. Power failure: why small sample size undermines the reliability of neuroscience. Nat Rev Neurosci. 2013;14(5):365-76.

Halsey LG, Curran-Everett D, Vowler SL, Drummond GB. The fickle P value generates irreproducible results. Nat Methods. 2015;12(Go *et al.*):179-85.

Lazic SE. The problem of pseudoreplication in neuroscientific studies: is it affecting your analysis? BMC Neurosci. 2010;11:5.

Word count

Original Articles may contain a maximum of 6000 words in the main text excluding the abstract, title page, tables, figure legends and references. **Reviews** may contain up to 9000 words in the main text. Abstracts of **Original Articles** and **Reviews** may contain up to 400 words. **Reports** may contain a maximum of 2500 words in the main text and up to 200 words in the Abstract and are limited to 30 references. **Updates** may contain up to 3000 words in the main text and 200 words in the abstract. **Grey Matter** articles may contain a maximum of 4000 words, have no abstract and are limited to 10 references. **Letters to the Editor** may contain up to 1500 words and have no abstract.

Tables

Each table should be self-explanatory and include a brief descriptive title. Tables must be supplied in Word (.doc) format to enable editing. Please avoid abbreviating words in tables unless already defined in the abbreviations list. Abbreviations must be listed below the table if used. Please supply landscape tables in a separate file. PPT and XLS files can be uploaded but the layout may change when converted to PDF for review.

Figures

For the review process, figures can be embedded in the main text if they are of sufficient quality, but separate files are preferred. For review, the high resolution images you upload will automatically be converted to PDF and HTML for reviewers to download. Please label and number your figures and figure legends clearly. In the text refer to figures as Fig. 1, Fig. 2A, Fig. 2B, Supplementary Fig. 1 etc. Each figure should be given a short heading, which will be published in bold font.

For publication, you will be required to supply separate high-resolution files at resolutions of 300 dpi for colour and half-tone (grey shaded) artwork or 600 dpi for black and white line drawings. TIF files are preferred. PDF files are not recommended. We advise that you create your high-resolution images first as these will be easily converted into low-resolution images by our online submission system for peer-review. For useful information on preparing your

figures for publication, click here. Figures should be prepared to fit into a single column (90 mm width) or two columns (185 mm). The journal reserves the right to reduce the size of illustrative material. *Brain* does not charge for printing colour figures.

Original articles and Grey Matter articles should contain no more than eight display items (figures and/or tables). Updates and Reports should contain no more than four display items. Authors of Updates and Reviews are encouraged to include figures, boxes and glossary terms, which might help the reader to understand technical or conceptual points. Letters to the Editor should contain no more than two display items.

Requirements for images

Image manipulation beyond minimal processing (for instance, to add arrows to a micrograph) is strictly forbidden. Unprocessed data and metadata files must be archived by the author(s) in case they are requested by the editorial team or reviewers during manuscript evaluation. This requirement for archiving data and metadata for images is particularly important because readers occasionally highlight issues with images after publication, and authors may be required to respond to such queries via the Editor. All digitized images submitted with the final version of the manuscript must be of high quality and have resolutions of at least 300 dpi for colour, 600 dpi for greyscale and 1200 dpi for line art. All images must accurately represent the original data in line with the latest standards now expected by the research community.

Please list in the methods all tools and software used to acquire images, including image-gathering settings and any required processing manipulations.

Single images created from separately acquired (e.g. different times or from different locations) are not permitted unless it is clearly stated in the legend that the combined image is, for example, time-averaged data or a time-lapse sequence. If comparative images are required in one figure then separate images must be demarcated in the whole figure and described in the legend.

Changing contrast or brightness may be acceptable when it is applied evenly over the whole image including over the controls. Reducing or increasing

contrast to hide data is forbidden. Processing to emphasize a region in an image to the detriment of other regions is inappropriate, particularly where an attempt is made to reinforce significance of experimental data relative to the control.

Use of cloning and healing tools, such as those available in Photoshop, or any feature that deliberately obscures manipulations, is considered inappropriate. Where such tools are used by necessity, for example to remove identifying data about patients from an image, then this should be explicitly mentioned in the figure legend.

Electrophoretic gels and blots

Brain allows cropped gels and blots in the main paper only if they improve understanding of the data reported. Cropping must be indicated in the image and mentioned in the figure legend. Full-length gels and/or blots are to be made available as supplementary data, which will be published online if the manuscript is accepted.
All gels must include positive and negative controls, as well as molecular size markers; where these are not visible in the cropped figure then such controls must show clearly in the expanded data supplementary figure.

Please provide a citation for characterized antibodies. Where a citation is not yet available, then a detailed characterization demonstrating the specificity of the antibody and the range of reactivity of the reagent in the assay, should be supplied as supplementary information. *Brain* recommends submission of data and linking with an antibody profile database (e.g. Antibodypedia, 1DegreeBio).

While *Brain* discourages quantitative comparisons between samples on different gels/blots, if this is part of the experiment reported, then the legend must state that the samples derive from the same experiment and that gels/blots were processed in parallel. Sliced images that compare lanes that were non-adjacent in the original gel must have a dark line delineating the boundary between the gels. Loading controls (e.g. GAPDH, actin) must be run on the same blot. Sample processing controls run on different gels must be identified as such, and distinctly from loading controls.

Cropped gels/blots in the paper must retain important bands, and *Brain* recommends at least six band widths above and below the band under investigation.

Overexposure may mask additional bands and high-contrast gels and blots are therefore discouraged. Grey backgrounds are expected as the norm. If high contrast is unavoidable then multiple exposures should be presented in the supplementary information.
For quantitative comparisons, appropriate reagents, controls and imaging methods with linear signal ranges should be used.

Checklist

(i) All micrographs must carry a magnification bar.

(ii) Each figure must have a short title.

(iii) Legends for figures should be listed at the end of the main text document.

(iv) Abbreviations and symbols used in a figure must be defined in the figure legend unless they have been used and defined in the main text and appear in the main text list of abbreviations.

(v) Submit files at a resolution of 300 dpi or higher, and at a size that allows the reader to see detail.

(vi) In laying out figure panels avoid unnecessary empty space or clutter. Identify figure panels with capital letters (A, B, etc) in 9 pt at the final figure size. Panels should be ordered from left to right and then from top to bottom.

(vii) Keys to symbols should be as simple as possible.

(viii) Axes should not extend beyond the range of the data. Use leading zeros on decimals (e.g. 0.1).

(ix) Solid symbols are preferable to open symbols except to indicate data overlap. Circles, squares, diamonds and triangles are preferable to crosses.

Symbols and lines should be distinguishable when the figure is reduced, and no smaller than 5 and 0.5 pt, respectively at the final size.

(x) Bar charts with a single bar or with a bar indicating 100% should be avoided. Keep bar width to the minimum required for legibility.

(xi) Avoid using different shades of grey or colours that are close in hue to identify different symbols or columns in a bar chart. Colour should be used sparingly to identify different categories of data, and red and green should not be used together in graphs. Avoid shadows and unnecessary 3D effects.

Figure files

Figures should preferably be saved separately but can be embedded in a DOC file for review. Figures in revised manuscripts should be uploaded separately, preferably as high resolution TIFF files. PDF and HTML renditions are made for the following file extensions: doc, rtf, htm, wpd, txt, ppt, xls. The following file extensions are handled as images and converted to .jpg: gif, jpg, avs, bie, bmp, cgm, cmyk, dcx, dib, dicom, epdf, epi, epsf, epsi, ept, fax, fig, fits, fpx, gray, hdf, histo-gram, hpgl, jbig, jpeg, ico, label, map, miff, mng, mono, m2v, pbm, pcd, pcds, pcl, pcx, pgm, pix, Plasma, png, pnm, ppm, psd, ps2, rad, rgb, rgba, rla, rle, sgi, shtml, sun, tga, tif, tiff, tile, tim, ttf, uil, uyvy, vicar, vid, viff, xc, xbm, xpm, xwd, yuv. Note: eps, eps2, ps and ai file extensions are special. If the file designation is a (configurable) type image then they are run through GhostScript to convert to PDF (picture), otherwise they are run through ActivePDF to convert to PDF (text). Please note that while you may upload other file types, they will not be converted to PDF files and will not be viewable by referees.

Other file types

Other file types, such as Microsoft Excel spreadsheets (.xls) and Powerpoint presentations (.ppt) may be uploaded, however the layout may change when these are automatically converted to PDF files for review. The journal cannot accept LaTex files.

Thumbnail figure

At submission, please provide a thumbnail figure (can be a cartoon or schematic) in jpeg format. This will be used on our website and electronic Table of Contents. The figure should be 100 pixels (width) × 130 pixels (height).

Supplementary material

Supporting material that is not essential for inclusion in the full text of the manuscript, but would nevertheless benefit the reader, can be made available by the publisher as online-only content, linked to the online manuscript. The material should not be essential to understanding the conclusions of the paper, but should contain data that are additional or complementary and directly relevant to the article content. Such information might include more detailed methods, extended data sets/data analysis, or additional figures (including colour).

It is standard practice for appendices to be made available online-only as supplementary material. All text and figures must be provided in suitable electronic formats. All material to be considered as supplementary material must be submitted at the same time as the main manuscript for peer review. It cannot be altered or replaced after the paper has been accepted for publication. Please indicate clearly the material intended as Supplementary material upon submission. Also ensure that the Supplementary material is referred to in the main manuscript where necessary (Supplementary Fig. 1; Supplementary Table 1).

Please note that Supplementary material will not be edited, so ensure that it is clearly and succinctly presented, that the style of terms conforms with the rest of the paper, and that there are no tracked changes. Also ensure that the presentation will work on any internet browser.

A maximum of 10 files is acceptable to make up the Supplementary material unit for the article. The maximum size per file should not exceed 1.5 MB. Smaller files will be downloaded more efficiently by readers.

Recommendations:

(i) Provide all files in PDF (.pdf). Files supplied in other formats will be converted to PDF.

(ii) Images should be a maximum size of 640 x 480 pixels (9 x 6.8 inches at 72 pixels per inch).

(iii) Provide sound clips in .mp3 format

(v) Provide video clips in .mpg or .mp4 format. If video files are too large to be uploaded onto the submission site, please send them by Dropbox to the editorial office (brain@ucl.ac.uk). The journal staff, editors and reviewers will only be able to view these unconverted files if they have the appropriate software, which cannot be guaranteed.

Please note that supplementary material is not edited or typeset in any way, and is uploaded exactly as we receive it. For this reason, we do not send out proofs of the supplementary material, and authors need to ensure that these files are correct before submitting their paper.

References

Citations in text

Brain uses parenthetical citations in-text with the following stipulations: all in ascending chronological order followed by alphabetical order; *et al*. is in italics and used if there are more than two authors; last name of the first author is followed by comma then a space then the year. Citations are separated by semi-colons. If an author appears on two citations in one year add a, b in italics after the year. References should not be numbered either in the text or list of citations.The punctuation in the text should follow the style of the journal (see current issue).

Example (Richardson, 1996; Alberts, 2001, 2009; Smith and Black, 2008a; Bolton *et al.*, 2010a, b).

Reference list

Bibliographic references should be limited to essential literature. They should be listed at the end of the paper in alphabetical order and not numbered. Author

names are listed to a maximum of six; further names should be indicated by *et al*. For helpful examples of reference formatting consult Uniform requirements for Manuscripts submitted to Biomedical Journals. Please see common examples below. Any manuscript with an incorrectly formatted reference list will be returned to the author.

Journal article

Triggs WJ, Ghacibeh G, Springer U, Bowers D. Lateralized asymmetry of facial motor evoked potentials. Neurology 2005; 65: 541-4.

Morecraft RJ, Herrick JL, Stilwell-Morecraft KS, Louie JL, Schroeder CM, Ottenbacher JG, *et al.*Localization of arm representation in the corona radiata and internal capsule in the non-human primate. Brain 2002; 125: 176-98.

Supplement

Jones-Gotman M, Harnadek MC, Kubu CS. Neuropsychological assessment for temporal lobe epilepsy surgery. Can J Neurol Sci 2000; 27 (Suppl 1): S39–43.

Articles with the same first author:
Those by the author alone are listed first, those with two authors listed after these and any with three or more authors last. Author names must be given up to a maximum of six and any more should be indicated by et al.

If there is more than one paper from the same author for a given year, these should be listed a, b, c, etc.

Friston K, Ashburner J, Frith C, Poline J, Heather K, Frackowiak R. Spatial registration and normalization of images. Hum Brain Mapp 1995a; 3: 165–89.

Friston K, Holmes A, Worsley K, Poline J, Frith C, Frackowiak R. Statistical parametric maps in functional imaging: a general linear approach. Hum Brain Mapp 1995b; 2: 189–210.

Review Article

Handwerker HO, Kobal G. Psychophysiology of experimentally induced pain. [Review]. Physiol Rev 1993; 73: 639-71.

Book chapter

Barkovich AJ. Disorders of neuronal migration and organization. In: Kuzniecky RI, Jackson GD, editors. Magnetic resonance in epilepsy. New York: Raven Press; 1994. p. 235-55.

Book

Costa DC, Morgan GF, Lassen NA, editors. New trends in neurology and psychiatry. London: John Libbey; 1993.

Article on advance access using digital object identifier (DOI)

Trimble, M. June 10, 2012. Musing about medical muses. Brain 10.1093/brain/aws116

Papers in which the reference citations do not follow this format may be returned to the author. References to papers 'in preparation' or 'submitted' are not acceptable; if 'in press', the name of the journal or book must be given. Reference citations should not include 'personal communications' or other inaccessible information; information derived from personal communications or from unpublished work by the authors should be referred to in the text.

Note: In the online version of *Brain* there are automatic links from the reference section of each article to cited articles in Medline. This is a useful feature for readers, but is only possible if the references are accurate. It is the responsibility of the author to ensure the accuracy of the references in the submitted article. Downloading references directly from Medline is highly recommended.